A DISSERTATION

entitled

KINETIC STUDIES BY THE LOW TEMPERATURE STOPPED-FLOW METHOD

by

DAVID JAMES BENTON, B.Sc.

Submitted to the University of Warwick in
partial fulfilment of the requirements for the
award of the degree of Doctor of Philosophy

January, 1972

The Low Temperature Stopped-flow Apparatus

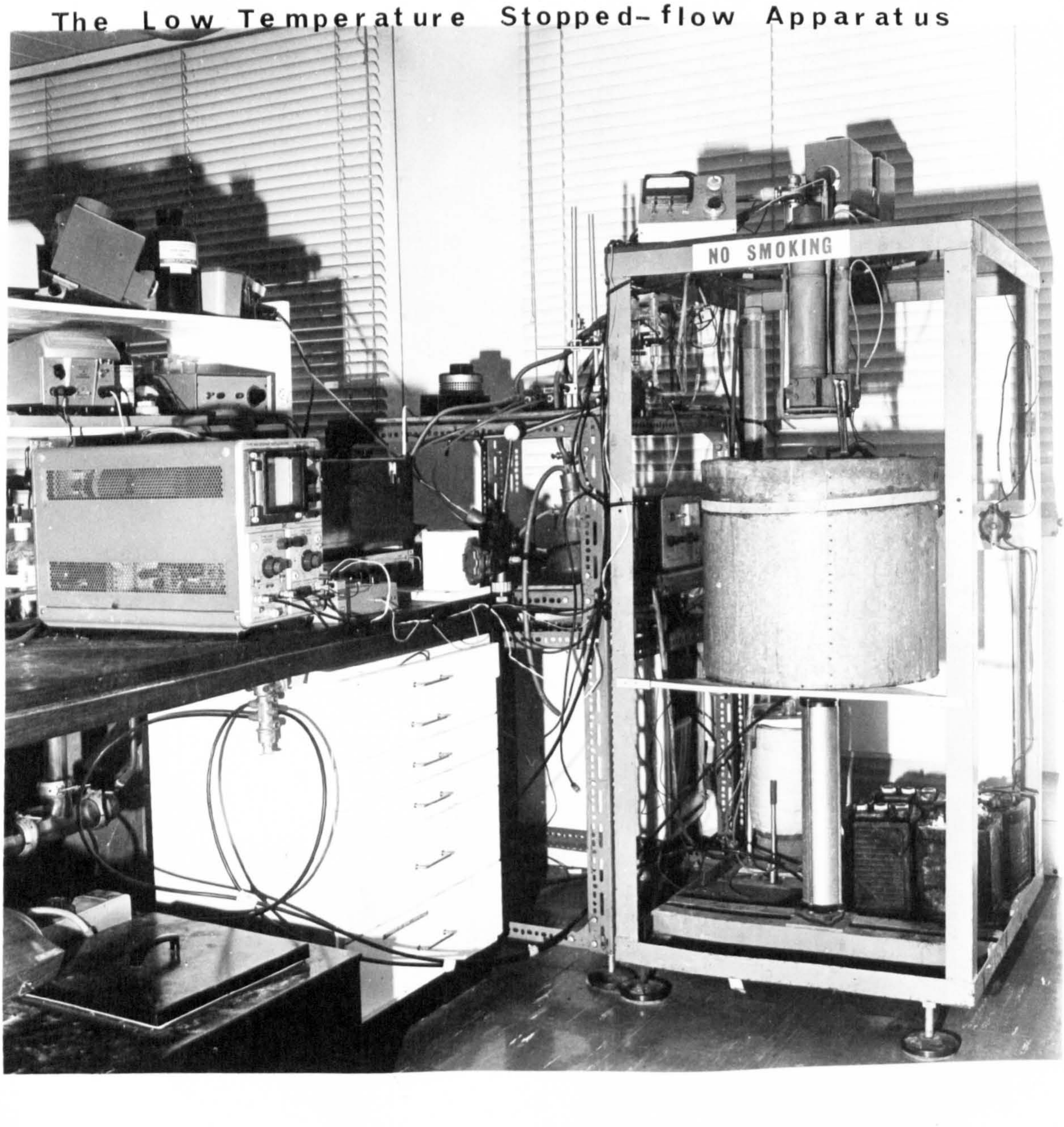

PREFACE

The studies described in this dissertation were undertaken in the School of Molecular Sciences of the University of Warwick between October, 1968, and September, 1971. The work is original and the author's own except where specific mention is made to the contrary. None of the information contained herein has been submitted either wholly or in part to this or another university for the award of a degree.

The author is indebted to his supervisor, Dr. Peter Moore for his constant advice and encouragement, to his former colleague, Dr. Terrence Matts for many helpful discussions, and to Professor V.M.Clark for providing research facilities. Thanks are also due to Messrs. K.Holden, C.Worland and A.Gurnham, of the School of Molecular Sciences Workshops, for their invaluable help in the construction of the low temperature stopped-flow apparatus.

The award of a Research Assistantship by the Science Research Council is gratefully acknowledged.

Parts of the work contained in this thesis have been published in the scientific literature, with the following references :

H.W.Alcock, D.J.Benton and P.Moore, Trans. Farad. Soc., 1970, 66, 2210.

D.J.Benton and P.Moore, J. Chem. Soc. (A), 1970, 3179.

CONTENTS

Contents (continued)

ABBREVIATIONS

S.I. units are used in this thesis unless alternative symbols are defined in the following list:

Å	angstrom unit (10^{-10} m)
DMSO	dimethyl sulphoxide
E.D.T.A.	ethylenediaminetetra-acetate
e.m.f.	electro-motive force
en	ethylenediamine
E.S.R.	electron spin resonance
exp	exponential function
h	Planck's constant
I	ionic strength
K (with subscript)	equilibrium constant
kcal	kilocalorie = 4184 J
k_d	dissociation rate constant
k_f	formation rate constant
k_o	first-order rate constant for water exchange at a metal ion
k_{obs}	observed first-order rate constant
N.M.R.	nuclear magnetic resonance
pK_a	$-\log_{10}$ (acid dissociation equilibrium constant)
R	gas constant per mol
Kel-F	polyfluorotrichloroethylene
Teflon	polytetrafluoroethylene
bipy	2,2'-bipyridyl
phen	1,10-phenanthroline
terpy	2,2',2"-terpyridyl
ΔH^*	activation enthalpy change
ΔS^*	activation entropy change
ϵ	extinction coefficient
λ	wavelength

SUMMARY

The design and construction of a low temperature stopped-flow apparatus is described. This equipment was developed to study reactions whose rates are too fast for other rapid flow methods and are not suitable for investigation by the rapid-reaction techniques which do not involve the mixing of reagents. Spectrophotometric observation is used and reactions may be monitored in both the ultraviolet and visible regions. The equipment is constructed from chemically inert materials and reactions may be studied down to ca. 220K.

The low temperature stopped-flow apparatus was used to study the formations of the 2,2'-bipyridyl, 1,10-phenanthroline and 2,2',2"-terpyridyl complexes of the manganese(II) ion in anhydrous methanol. The reactions between the manganese(II) ion and the first two ligands are too fast for flow methods at ambient temperatures but the kinetics and activation parameters were easily obtained at low temperatures.

Whereas in aqueous solution the formation reactions of the divalent metal ions have activation enthalpies very similar to that of water exchange at the metal ion, the activation enthalpies of the reactions studied in this work are considerably greater than that of methanol exchange at the manganese(II) ion. It is suggested that a steric effect causes the high activation enthalpies. Possibly, either the first metal-ligand bond is hindered, or ring closure is rate determining. Evidence that the 2,2'-bipyridyl complex is formed with a rate determining ring closure is presented from consideration of the relative magnitude of the acid and mercuric ion induced dissociation rate constants.

The kinetics of dissociation of the mono-(2,2'-bipyridyl)manganese(II) and mono-(1,10-phenanthroline)manganese(II) ions in anhydrous methanol are also reported. The rate constants are smaller than the corresponding reactions in water, as is expected from the relative labilising effects of co-ordinated water and methanol molecules.

In Chapter 3, the kinetics of formation of peroxynitrous acid (HOONO)

and its decay to nitrate ion (reactions (1) and (2)) are described.

$$HNO_2 + H_2O_2 \xrightarrow{H^+} HOONO + H_2O \qquad (1)$$

$$HOONO \xrightarrow{H^+} NO_3^- + H^+ \qquad (2)$$

The reaction rates are measured at much higher acidities than previous studies. The existence of an acid catalysed pathway for the isomerisation of the peroxynitrous acid, which previous workers had postulated, is confirmed.

The rate law for the formation process was found to be of the form (a, b and c are constants),

$$d[HOONO]/dt = a[H^+][HNO_2][H_2O_2]/(b + c[H_2O_2])$$

which is consistent with a mechanism in which NO^+ is formed as an intermediate.

The spectrum of peroxynitrous acid was recorded for the first time using a continuous-flow mixing cell.

Under the conditions used, reactions (1) and (2) are an example of a series first-order reaction. It was not possible to measure meaningful rate constants for the formation process directly because of the overlap with reaction (2). A least-squares method of analysing spectrophotometric data for a series first-order reaction

$$A \xrightarrow{k_1} (B) \xrightarrow{k_2} C$$

is described where the unknown parameters are k_1, k_2 and the extinction coefficient of the intermediate B. Care is needed, since two solutions fit the data equally well. These solutions correspond to a faster formation of a weakly absorbing intermediate, and a slower formation of a more strongly absorbing species. Methods of resolving the ambiguity are discussed.

CHAPTER I

INTRODUCTION

The ability to study the kinetics of a reaction provides a most powerful tool for the elucidation of the mechanism of that reaction. Increasingly, kinetic methods have been applied to gain an understanding of the reactions of metal complexes.

A substitution reaction is the most fundamental process that a metal complex in solution may undergo, and has an important role in a wide range of processes. A substitution step, for example, is involved in an inner-sphere redox reaction, and often in metal ion catalysis. Again, in biochemical systems, substitution and the rate at which it occurs, is important in determining the role of metal ions in metalloenzyme or coenzyme function. In consequence, the kinetics of substitution reactions have received a great deal of attention.

Taube[1] has defined metal complexes as "inert" or "labile" as regards their rates of substitution processes. Metal complexes whose reactions are complete within one minute, at room temperature, and concentrations ca. 0.1 mol l^{-1} are said to be labile. Other metal complexes are classified as inert. Some borderline cases do exist, of course, and the division is purely arbitrary. Essentially, this definition divides metal complexes into those whose rates of reaction are measurable by conventional methods and those which require special techniques.

The substitution reactions of inert complexes have been extensively studied by a variety of techniques[2] which includes isotopic exchange, electrochemistry, polarimetry, pH measurements, and, of course, chemical analysis. Results on these systems are well documented[3,4]. In favourable cases, rapid reactions may be rendered suitable for study by simple methods[5a]. A common method for a second-order reaction is the use of low reagent concentrations, provided that a suitably sensitive method of detection is available. Low temperatures have been used to slow a reaction rate, either by working in non-aqueous solvents[6], or by the addition of a salt to depress the freezing point

of aqueous solution[7]. Competition methods or the combination of an equilibrium constant and a measurable reverse rate constant may also be used occasionally.

In the vast majority of cases, however, study of labile systems has had to await the widespread availability of rapid-reaction techniques. These methods have been well reviewed[5,8-12]. The various methods may be divided into two general categories:

a) those that involve the mixing of reagents and

b) those that utilise a static sample.

Due to the finite time taken to mix and observe a reaction, the majority of current equipment involving mixing is limited to processes of half-lives approximately $\geqslant$ 1 ms. The techniques using a static sample have no such limitation and half-lives down to nanosecond values can be measured by some methods.

Some improvement over the usual method of mixing reagents can be obtained by use of syringes. For example, injection of one reagent into another in a spectrophotometer cell is adequate for reactions taking several seconds to completion[13]. Another mixing in situ technique is the baffle method[14], where the reagents are initially separated by a baffle, which is suddenly removed by a strong spring, giving about 90% mixing in 50 ms or so. However, the best method to obtain both rapid and efficient mixing in a short time interval is to use a flow method.

Flow techniques were the first of the rapid-reaction methods to be developed, originally by biochemists and physiologists. Only in recent years have they been adopted by inorganic chemists, but in a decade or so have yielded a vast amount of rate data on the reactions of metal complexes. The two reagent solutions are forced along separate narrow-bore tubes under turbulent conditions into a mixing chamber. Observations on the ensuing reaction are then made in the exit tube from the mixer. Alternatively, the mixed solutions may be quenched by flowing into a third reagent which stops the reaction, or by rapid cooling. With quenched-flow methods no special

detection system is required, the sample being analysed at leisure to determine the extent of reaction at the point of quenching.

The efficiency of a flow apparatus is dependent upon many factors[10a], for example, the rate of the flow, and the sensitivity of the detection system, but none is perhaps more critical than the performance of the mixer into the design of which has gone much effort and ingenuity[8a,11].

The original apparatus of Hartridge and Roughton[15] was of the continuous-flow type. In this mode solutions are driven continuously through the system, while measurements are made either at a number of positions beyond the outflow from the mixer, or at a single point and varying the extent of reaction at that position by using different flow rates. A variety of techniques has been used to follow the progress of the reaction including photometry, conductivity, temperature and pH measurements, and an adaption to use a commercial spectrophotometer has been designed[16]. Originally, gas pressure was used to drive the solutions but motor driven syringes, first introduced by Dirken and Mook[17], are now generally employed. A dead-time of the order of 1 ms can easily be achieved and the utilisation of very sensitive observation methods permits high accuracy and the use of dilute reagents. Although this method can be used for reactions with half-lives down to about 1 ms, the requirement for turbulent-flow in the observation tube limits the continuous-flow technique to reactions which are complete within about 0.1s. Continuous-flow is a comparatively simple technique in that rapid-response detectors are not required but it does lead to the consumption of large amounts of reagents which is a grave disadvantage for many systems, especially the biochemical ones. Fast-response detectors and recording instruments have reduced the quantity of reactants required from the 3-4 litres of Hartridge and Roughton's apparatus down to a few millilitres. The improvement in electronic devices has, however, made other rapid-reaction methods possible.

Chance[18] developed an accelerated-flow system. The reagent solutions are contained in small syringes and driven forward by a sharp manual push,

which produces an accelerated flow for ca. 0.1s. The reaction is followed spectrophotometrically in one position directly after the mixer. The light intensity is converted to a voltage which is displayed on the Y-scale of an oscilloscope. The flow rate varies during a run, but is sensed from the movement of the driving syringes and displayed on the X-scale of the oscilloscope. The trace is photographed and a reaction-time curve deduced. This method can measure reaction half-lives down to about 1 ms and is thus comparable to continuous-flow, but accelerated-flow has the great advantage of requiring only about 0.1 ml of each reagent. However, this latter advantage is also possessed by the stopped-flow method which also uses simpler electronic circuits.

The stopped-flow technique (SF) has developed into one of the most widely used of all the rapid-reaction methods, and this is no doubt due in part to the commercial availability of such instruments. A manual, motor, pneumatic or hydraulic drive forces the reagents out of syringes and rapidly through the flow system. When sufficient volume of fresh reagents has been delivered to purge the mixer and observation tube (ca. $\frac{1}{2}$ ml total), the flow is brought to an abrupt halt. Apart from the reaction that occurs in the mixer and during the time taken to reach the point of observation, (the so called "dead-time" of the apparatus), the whole course of the reaction is then observed at a point immediately behind the mixer. The method was first described by Roughton[19], improved by Chance[20], and finally perfected by Gibson[21].

A multitude of designs[11a, b, 20-25] of SF equipment has been described with dead-times between two and fifteen milliseconds. The time resolution of SF is thus not quite as good as that of continuous-flow but SF is much more versatile in that not only reactions in the millisecond region can be studied but also those extending over periods of minutes. SF thus overlaps with the conventional methods. An example of how the stopped-flow technique can extend conventional kinetic studies of a reaction is shown in Chapter 3, where the kinetics of formation and decay of peroxynitrous acid are described. The main drawback to SF is the requirement of rapid-response

detectors, spectrophotometric devices being most common, but e.m.f. and conductivity measurements have also been used.

Current advances in SF technology include the application of on-line computing[8b,26] for the rapid calculation of rate data, and rapid scanning spectrometry to obtain the spectra of intermediates[27].

Relaxation methods, pioneered by Eigen and co-workers[9a], involve the perturbation of a chemical system in equilibrium, and the observation of the subsequent re-equilibration. In the case of the temperature-, pressure- and electric field-jump methods, the disturbance is applied to the system as a single pulse, in a time short compared to the half-life of the reaction. The relaxation to a new equilibrium position is followed by fast conductiometric or spectrophotometric methods. Providing that the impulse does not greatly disturb the equilibrium, the relaxation process is first-order, irrespective of the molecularity of the reaction, and can be related to the rate constants of the forward and reverse reactions[28a,10b].

In addition to the pulse methods, periodic disturbances may also be used, as with ultrasonic waves or high frequency alternating electric fields. When the periodic time of the perturbing influence is comparable to the relaxation time of the reaction, energy is absorbed. The frequency at which the absorption is a maximum can be related to the relaxation time[5b].

Relaxation methods have proved especially useful in the study of the formation and dissociation reactions of those labile complexes whose rates are too fast for flow equipment, the temperature-jump method employing photometric read-out having, perhaps, the widest application. The original joule heating apparatus of Eigen[29] is limited to studies of relaxation times of about $\geq$ 1 μs in conducting solutions. The use of lasers[30,31a] and improved modes of joule heating[31b] can extend the time limit well into the nanosecond region, whilst both laser and microwave heating[32] make the technique applicable to non-conducting solutions.

Magnetic resonance methods also enable systems in equilibrium to be studied, and have the advantage of permitting the study of reactions which do

not involve any net chemical change, (provided, of course, a suitable nucleus is precent for N.M.R., or a paramagnetic species for E.S.R.). The line width of an N.M.R. signal is related to the lifetime of a nucleus in a particular environment. If the reaction rate is increased by addition of reagents or a rise in temperature, the line-width broadens. The broadening may be related to the rate constant[5c]. Similar considerations apply to the use of E.S.R. The greatest kinetic use of the magnetic resonance methods to the study of metal complexes has probably been the determination of solvent exchange rates by the N.M.R. line-broadening technique. Additional factors are involved when paramagnetic metal ions are studied and recent reviews present the methods and results published to date[33,34]. E.S.R. has not been widely used in connection with metal complexes but a few studies on the detection of outer-sphere association[35] and substitution reactions[36] have been reported.

The rapid photolytic and electrochemical methods of studying reaction rates, while extremely useful for many chemical systems, have not found extensive application to the reactions of metal complexes, though some polarographic investigations have been published[37].

Most of the data on fast substitution reactions have been measured by either the stopped-flow or temperature-jump techniques. However, many labile systems whose rates are too fast for stopped-flow investigations are not readily measurable by the temperature-jump method. Relaxation techniques suffer from the disadvantage that they are only applicable to systems in equilibrium, where the concentrations of reactants are comparable[8c]. Thus, with a reaction of large equilibrium constant it may not be possible to arrange conditions such that a perturbation will provide a measurable change in the concentration of one of the species present. Even for those systems that do possess a viable equilibrium, the applied disturbance must produce a detectable change in the equilibrium e.g. in temperature-jump studies, the enthalpy of reaction must be large enough. If the latter condition is not fulfilled, the difficulty may be circumvented in certain systems; thus

reactions whose equilibrium is controlled by pH may be coupled to a buffer whose ionisation constant is temperature dependent. Alternatively, the reaction may also be coupled to a second faster reaction that does have a large enough enthalpy of reaction, but often such methods are restricted and may introduce interpretational difficulties.

One approach to develop a device capable of studying fast irreversible reactions that are outside the time scale accessible to conventional flow methods has been to combine stopped-flow with another rapid-reaction technique. Examples include a SF/temperature-jump[38] and a SF/flash photolysis apparatus[39]. The stopped-flow component is used to establish a steady-state which may then be perturbed by the other technique.

A more promising development might be an improvement in the range of rates accessible to the stopped-flow method. A recent design of Berger *et al.*[40] uses very high driving pressures and special valves to arrest the flow. It is claimed that half-lives of less than $\frac{1}{2}$ ms can be studied with this apparatus. A second method that has been used is to combine low temperatures with the stopped-flow technique. A number of low temperature stopped-flow instruments have been reported[41-3]. The development of a similar apparatus forms the basis of this work, and in a later chapter its application to some formation studies of metal complexes will be described.

The formation reactions of metal complexes have second-order rate constants which vary from about 10^{-6} to 10^{+10} l mol^{-1} s^{-1}, and this is one field to which the rapid-reaction techniques have been widely applied. Many reviews[33,44-47] have been devoted to the compilation and interpretation of formation rate data. For this work we will be concerned with the behaviour exhibited in the formation reactions of the mono-complexes of the divalent metal ions of the first transition series. Most of the rate data reported so far refers to this class, but is restricted mainly to aqueous solutions, in which there has been general agreement on the mechanism by which these complexes form.

For reaction with a given ligand, the order of reactivity of this series of metal ions is:

$$V^{2+} < Ni^{2+} < Co^{2+} < Fe^{2+} < Mn^{2+} < Zn^{2+} < Cr^{2+}, \quad Cu^{2+}$$

This order is not understandable in terms of a simple electrostatic theory involving charge and radius considerations. Apart from the Cr^{2+} and Cu^{2+} ions (which are subject to Jahn-Teller distortion), the order can, however, be correlated in terms of the Crystal Field or Ligand Field Theories, as discussed by Basolo and Pearson[3a,b].

For the formation reactions of the divalent metal ions in aqueous solution, several experimental trends are prominent[45,47].

1. The rate law is second-order overall, first order in both metal ion and ligand.
2. Although across the series, the second-order rate constants vary by many orders of magnitude, the rate constants for any one particular metal ion, reacting with a wide variety of ligands, cover a much smaller range.
3. For a particular metal ion the second-order rate constants for reaction with neutral ligands are similar to the second-order rate constant for water exchange. With ligands of the same charge, the observed rates are very insensitive to the type of ligand, there being no correlation with the nucleophilicity of the entering group. The second-order rate constants increase as the charge on the ligand becomes more negative.
4. The enthalpies of activation connected with the observed second-order rate constants for a particular metal ion show a remarkable constancy for a wide variety of ligands of varying charge type and structural properties. The enthalpies of activation are usually close to that associated with the solvent exchange process. The entropies of activation for neutral ligands are about zero and progressively become more positive for ligands of increasing negative charge.

The lack of dependence of the rate constant and energetics of the reaction upon the incoming ligand is one of the principal criteria of a dissociative process[4], for the ligand cannot be contributing significantly

to stabilisation of the transition state. The minor role of the ligand discounts an associative mechanism and solvent loss occurs without any assistance from the incoming ligand. Langford and Gray[4] have classified dissociative mechanisms into a D mechanism, in which a five co-ordinate intermediate is generated, or an I_d mechanism in which solvent-ligand interchange occurs. A D mechanism has an intermediate of sufficient lifetime to survive rearrangement of its second co-ordination sphere and hence discriminate between different ligands. The I_d mechanism has the entering group as a stoicheiometric component of the transition state. It arises when the five co-ordinate complex does not have sufficient lifetime relative to the lifetime of the second co-ordination sphere to react selectively. Rather it must react with the molecule in the second co-ordination sphere at the instant of formation of the transition state.

If we consider the simplest case of a unidentate ligand (L) forming a complex, the following schemes are possible:

(S = solvent molecule, and charges have been omitted)

(i) $MS_6 \underset{k_{-1}}{\overset{k_1}{\rightleftharpoons}} MS_5 + S$

$MS_5 + L \underset{k_{-2}}{\overset{k_2}{\rightleftharpoons}} MS_5L$

(ii) $MS_6 + L \underset{k_{-o}}{\overset{K_o}{\rightleftharpoons}} MS_6,L \overset{k}{\rightleftharpoons} MS_5L + S$

In scheme (ii) complex formation is preceded by the formation of an ion-pair, or outer-sphere complex if the ligand is uncharged. The conversion to the complex may proceed via either a D or an I_d path.

Most experiments are performed with the metal ion in excess to limit the formation to the mono-complex, and then both schemes give a similar rate law[47] (neglecting the back reactions with rate constants k_{-2} or k_{-o})

$$d[MS_5L]/dt = A[MS_6][L]/(1 + B[MS_6]) \qquad (1.1)$$

where for scheme (i) $A = k_1k_2/(k_{-1}[H_2O])$ and $B = k_2/(k_{-1}[H_2O])$

and for scheme (ii) $A = K_ok_o$ and $B = K_o$

Much of the current interpretation of these reactions is based upon the proposal of Eigen[48] that scheme (ii) is operating. Eigen and Tamm's[49] ultrasonic studies on the divalent metal ion sulphate systems revealed two absorption-frequency maxima, the position of one maximum being independent of the metal ion used. They proposed that the reactants diffused together to form an ion-pair in which the metal ion and ligand are separated by two water molecules which then collapses to the outer-sphere complex. This ion-pair loses a co-ordinated water molecule and proceeds to the product. It was this last step that produced the metal ion dependent peak. Significantly, the slower step agreed closely with the water exchange rate of the same metal ion as determined by N.M.R. studies[50].

Under the conditions of most experiments $[MS_6]$ is very small, and if K_o is also small, then the rate law for scheme (ii) reduces to:

$$d[MS_5L]/dt = K_ok_o[MS_6][L]$$

That is, second-order as experimentally observed with the observed formation rate constant $k_f = K_ok_o$. This mechanism is then able to account for the experimental observations noted above by considering, for example, the effect of negatively charged ligands upon the magnitude of K_o and hence k_f.

However, it is important to realise that most kinetic studies on the divalent metal ions have resulted from the application of temperature-jump and stopped-flow methods, techniques which do not permit ion-pair formation to be directly determined. Only rate constants which may be equated to the product K_ok_o are obtained. The equality $k_f = K_ok_o$ provides a test of mechanism (ii) if it is possible to estimate K_o and k_o separately, an approach that has been used by many workers. The presence of ion-pairs in inert systems, such as Cr(III) and Co(III) complexes, is well established from thermodynamic and kinetic studies[51-3]. There is evidence

from substitution reactions in such systems that ion-pair formation does not significantly affect the solvent exchange rate[54]. Therefore, the solvent exchange rate constant measured by N.M.R. line-broadening methods should provide a very close approximation to k_o. The direct determination of K_o values for labile systems is not easy, a few experimental values from ultrasonic studies of metal sulphates[55-56], E.S.R. measurements[36] and one particular temperature-jump study[57] where the ion-pair is particularly stable, are available. Resort is, therefore, made to calculation of K_o values from the equation:[58-9]

$$K_o = (4\pi Na^3/3000)\exp(-U_{(a)}/kT) \qquad (1.2)$$

where $$U_{(a)} = Z_1Z_2e^2/aD - Z_1Z_2e^2\underline{k}/D(1+\underline{k}\,a)$$

and $$\underline{k}^2 = 8\pi Ne^2I/1000\,D\,kT$$

N is Avagadro's number, a is the distance of closest approach of the ligand and metal ion, k is Boltzmann's constant, T is the absolute temperature, Z_1 and Z_2 are the charges on the metal ion and ligand, e the electron charge, D is the dielectric constant of the medium, and I is the ionic strength.

For the inert systems values of K_o may be found from spectrophotometric and other methods[60], and yield a value for a of about 4Å to 5Å. Assuming similar distances apply to labile systems, K_o values are calculated and the quotient k_f/K_o ($=k_o$) compared to the experimental first-order rate constant for solvent exchange. In general, the spread of derived k_o values for different ligands in aqueous solution is small and these values are close to the water exchange rate constant. Due to the assumptions made in the derivation of equation (1.2), K_o values for oppositely charged reactants are estimated to be accurate to within a factor of two to four[47]. The weakness of this approach is estimating the magnitude of K_o for neutral, particularly bulky, multidentate ligands where steric effects might arise. This type of consistency of large amounts of data provides strong support for the Eigen mechanism. However, most rapid reactions are also compatible with a

D mechanism in which no outer-sphere complexes are present, for any ligand which could capture the five co-ordinate intermediate preferentially could exhibit a reactivity paralleling a calculated outer-sphere association constant[61].

Whether the outer-sphere complex reacts to give product via a D or I_d mechanism is difficult to establish. Langford and Stengle[61] have suggested a possible method of distinction. If the ion-pairing constant is known, or a limiting rate of ligand entry corresponding to saturation of the association is observable, then all ligands should enter at a rate, which for an I_d mechanism, should lie below the water exchange rate. The reason for this is that the ion-pair has a number of water molecules in its outer-sphere in addition to the ligand. The most probable result of water loss will be water exchange. If a D mechanism is operating, the rate of ligand entry should match the water exchange rate. It has been possible for certain inert systems to arrange experimental conditions to distinguish the two mechanisms. Thus $Co(CN)_5 H_2O^{2-}$ anation proceeds by a D mechanism[62] and $Co(NH_3)_5 OH_2^{3+}$ anation by an I_d mechanism[53]. Unfortunately, in labile systems it is not usually possible to achieve the required experimental conditions and such a comparison has to be made via estimates of K_o, which are not accurate enough for such subtle distinctions.

Even though the Eigen mechanism has been generally accepted in aqueous solution, the demonstrated presence of an outer-sphere complex in a reacting system does not necessitate it being an essential intermediate in the reaction[63]. The close proximity in which the metal ion and ligand are then held, however, does make the outer-sphere complex an attractive possibility. In addition, as Prince and Hewkin[33] have pointed out, there are often great differences in the experimental conditions and techniques used to measure solvent exchange and complex formation. For instance, the temperature ranges and concentrations of metal ion are often completely different, and the presence of the large quantity of electrolyte necessary for temperature-jump experiments may influence the rate of solvent exchange,

thus invalidating the comparisons described above.

The Eigen mechanism may be extended to include multidentate ligands if additional steps are taken into account, thus for a bidentate ligand, L–L, and omitting charges:

$$S_6M + L\text{–}L \underset{}{\overset{K_o}{\rightleftharpoons}} S_5MS,L\text{–}L \qquad (1.3)$$

$$S_5MS,L\text{–}L \underset{k_{-1}}{\overset{k_1}{\rightleftharpoons}} S_5M\text{–}L\text{–}L + S \qquad (1.4)$$

$$S_5M\text{–}L\text{–}L \underset{k_{-2}}{\overset{k_2}{\rightleftharpoons}} S_4M\langle^{L}_{L}) + S \qquad (1.5)$$

If reaction (1.3) is assumed rapid compared to the succeeding steps, and applying the steady-state approximation to the intermediate, the rate law (1.6) results[64]:

$$\text{Rate} = k_f[MS_6]\,[L\text{–}L] - k_d[M\langle^{L}_{L})] \qquad (1.6)$$

$$\text{with } k_f = K_o\,k_1\,k_2/(k_{-1} + k_2) \qquad (1.7)$$

$$\text{and } k_d = k_{-1}\,k_{-2}/(k_{-1} + k_2) \qquad (1.8)$$

There are a great many results, at least for the simpler multidentate ligands, where the rate constants for a given metal ion are comparable to those of unidentate ligands of the same charge. For example, the rate constants of the Ni(II) ion reacting in water with pyridine, 2,2'-bipyridyl, 1,10-phenanthroline and 2,2',2"-terpyridyl are all within a factor of four[45]. This has been interpreted as showing $k_2 \gg k_{-1}$; a mechanism in which attachment of the first bond is rate determining and $k_f = K_o k_1$. This can readily be understood when it is recognised that the ring closure step is a first-order process and the remaining co-ordination sites of the ligand are held in close proximity to the metal ion, hence having a high effective concentration.

In some cases, however, there is a marked difference between the rate

constant observed for uni- and bidentate ligands and this can sometimes be rationalised in terms of ring size and the nature of the binding groups. Kustin and co-workers' study[65] of the Mn(II) and Co(II) ions reacting with α- and β-alanine revealed that β-alanine, which forms a six-membered ring, reacted much more slowly than the α-form. Yet the Ni(II) ion reacted with both ligands at about the same rate. This was attributed to the rate determining step involving ring closure (rate constant k_2 equation (1.5)). More energy must be required for ring closure of the β-alanine than with α-alanine. Either ring strain or entropy loss from forming a six, as compared to a five, membered ring could be the cause of the slow rate constant. This behaviour has been termed sterically controlled substitution (SCS) and may be expected for the most labile metal ions such that $k_{-1} > k_2$. SCS has also been postulated for other reactions of Co(II)[66] and Cu(II) ions[67-9]. Although expected for the most labile ions, SCS has been invoked to account for the relatively slow rate of reaction between the Ni(II) ion and the enol form of acetylacetone[69]. These conclusions are deduced from the observed rate constants, but more direct evidence comes from the detection of two relaxation times in a pressure-jump study[70] of the formation of the malonatonickel(II) ion. The rapid process was assigned to the formation of the unidentate intermediate, and the slower step to ring closure.

Cases do occur where formation rate constants are higher than would be predicted from expected values of K_o and k_o. Some polyamines react with the Ni(II) ion in aqueous solution faster than other ligands of like charge. Rorabacher[71] has proposed an internal conjugate base mechanism (ICB). Hydrogen bonding occurs between one end of the amine and a co-ordinated water molecule, which stabilises the outer-sphere complex and leads to a greater K_o. The hydrogen bonding imparts some hydroxide character to that water molecule, which causes labilisation of the remaining co-ordinated water molecules. A second donor atom, from the same ligand, is thus in a favourable position to take advantage of the greater rate of water loss.

The ICB mechanism only occurs with amines more basic than the co-ordinated water molecules. A similar type of acceleration has also been reported in Co(II)[72] and Cu(II)[73] systems.

The application of a low temperature stopped-flow obviously requires the use of solvents other than water, or possibly solvent/water mixtures if their flow properties are suitable. Data upon formation reactions of the divalent metal ions in non-aqueous solvents are very restricted. Recently, a number of studies have been performed in non-aqueous and mixed solvents, and the factors that influence formation rates in these solvents have become a topic of discussion. Pearson and Ellgen's work on the formation rates of some Ni(II) ion complexes in methanol, with neutral and negatively charged ligands, was in excellent agreement with the predictions of the ion-pair mechanism.[74] The difference in rates between the variously charged ligands in methanol, and comparisons with their rates in water, could logically be accounted for by considering the different exchange rates of the two solvents, and the effect of the dielectric constant upon the magnitude of K_o. Similarly, Hoffmann et al.[75] argued in terms of the Eigen mechanism in their study of the Ni(II)/SCN^- formation reaction in methanol. A pressure-jump study[76] of some divalent metal ions formation rates with m-benzenedisulphonate in methanol was discussed in terms of an I_d mechanism. The difference between the rate of solvent exchange and ligand entry into the inner co-ordination sphere was much larger in methanol than that usually found for I_d mechanisms in aqueous solution. This was attributed to the metal ions having a larger second co-ordination sphere in methanol than water, causing solvent exchange to be more probable. In this paper it was also reported that the formation rate constants of the six metal complexes studied differed only by a factor of two.

A study[77] of the formation of the mono-(2,2'-bipyridyl)Ni(II) ion in mixed methanol/water solutions, led Bennetto and Caldin to suggest that solvent structure was important in determining the observed rate. This same reaction, when studied in several non-aqueous solvents[78], gave results that

could not be accounted for by the Eigen mechanism. The ratio $n = k_f/K_o k_o$, which should equal unity, or at least be a constant in a variety of solvents if the Eigen mechanism is applicable, varied by a factor of 200 over the range of solvents used. Moreover, the activation enthalpies for formation differed considerably in some cases from those of the respective solvent exchange. There was a linear relationship between log n and the solvent fluidity, which was taken to show a dependence on the solvent structure. This has been criticised[47] for using a constant K_o value and the assumption that the bidentate ligand will display normal substitution in these solvents. With regard to the latter suggestion, Rorabacher and MacKellar[79] have reported a different profile of rate versus solvent composition in methanol/water mixtures for the formation of the mono-ammine-Ni(II) ion to that observed in the similar study of the 2,2'-bipyridyl reaction[77]. The results of the mono-ammineNi(II) ion formation[79] are discussed in terms of the outer-sphere complex scheme and the differing labilities of the various solvated species. Any steric effects are likely to be less with the smaller ammonia molecule. Rorabacher and MacKellar also suggest that the 2,2'-bipyridyl results[77] in the mixed water/methanol solutions could be due to a steric effect or a rate determining ring closure.

Bennetto and Caldin, however, have extended their work with Ni(II) to include other ligands and have also studied reactions with the Co(II) ion in non-aqueous solvents[80]. A mechanism based on a model for solvated metal ions, due to Frank and Wen[81], is proposed, in which solvent structure and solvent re-organisation in the region of the metal ion can have a large effect upon the transition state.[82]

Langford and Tsiang[83] have reported that the reactions of murexide and thiocyanate anions with the Ni(II) ion in dimethyl sulphoxide solution proceed very much below the solvent exchange rate, a similar trend to that observed[78] with the Ni(II)/2,2'-bipyridyl reaction in DMSO. The slow rate is attributed to a five co-ordinate intermediate (D mechanism) which appears to respond to kinetic tests. Frankel's N.M.R. study[84] of the solvent

exchange at the $Ni(DMSO)_6^{2+}$ ion in DMSO and DMSO/mixed solvents is also consistent with a D mechanism.

As with early studies in aqueous solution, formation reactions in non-aqueous solvents have so far been largely confined to the Ni(II) ion. For the reactions of the more labile divalent metal ions in non-aqueous solution, it was expected that a low temperature stopped-flow would prove very suitable. This is especially so in view of the hypothesis[82] that the activation parameters may be useful in understanding the mechanism of the system, and these are best obtained over as wide a temperature range as possible.

CHAPTER 2

EXPERIMENTAL

2.1. The Low Temperature Stopped-flow Apparatus

The requirements for the efficient operation of a rapid flow apparatus have been discussed by Roughton and Chance[10a], with particular reference to continuous-flow equipment, although many of these considerations also apply to the stopped-flow method. The main points to which special attention must be devoted are summarised below.

1. The mixing must be rapid and efficient.
2. A high linear flow velocity is required. It is usual to try to achieve a flow rate above the critical velocity of the liquid, at least in the vicinity of the mixer. This will aid the mixing process. Fortunately, and in contrast to the continuous-flow method, provided that the mixing is efficient, the velocity profile for the subsequent flow does not matter. A high flow velocity also minimises the dead-time.
3. The stopping of the flow must be very sharp. The efficiency of mixing falls if the flow rate is too slow. Consequently, if the flow decreased gradually, the liquid which ultimately came to rest at the observation point might be incompletely mixed, and the apparent reaction rate would initially be too low. Moreover, the more sudden the stopping, the faster the reaction that can be observed.
4. The thermostating arrangements must give good temperature control and prevent differences of temperature between the solutions and the components of the stopped-flow apparatus with which they come into contact.

In addition to the above considerations the apparatus required in this work had to be inert to acids and strongly complexing ligands which are known to attack stainless steel, and also be operable to low temperatures down to about 220K. Inertness was satisfied by ensuring that the solutions only came into contact with glass, and the plastics Kel-F, Teflon and glass impregnated Teflon. The low temperatures were achieved

by following a similar pattern to Caldin et al.[41].

General Arrangement

A schematic side view of the equipment is shown in Figure 1. The apparatus was designed for total immersion in a low temperature thermostat. Heat losses through the faces of the components due to large temperature differences between the laboratory and the components are then avoided. The stopped-flow apparatus is suspended from a large rigid metal stand (A, Fig. 1), with the thermostat (L, Fig. 1) mounted beneath. In use, the thermostat is raised pneumatically to surround the stopped-flow; an arrangement chosen to avoid movement of the carefully aligned light beam. The roof of the stand is available to mount the light source, monochromator and stirrer (not shown in Fig. 1 for clarity). The controls for emptying the stopping syringe (B, Fig. 1) and operating the exit valve (C, Fig. 1) extend out of the thermostat through the roof.

As many of the moving parts as possible are mounted external to the thermostat to prevent complications due to contraction. The hydraulic ram, (I, Fig. 1) drive syringes (H, Fig. 1) reservoirs and associated connecting taps (J, N, Fig. 1) are mounted on a separate stand to prevent transmission of vibration to the optical system during a run. The hydraulic master unit (O, Fig. 1) is mounted separately to the two stands, again to eliminate vibration.

The detailed description of the components of the low temperature stopped-flow now follow. The diagrams are not drawn to scale but illustrate important features of design and construction.

The Observation Block

To keep the stopped-flow apparatus as compact as possible, a single block was designed to incorporate the mixer and observation tube, and to mount the stopping syringe and exit valve. This block (Fig. 2) is machined from a piece of Kel-F, 100 x 50 x 50 mm. This material was chosen not only for its chemical inertness but also for its greater rigidity compared to Teflon or glass impregnated Teflon, which aids machining. In

FIGURE 1

Schematic side view of the low temperature stopped-flow apparatus

Key

A Main support stand.

B Stopping syringe emptying rod.

C Exit valve control.

D Monochromator.

E Light inlet tower.

F Photomultiplier tower.

G Glass tubing.

H Drive syringes.

I Hydraulic ram.

J Reservoirs.

K Inner thermostat tank.

L Outer thermostat tank.

N Three-way taps.

O Hydraulic master unit.

SF Stopped-flow apparatus.

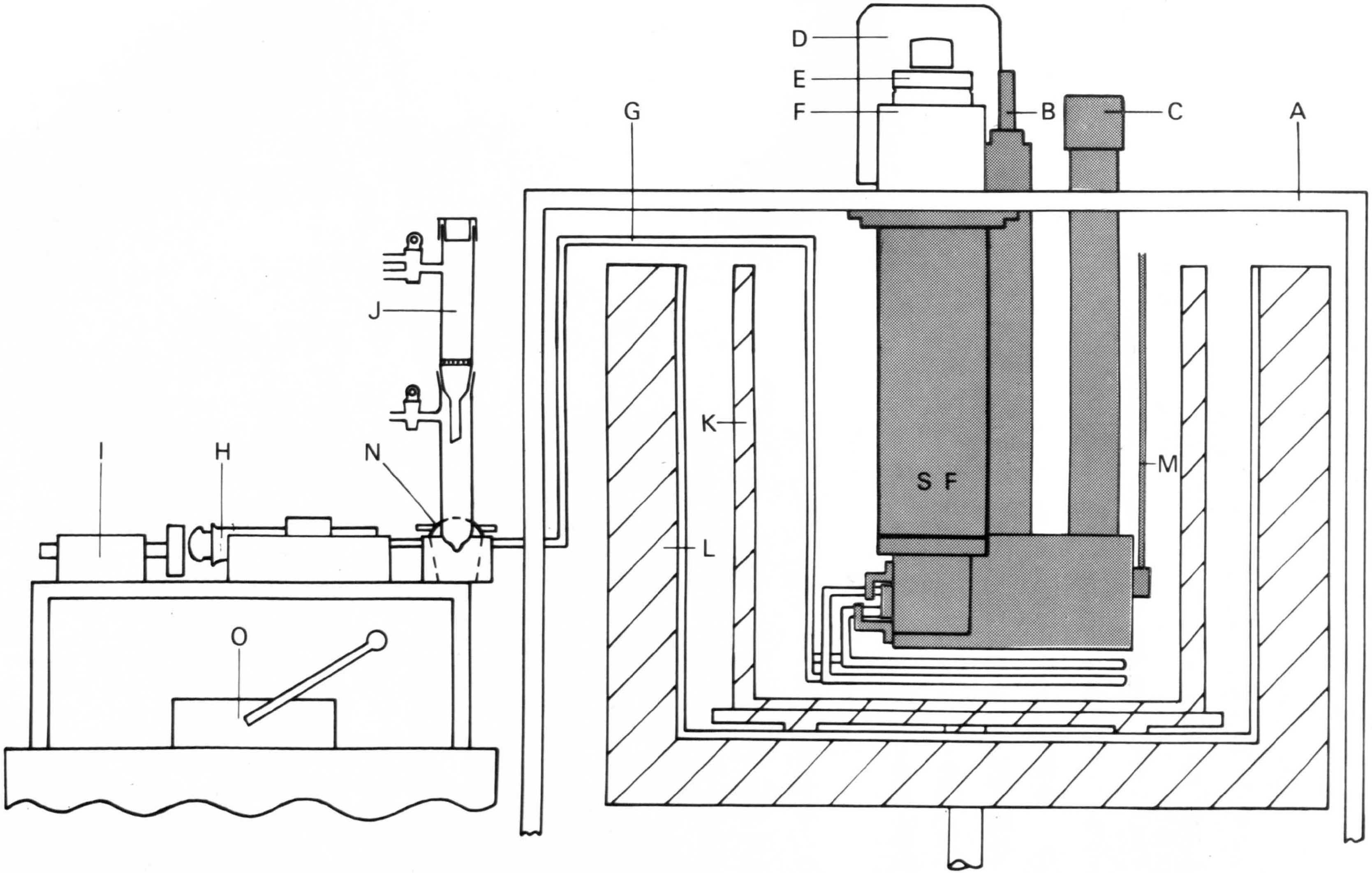
D
E
F
G
B
C
A
J
K
L
M
S F
I
H
N
O

particular, Kel-F will take threads much more successfully than either of the other two plastics, and has the additional advantage for this work of a low temperature coefficient of expansion. The observation block is enclosed on all faces by stainless steel plates which act as light seals for the translucent Kel-F. The solution pathways are shown in Figure 2 (a). They are all of 2 mm diameter. The "blind" holes are closed by Kel-F plugs cemented in position by the epoxy resin "Araldite". The mixer (M, Fig. 2) fits into the front face of the block. The windows are made from quartz rod 8 mm long and 6 mm diameter at their wide face. A cylindrical projection, 2 mm long and of 2 mm diameter, is ground on one end of each window. This projection fits into the 1.45 cm pathlength observation cell. The faces of both ends are ground and polished optically flat. The windows seal onto 0.5 mm thick Teflon gaskets and are held firmly in place by threaded backing pieces (T, Fig. 2 (b)).

The stopping syringe (S, Fig. 3) is positioned on the top face of the observation block, at the bottom of a threaded recess (marked A, Fig. 2 (c)). It is constructed from a 2 ml all-glass syringe with the two ends sawn off and a glass flange, both faces of which are ground flat and square to each other, blown on one end. In position, the syringe sits on a 6 mm diameter silicone rubber "O" ring and is held firmly in place by a threaded tube turned from glass impregnated Teflon (R, Fig. 3). This tube screws down into the Kel-F block and over the stopping syringe. The length of this holding tube is such that as it tightens into position a seal between it and the block is made by compression of a silicone rubber "O" ring, thus keeping thermostat liquid out of the apparatus. A glass impregnated Teflon tube (32 cm x 3 cm), (U Fig. 3) screws onto the outer threads of the syringe holder (R, Fig. 3) and over the stopping syringe, also sealing onto a silicone rubber "O" ring. This design gives easy access to the stopping syringe in order to remove air bubbles and for inspection. The tube (U, Fig. 3) is drilled to half its length with a 20 mm diameter hole and for the remaining half with a 12 mm diameter hole. A 45° shoulder (D,

FIGURE 2

The observation block.

Fig. 2(a) TOP FACE

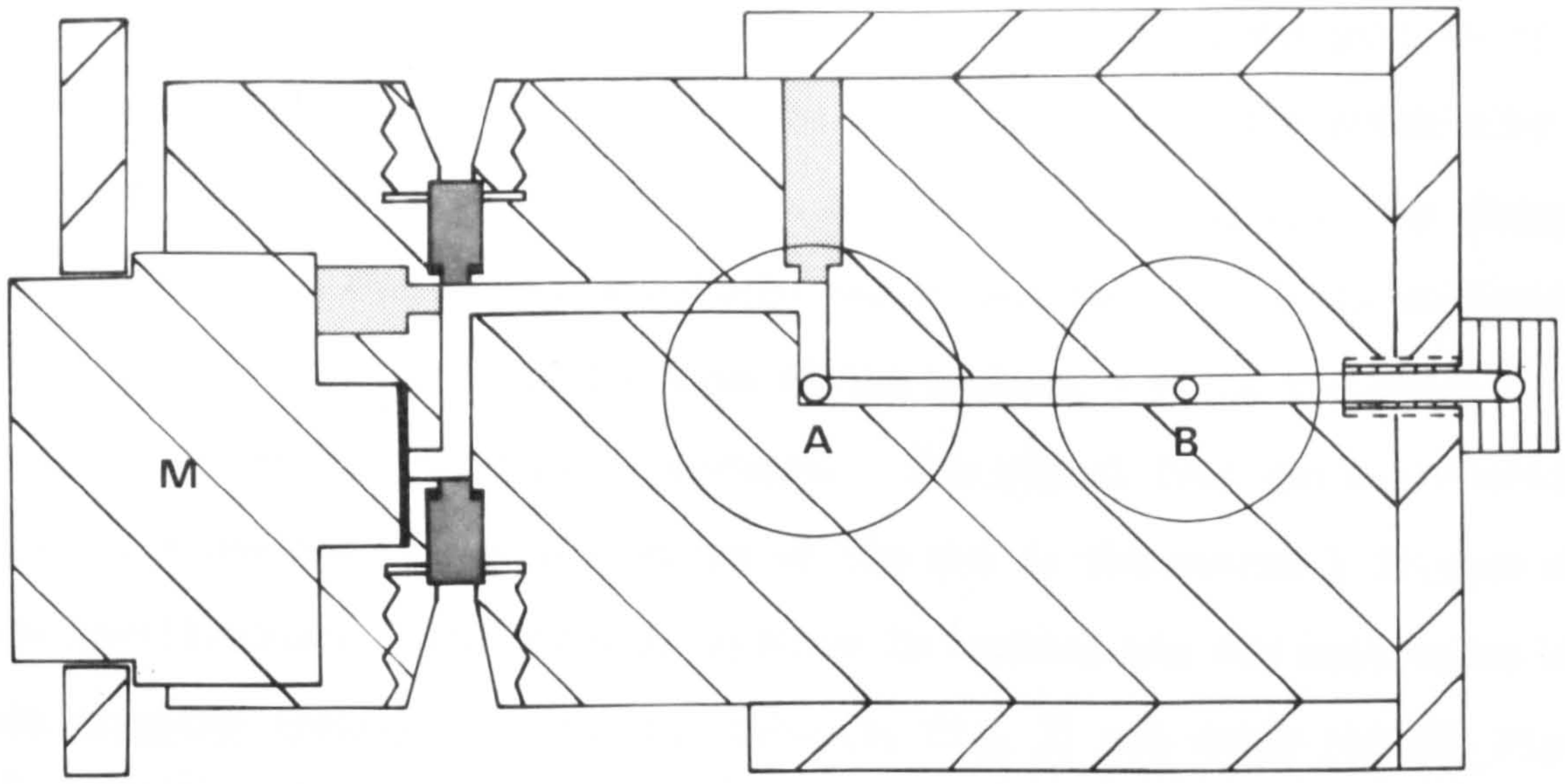

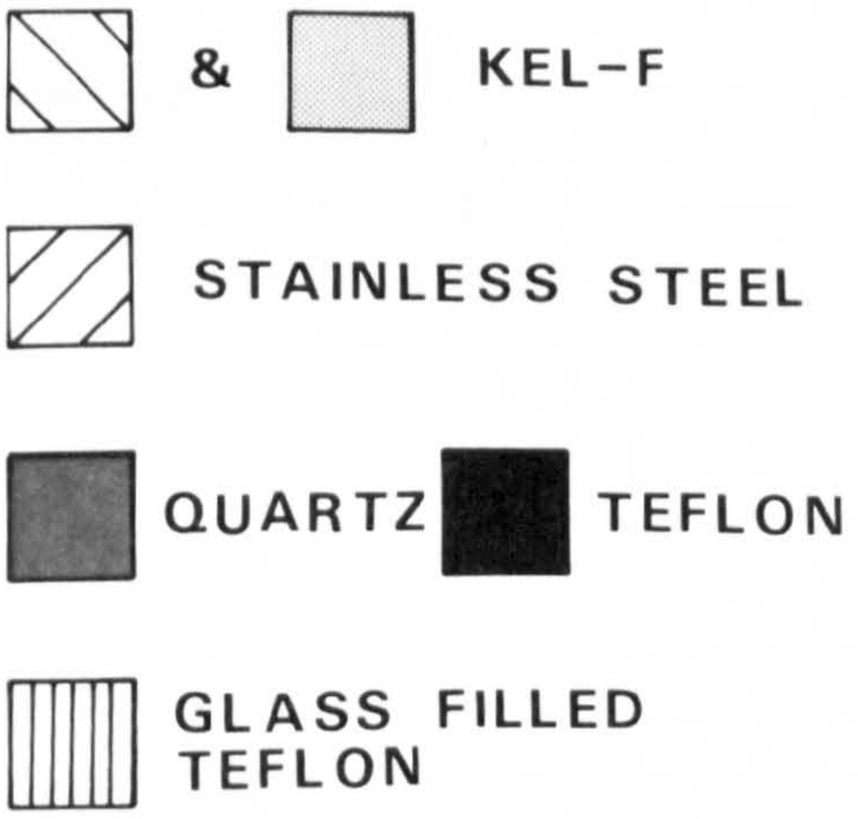

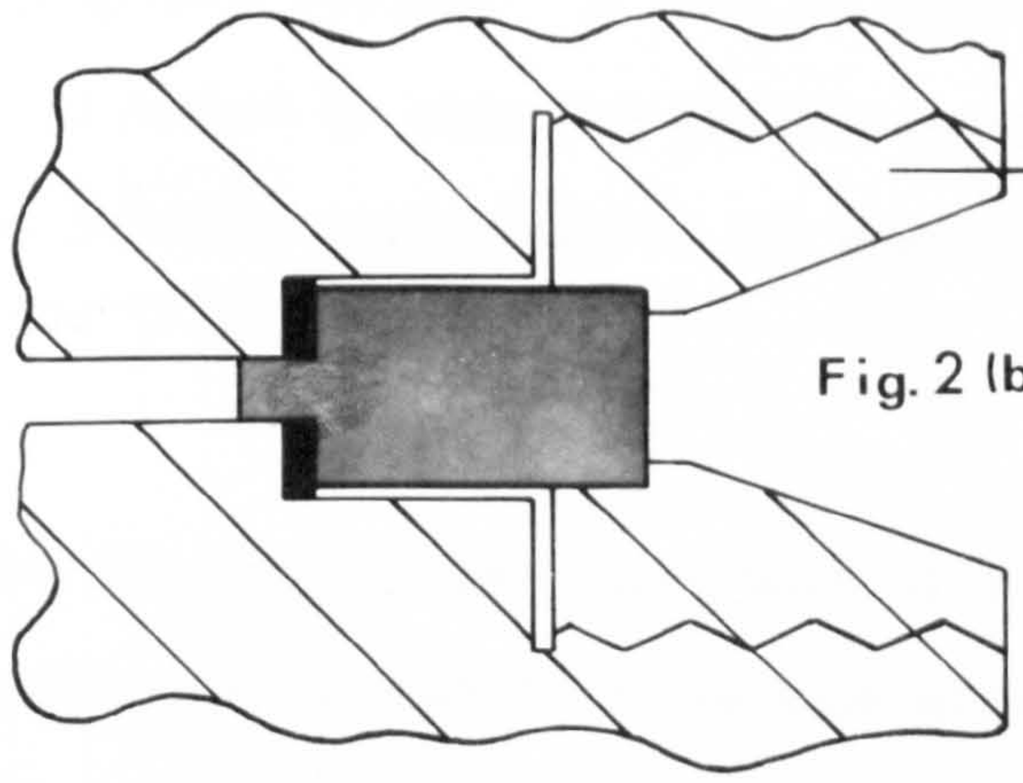

Fig. 2 (b)

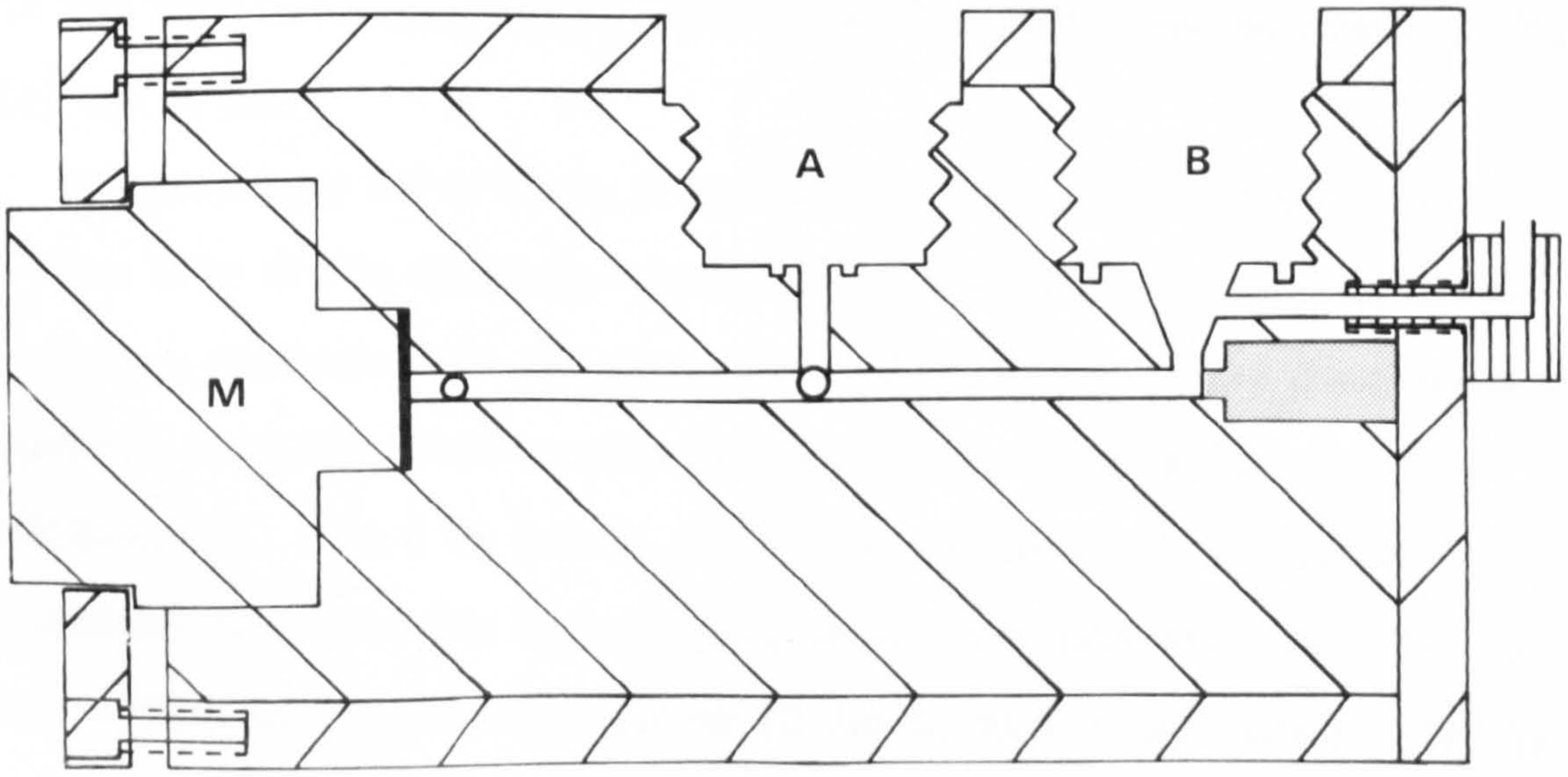

Fig. 2(c) SIDE FACE

Fig. 3) is cut at the junction of the two holes. A perspex rod (C, Fig. 3) of 11 mm diameter, fitted with a short extension of 19 mm diameter whose top surface is inclined at 45°, fits inside the outer tube and up against the shoulder, (D, Fig. 3). The extension acts as a stop to the plunger of the stopping syringe. The rod passes out of the top of the outer tube (U, Fig. 3) and is held in place by a ball-catch (E, Fig. 3). By pressing down on the rod, the stopping syringe can be emptied. A small microswitch (M, Fig. 3), positioned in the base of the perspex rod, is triggered by the rising plunger of the stopping syringe. The signal from the microswitch is fed via wires passing up the centre of the rod to the external trigger of the oscilloscope. The stopping syringe is emptied via the exit valve behind the stopping syringe. The outer tube (W, Fig. 3) and inner rod (V, Fig. 3) are both machined from glass impregnated Teflon. A 1 in 10 taper, on the end of the rod, is pushed into its socket by screwing the aluminium cap down (F, Fig. 3). The expended solution passes out of the apparatus through the waste pipe (K, Fig. 3).

The Mixer

This is a single stage eight jet design, based upon that of Gibson[24], and machined from Kel-F. The main modification to those used previously[13] is that in constructing the mixer in modular form, it is possible to dispense with the need for Gibson's pre-mixer block[24]. The mixer is shown in Figures 4 (a) and 4 (b).

The solutions enter along 2 mm diameter holes (a,a', Fig. 4 (a)). The main body of the mixer is drilled to divide each flow line into two 1 mm holes, which pass to the front part of the mixer. The 2 mm holes are introduced into the mixer on adjacent diagonals, (Fig. 4 (b)), so that after division into 1 mm holes, the latter may surround the direction of the central exit hole (E, Fig. 4 (a)), in an ABAB pattern. Four 0.5 mm holes in each of two parallel planes (C and D, Fig. 4 (a)) are drilled to enter tangentially to the cross-section of the exit hole (E, Fig. 3). One bank of four is inclined anticlockwise and the other bank clockwise. In this way a rotary motion is impressed upon the entering fluid before it

FIGURE 3

The stopping syringe and exit valve.

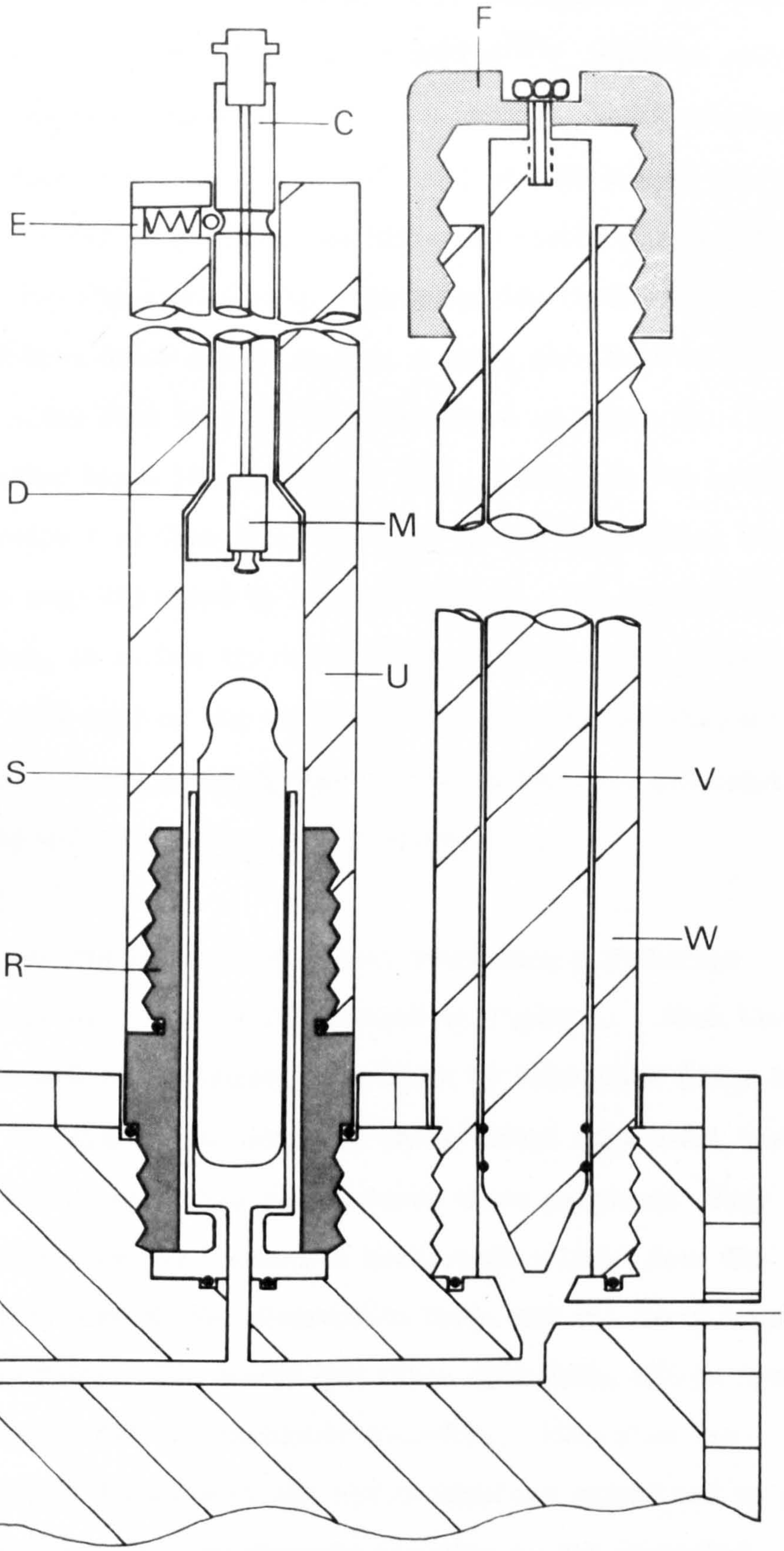
F
C
E
D
M
U
S
V
W
R
K
&
GLASS
FILLED
TEFLON
KEL–F
ALUMINIUM
STAINLESS
STEEL

passes perpendicularly down the exit tube. This arrangement has been shown to improve the speed and efficiency of mixing[10a]. The two sets of jets are placed as close together as possible to reduce errors arising from the different distances that fluid from each bank of jets has to travel. The unwanted parts of the 2, 1 and 0.5 mm holes are closed off by Kel-F plugs cemented in place by "Araldite". The extension containing the jet system is enclosed by a Kel-F cap (H in Fig. 4 (a)), also held in place by "Araldite". The mixer fits into the block as shown in Figure 2. The main body of the mixer has a lip (L, Fig. 4 (a)), which when the mixer is in position, protrudes 1 mm from the front face of the observation block. A metal plate fits over the mixer up against the lip. As this plate is bolted into position, it pushes the mixer firmly against a 0.5 mm Teflon washer (Fig. 7). The exit of the mixer is set 6 mm from the observation tube; a compromise between ensuring that mixing is complete and keeping the time between mixing and observation to a minimum.

The Optical System

As the apparatus was designed for total immersion, a periscope arrangement was adopted. This is illustrated in Figure 5. Each tower (T, Fig. 5) is attached to the observation block by four bolts (only one of which is shown in Figure 5 for clarity) which thread into metal inserts embedded in the Kel-F block. The towers serve three purposes: they suspend the apparatus into the thermostat bath, enable light from the monochromator to pass through the observation tube, and one tower houses the photomultiplier tube. The towers are nylon cylinders, 25.6 cm long, 7.6 cm outside diameter and 4.8 cm inside diameter. This size was dictated by the outside diameter of the photomultiplier shield and by a wall thickness sufficient to give adequate rigidity to the suspended apparatus. One end of each tower is closed by a stainless steel cup (A, Fig. 5) to which a 5 cm square stainless steel block is bolted. Silicone rubber and silicone rubber "O" rings seal the joints. The base plates of the metal blocks (E, Fig. 5) are machined to include a cylindrical rod whose

FIGURE 4

The mixer.

Fig. 4 (a)

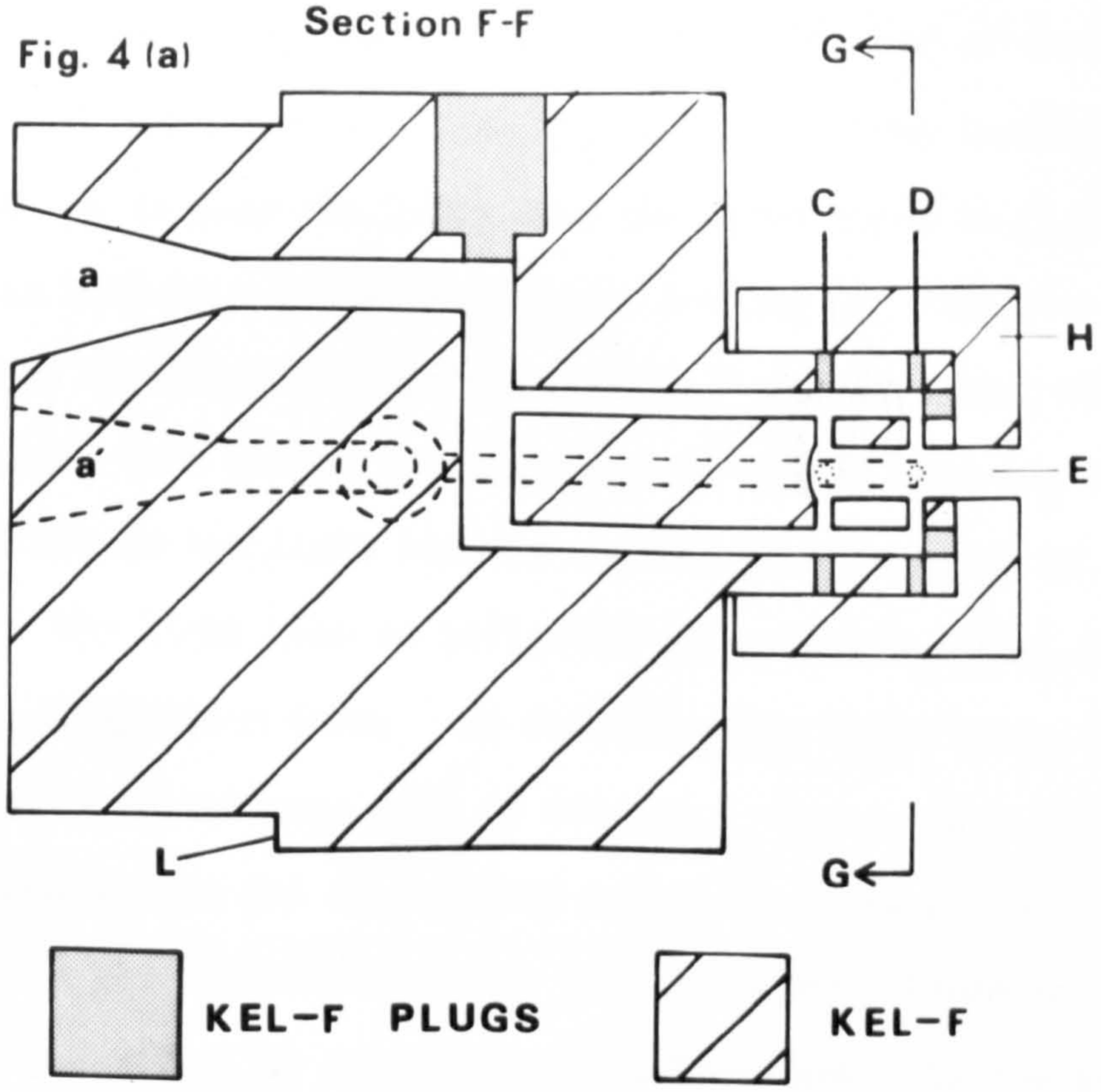

Fig. 4 (b)

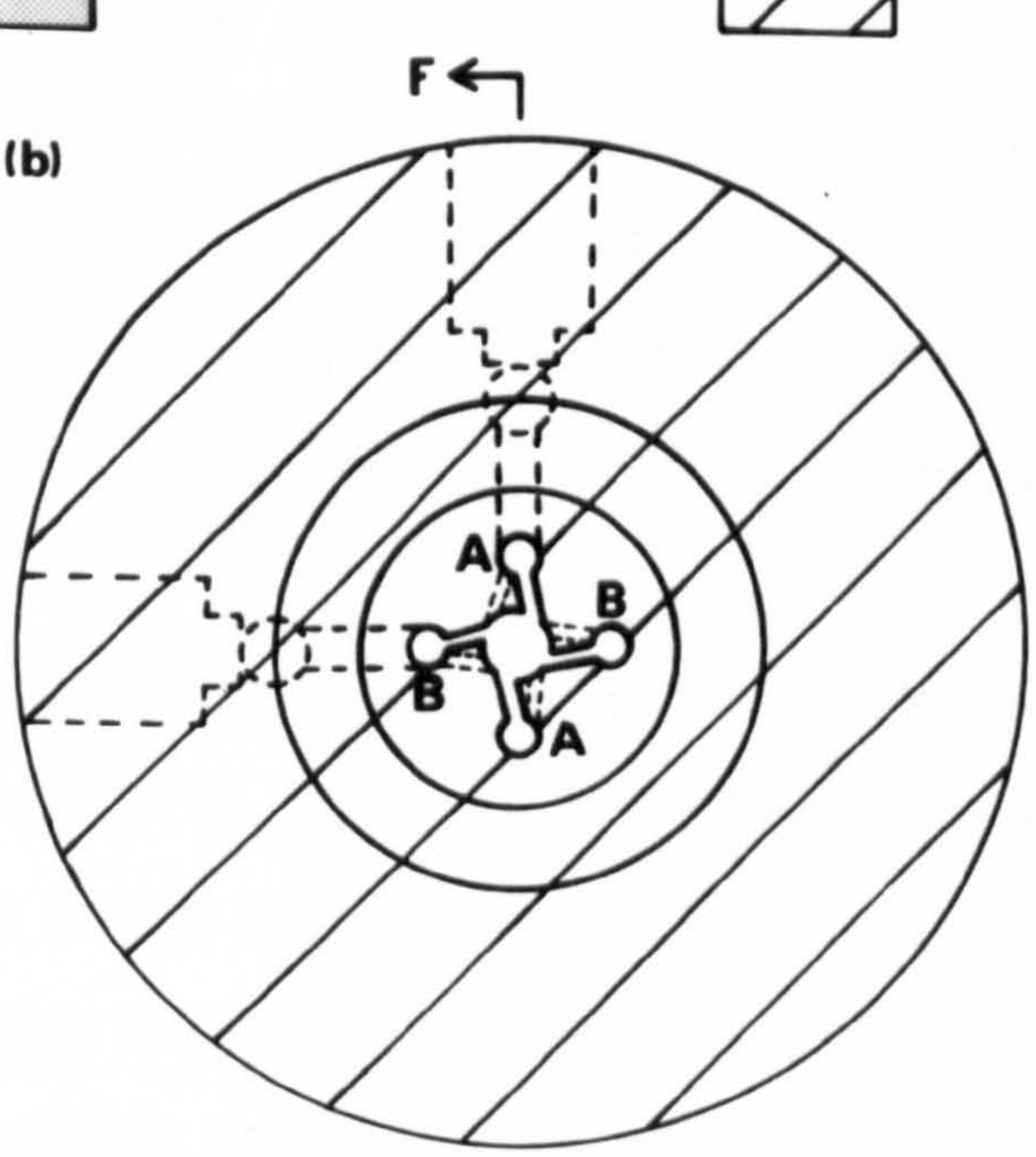

top face is inclined at 45° towards the observation tube. Each rod mounts a front surface aluminiumised mirror. Both U.V. and visible light may be reflected off these mirrors. The monitoring light emerges from the monochromator as an f 3.5 cone. It is reflected off an aluminiumised mirror, (M_1, Fig. 5), set at 45° to the horizontal at the end of the monochromator, through 90° onto a quartz lens (L_1, Fig. 5). The focal length of the lens is such as to pass the light down the first tower as a parallel beam. The lens is held in a cylindrical brass housing (B, Fig. 5), whose height can be varied to "tune" the optical system. At the bottom of the first tower, the light beam passes through a second quartz lens (L_2 Fig. 5) whose focal length brings the light beam to a focus at the centre of the observation tube. The light beam is reflected off mirror M_2 (Fig. 5) and passes through the observation tube. By focussing the light beam, the "stop" effect of the 2 mm entrance hole is reduced. Hence, more light through the observation tube and an improved signal to noise ratio is obtained. After passing through the observation tube, the transmitted light is reflected off mirror M_3 (Fig. 5) into the second tower and onto the photomultiplier face. The photomultiplier (PM, Fig. 5) is held inside a brass tube (S, Fig. 5) which slips inside the second tower. To prevent icing, the high voltage terminals (R, Fig. 5) of the photomultiplier are enclosed in a cylindrical "Tufnol" case (C, Fig. 5) which also supports the photomultiplier.

A collar (G, Fig. 5) fits over the top of each tower and is screwed into a rectangular base plate (F, Fig. 5). The latter fits into the roof of the main stand and is firmly bolted down.

During operation, air, dried and filtered by first passing it through a column of silica-gel, then a one micron air filter and finally a solid carbon dioxide/methanol trap, is blown into the bottom of each tower (at D, Fig. 5). This keeps the optics and photomultiplier face free from condensation. The dry air also passes over the terminals of the photomultiplier.

To ensure completeness of the light seal and as a precaution against

FIGURE 5

Cross-section of the optical system.

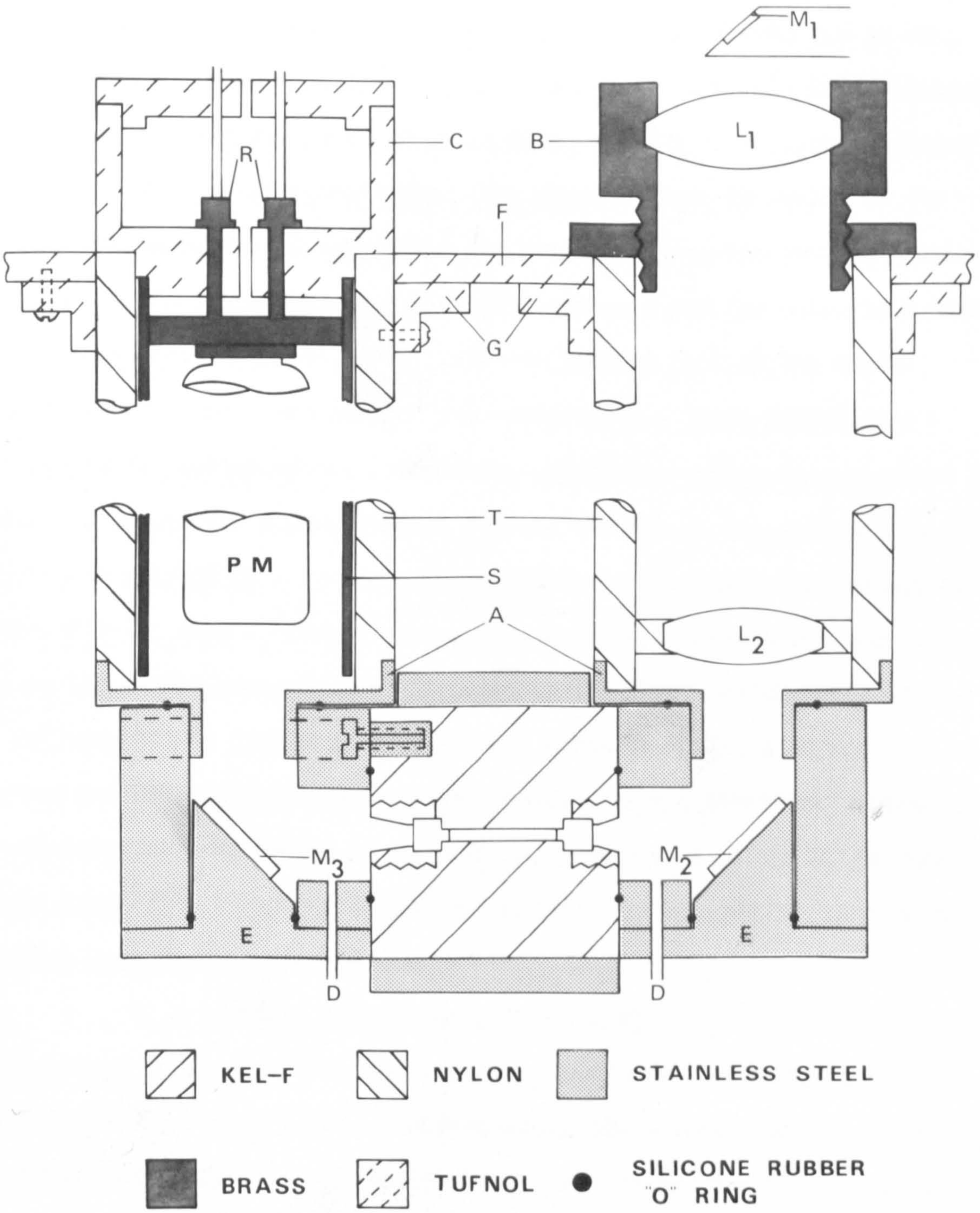
M1
L1
B
C
R
F
G
PM
T
S
A
L2
M3
M2
E
E
D
D
KEL-F
NYLON
STAINLESS STEEL
BRASS
TUFNOL
SILICONE RUBBER
"O" RING

leaks, the entire apparatus is sprayed with a thin coat of silicone rubber.

The Thermostat

The thermostat is based upon the design due to Scott and Brickwedde[85]. It consists of two copper tanks (K, L, Fig. 1), one inside the other. The outer tank, of 33 cm diameter and 35.5 cm depth, is lagged with 7.6 cm of expanded polyurethane foam as insulation. The inner tank is a double walled vessel, 20 cm internal diameter and 32 cm deep, sitting on a tripod to raise it from the bottom of the outer tank. The space between the walls of the inner tank can be evacuated to control the heat loss from the inner to outer tank. In use the inner tank is filled with methanol and the outer tank with solid carbon dioxide/methanol. Temperatures between that of the carbon dioxide/methanol mixture and ambient are achieved by a 150W, 100V heater, positioned at the bottom of the inner tank. The heat output is controlled by a thermistor sensor and a proportional control circuit. The methanol in the inner bath is stirred by a compressed air driven Archimedean screw of 2.5 cm diameter, fitting into a "Tufnol" tube. This stirrer ensures movement of the whole liquid and prevents any streaming of the liquid which might occur if an ordinary paddle type stirrer was used. The temperature is measured by a platinum resistance thermometer, in conjunction with a Wheatstone bridge. The thermometer was calibrated at the melting points of a series of freshly distilled liquids[86]. The resistance was found to be linearly related to the temperature according to the equation :

$$R_T = 1.2068T + 575.27 \text{ (where T is in K)}$$

The temperature may be measured to at least $\pm$ 0.01K and the stability of the bath is better than $\pm$ 0.1K. Unfortunately, the thermal inertia of the apparatus is considerable. About five hours is required for the observation block to come to temperature at the lowest temperatures used. The addition of a commercial refrigerating bath, which could run continuously, would add considerably to the effectiveness of the apparatus.

An early problem of icing of the exposed parts of the stopped-flow apparatus below the roof was greatly reduced by suspending a circular rubber skirt from the roof and using "Velcro" to adhere the skirt to the

sides of the thermostat.

The Inlet System

The inlet system is shown in Figure 6. The drive syringes (A, Fig. 6) are of the 5 ml Everett "Record" all-glass type. The syringes are half embedded in a perspex block (B, Fig. 6). A perfect fit between glass and perspex is made by laying the syringes onto freshly mixed silicone rubber and allowing the rubber to set. The syringes are held in position by a perspex plate (C, Fig. 6) which prevents movement during driving. The syringes are joined to Teflon keyed three-way capillary taps supported in a perspex block (D, Fig. 3). The straight through section of the taps leads on to the stopped-flow apparatus. The third arm joins on to the reservoir tubes which are mounted vertically. The reservoirs have two- and three- way taps on their sides so that dry nitrogen can be flushed through the system. The top sections are sealed by "subaseals" (S, Fig. 6) and are fitted with glass sinters (T, Fig. 6). Dry or oxygen sensitive solutions can therefore be handled in the reservoirs and filtration prevents any solids being introduced into the flow line. The flow line consists of 2 mm bore glass capillary tubing extending from the three-way taps up and over the thermostat tanks (G, Fig. 1), and down to just below the bottom of the apperatus (Fig. 1). Each glass tube is coiled once (diameter ca. 15 cm) beneath the apparatus (Fig. 1) and then passes into the mixer. The coils ensure an adequate supply of thermostated reagents, enough for about twenty runs. Glass tapers (A, Fig. 7), on the end of the glass tubes, fit into the corresponding sockets machined in the mixer. A metal bracket (B, Fig. 7) fits over a shoulder carefully ground onto each glass tube about three centimetres from the taper. As the metal bracket is bolted up to the front stainless steel plate, it pulls the taper firmly into the socket (Fig. 7). A thin layer of silicone rubber seals the glass to the Kel-F.

Peripheral equipment used with this stopped-flow apparatus is summarised below:

Oscilloscope. Tektronix storage oscilloscope, type 564, with 2A63

FIGURE 6

The inlet system.

GLASS

TEFLON

PERSPEX

"SUBASEAL"

GLASS SINTER

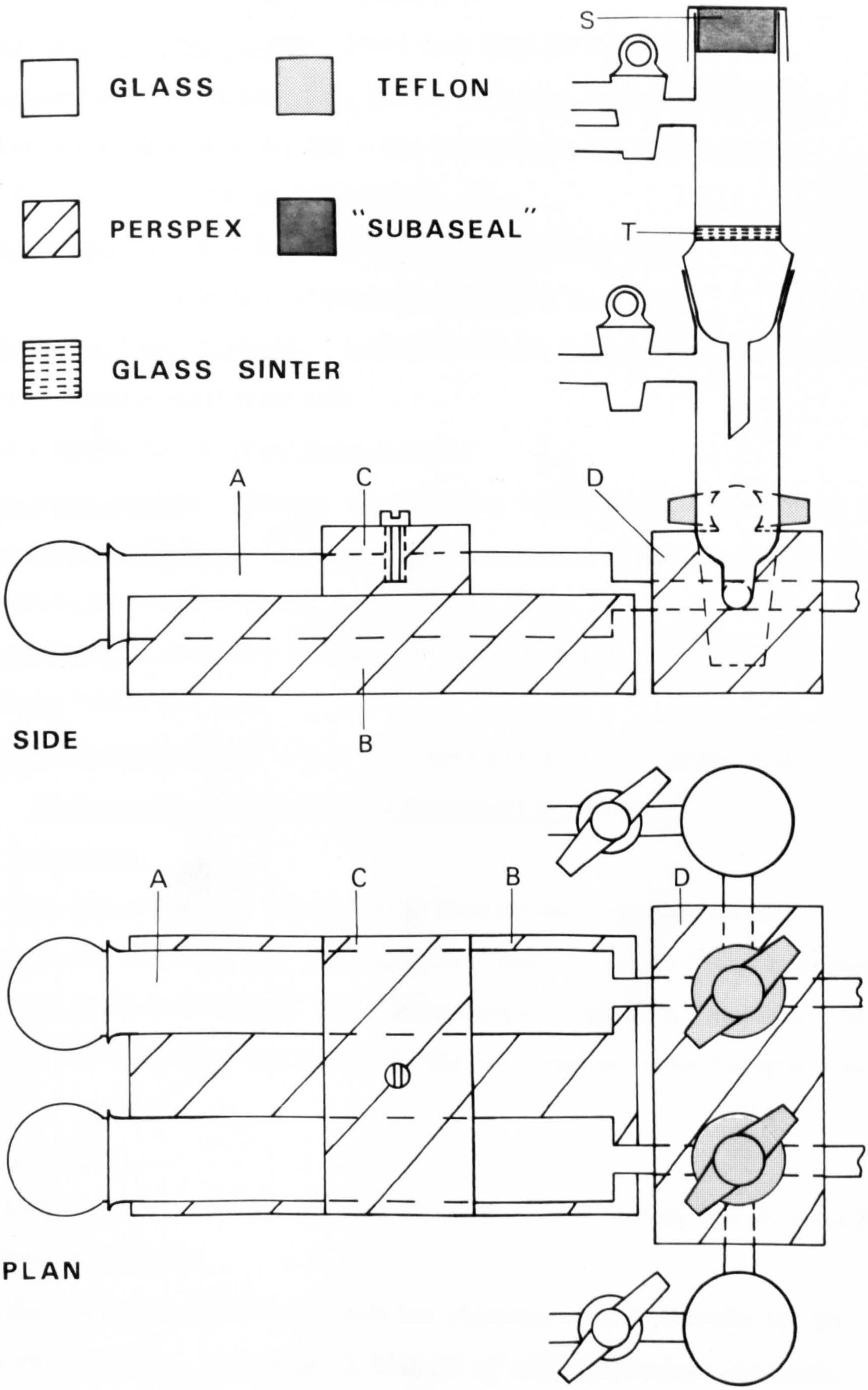

SIDE

PLAN

differential amplifier and 2B67 timebase.

Photomultiplier. E.M.I. type 9529B (quartz end window). All dynodes are utilised, connected by 100K resistors.

Photomultiplier Power Supply. Fluke type 412B (0 - 2.1 kV).

Monochromator. Baush and Lomb, fitted with high intensity gratings, Catalogue No. 33 - 86 - 01, 400 - 180 nm for U.V. and Catalogue No. 33 - 86 - 02, 800 - 350 nm for visible.

Light Sources. U.V. - Baush and Lomb 45W deuterium lamp.

Visible - Silvania 45W Tungsten lamp.

Light Source Power Supplies. U.V. lamp - 0.6A constant current stabilised, built by Gronson Electronic Ltd.

Visible lamp - Six 6V Osram accumulators.

Oscilloscope Camera. Telford type A, using Polaroid 46-L transparency film.

Temperature Controller. Accuron Ltd. Temperature Controller providing proportional control over the range 193K to 283K.

Syringe Drive. Hydraulic Actuator, circuit type A 8 - LT8/15, Armstrong Patent Co. Ltd.

Emitter-follower Circuit. This was constructed to the design used previously[13].

2.2. Tests on the low temperature stopped-flow apparatus

Cavitation

This phenomenon was tested for by flowing solvents through the apparatus and observing the light output. Had cavitation been occurring, large and sharp decreases in light transmission would have resulted. No evidence for cavitation was observed, the oscilloscope trace being a straight line.

Flow rate

It was not possible to measure the flow rate directly, but an estimate was found as follows:

The fast reaction of hydroxide ion reacting with dichromate ion in water was studied. The internal trigger of the oscilloscope was used, with the trigger level set as close to the infinity of the reaction as possible. An example of the resulting trace appears in Figure 8 (a).

FIGURE 7

Method of joining glass tubing to mixer.

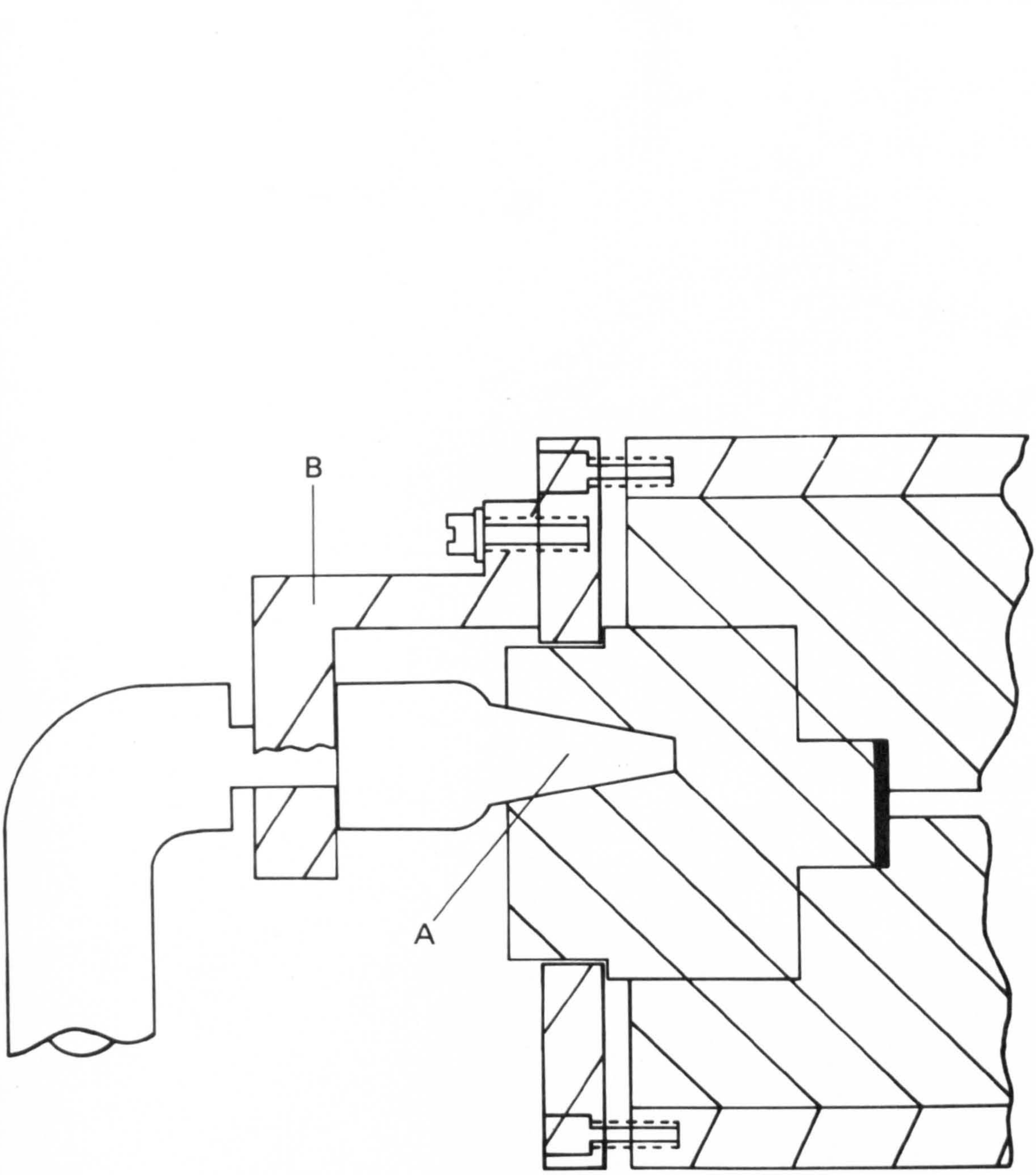

STAINLESS STEEL

KEL-F

GLASS TUBING

TEFLON

The time taken to reach the break in the plateau, where the reaction starts, is the time to the "stop". Knowing the volume of reagents used and the dimensions of the flow line it was possible to calculate the average velocity. The observed velocity with water at room temperature was over 4 m/s. However, the above observation takes no account of acceleration time, and so is only a minimum estimate.

Mixing tests[10a, 41]

The apparatus was checked for 1:1 mixing by optical density measurements of alkaline chromate solutions and found to be satisfactory.

The mixing efficiency was tested in two ways. At room temperature, with water as solvent, a 20% ammonium sulphate solution in one drive syringe was flowed with water in the other. When poorly mixed, this solution becomes turbid due to multiple refractions, which leads to low light transmission. The trace obtained was very erratic for the first 15 ms or so, but then became a straight line. The initial irregularities were due to poor mixing at the low velocity at the start of flowing, but the mixing rapidly becomes efficient. As the "stop" is known to occur after about 50 ms, it can safely be assumed that the mixing is adequate by the time observation of a reaction takes place.

The mixing efficiency in methanol solutions was tested by flowing a methanolic NaOH solution containing a trace of phenolphthalein with a methanolic solution of HCl of equivalent titre. The neutralisation reaction was followed at 550 nm. At all temperatures, down to 225K, the trace was a straight line about 16 ms after flow began. The rate of this reaction is beyond the range of flow methods even at 225K and so the trace should coincide with the infinity reading of the reaction as soon as the flow rate is high enough. Any deviations from adequate mixing would have appeared as irregular fluctuations on the oscilloscope trace.

The stopping time

The stopping time could not be measured directly, but examination of the "break" of typical traces, e.g. Figure (8a), showed that the stop was sharp and that the fluid came to rest in about 1 ms.

FIGURE 8

Figure 8(a)

Photograph of oscilloscope trace showing flushing out, attainment of maximum flow velocity and subsequent reaction after flow has stopped. The reaction is

$$Cr_2O_7^{2-} + OH^- \longrightarrow HCrO_4^- + CrO_4^{2-}$$

$[K_2Cr_2O_7] = 1 \times 10^{-3}$ mol l^{-1}, $[OH^-] = 0.04$ mol l^{-1}

I = 0.1 (KNO_3), λ = 475 nm

Sensitivity = 0.1V/division

timebase = 10 ms/division.

The straight line below the reaction trace is the infinity reading of the reaction.

Figure 8(b)

Example of the temperature difference artifact in the low temperature stopped-flow apparatus.

The injected methanol was approximately 65K warmer than the observation block.

The upper straight line is 0% transmission, and the lower line 100% transmission.

Sensitivity 0.2V/division

Timebase 0.5 s/division.

Figure 8 (a)

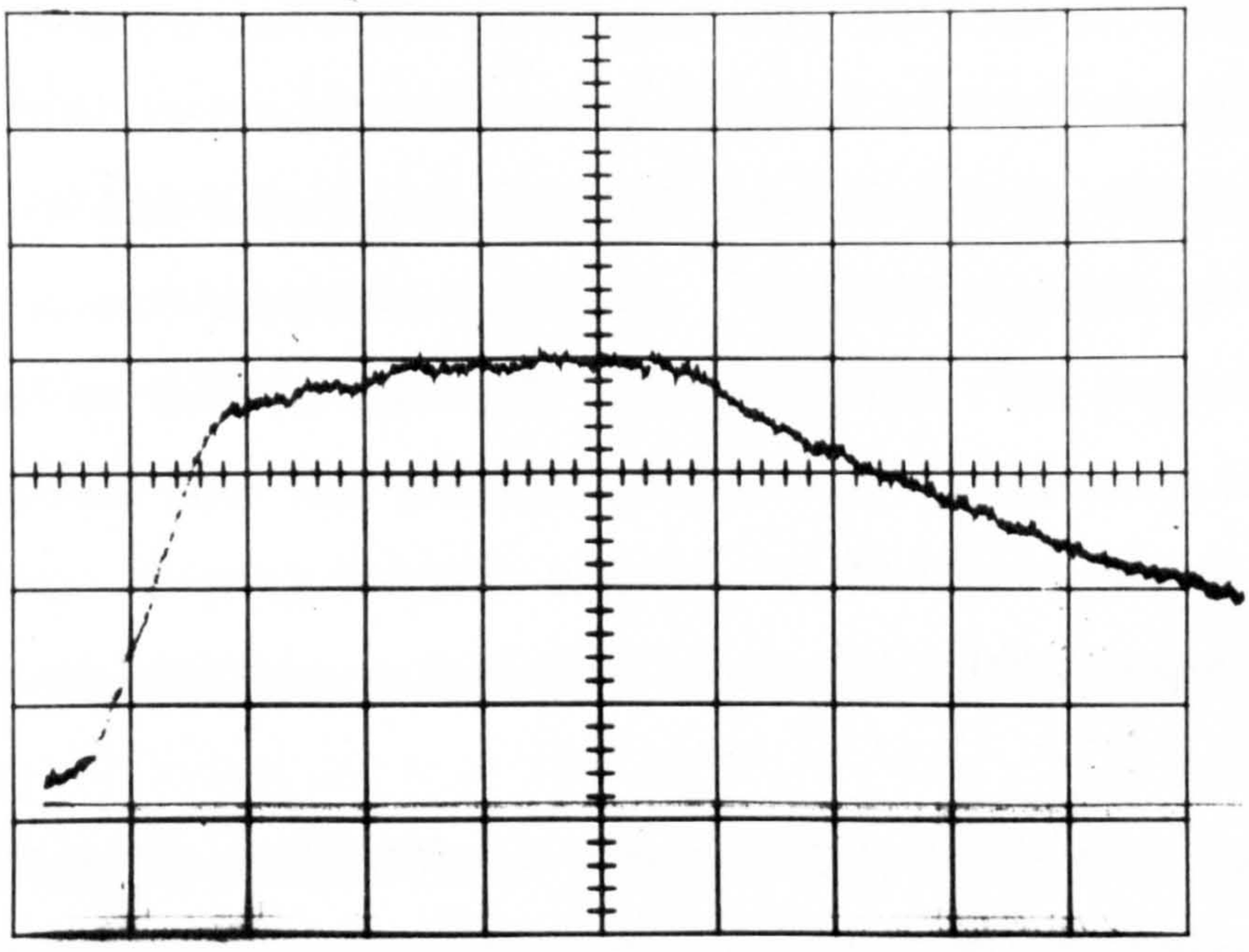

Figure 8 (b)

The dead-time

This is the time taken to mix the reactants, pass them to the observation tube and stop the flow. At room temperature it was measured by taking the second-order reaction between dichromate ion and hydroxide ion[87] under pseudo-first-order conditions with hydroxide in excess. An hydroxide concentration was chosen such that the half-life was ca. 0.1s. The initial optical density, which under these conditions corresponds essentially to zero reaction, was noted. The hydroxide ion concentration was increased so that the half-life was about 5 ms. The initial optical density was lower than that previously because of the reaction lost during the dead-time. Knowing the rate constant for the fast reaction and the two initial optical densities, a dead-time of 4.1 ± 0.3 ms was calculated.

Kinetic Runs

To confirm the suitability of this apparatus for kinetic measurements, some data of Wilkins and Moore[87] for the reaction between hydroxide and dichromate ions were reproduced.

2.3. Operation and Performance

Anhydrous reagent solutions are injected into the reservoirs through the "Subseals" by hypodermic syringes. Each run requires about 0.3 ml of each reagent. However, the minimum volume required for each reaction condition is about 40 ml to ensure that flushing out of the driving syringes and glass coils with fresh solution is complete. The solutions are left to thermostat for at least one hour. Kinetic runs down to 221K have been performed. The overall performance of this apparatus is very similar to the Gibson stopped-flow used in this laboratory[13]. First-order rate constants of up to 150 s^{-1} have been successfully measured. A typical set of oscilloscope traces and the corresponding rate plots are illustrated in Figure 9, which shows the excellent reproducibility attainable.

The signal from the photomultiplier is taken to the oscilloscope via an emitter-follower circuit[13]. The anode current of the photomultiplier is monitored using this circuit, and high frequency noise can be attenuated

using an R/C filter circuit. The circuit also generates an adjustable "backing off" voltage which is applied to the second input of the oscilloscope differential amplifier. A low range of photomultiplier anode current is employed (2-10μA). Photomultiplier voltages in the range 600-700V were found to be convenient. When using the R/C filter circuit to reduce noise on traces, care was taken to ensure that the time constant did not exceed 5% of the half-life of the reaction being measured, to ensure no distortion of the traces occurred[24]. The amplifier sensitivity and time base of the oscilloscope were calibrated using the oscilloscope's internal standard.

As mentioned previously, the apparatus has considerable thermal inertia. To test whether the apparatus has come to temperature, an interesting effect that had been observed with methanol solution is used. Both the thermostat liquid and the solvent in the reservoir coils attain the desired temperature very quickly, but the observation block initially lags behind. If methanol at the temperature of the thermostat is flowed into the unthermostated observation block, a bowed trace results (Figure 8 (b)). The trace is bowed upwards if the block is warmer than the methanol and downwards if the block is cooler. The apparent change in absorbance reaches a maximum in about 0.5 seconds and disappears in the course of about 7 seconds. If both the block and the methanol are thermostated, a straight line results. This artifact was later reported by Gibson[8d] with water near to room temperature. He attributed it to the establishment of a temperature gradient across the liquid after stopping. There is a corresponding gradient in refractive index with an effect equivalent to a lens. As the whole liquid equilibrates the lens effect disappears.

2.4. Calculation of Results

All kinetic runs carried out with the low temperature stopped-flow apparatus were performed under pseudo-first-order conditions. Two to four runs under the same reaction conditions were recorded on the oscilloscope screen, with a small vertical displacement between each one (Figure 9 (a)).

FIGURE 9

Figure 9(a)- Photograph of oscilloscope screen showing three consecutive kinetic runs.
Sensitivity 50 mV/division, timebase 0.1 s/division.

Figure 9(b) - Computer plotter output showing the rate plots of the above runs.
Computer program SFDATA (Appendix).
Each plot is separated from its predecessor by 0.1 log units.

The reaction portrayed is the formation of the mono-(1,10-phenanthroline)manganese(II) ion in anhydrous methanol.

$[Mn^{2+}] = 1.01 \times 10^{-3}$ mol l^{-1}

$[phen] = 5.08 \times 10^{-5}$ mol l^{-1}

Temperature = 251.6K, I = 0.2 ($NaClO_4$), λ = 300 nm.

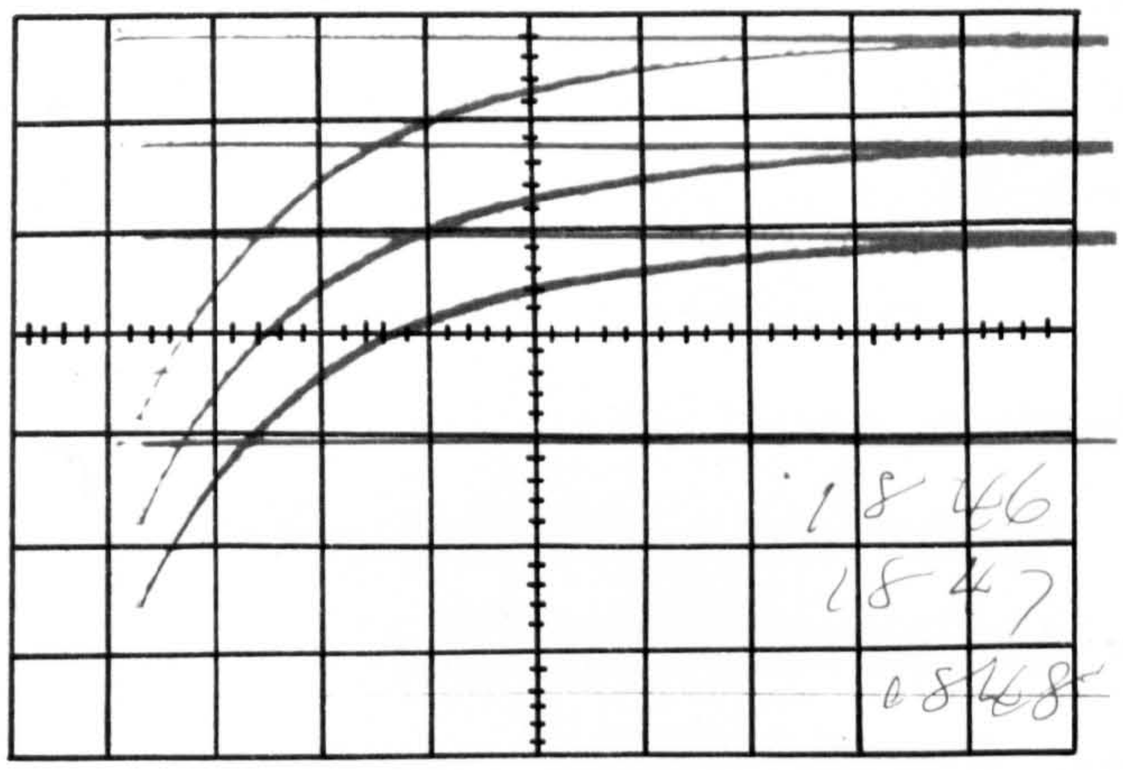

SFDATA RUN NO 1846 1847 1848

1846 +
1847 ◇
1848 X

LOG [D(INF) - D(T)] + 2

1.900
1.800
1.700
1.600
1.500
1.400
1.300
1.200
1.100
1.000
0.900
0.800
0.700
0.600

0 50 100 150 200 250 300 350 400 450 500

TIME / MS

The screen was photographed and the resulting transparency projected by means of a photographic enlarger. The reaction curves were traced onto graph paper and reduced to sets of (x,y) co-ordinates by manual measurements. The sets of co-ordinates, together with factors to convert x readings to time, and y deflections to transmission values were analysed by computer program SFDATA. A listing is given in the Appendix.

The computer program carries out the following operations:

a) Conversion of transmission to absorbance values.

b) A linear least-squares determination of the best straight line fit to a plot of ln $(D_t - D_{inf})$ versus t (where D_t and D_{inf} are the absorbances calculated for time t and infinity respectively). For a first-order reaction ln $(D_t - D_{inf}) = -kt + C$.

c) Print out of the rate constant, k, with its associated error.

d) Presentation of the rate plot derived above by means of a digital plotter accessory (see Figure 9 (b) for an example of this output).

The rate plots of every run were examined since it was found by experience that quite marked curvature could be exhibited with little effect on the magnitude of the calculated error. The results of any run showing curved rate plots were rejected.

2.5. Activation parameters

Computer program ACTPAR (Appendix) was used for the calculations. The Arrhenius factors E_a (activation energy) and A (frequency factor) from the relation, $k = A\exp(E_a/RT)$ were calculated from a linear least-squares best fit line to a plot of weighted values of ln k versus 1/T. Values of ΔH^* and ΔS^* from the transition-state theory equation, $k = (RT/Nh)\exp(\Delta S^*/R).\ \exp(-\Delta H^*/RT)$, were derived for 298.1K by means of the relations:

$$\Delta H^* = E_a - RT$$

$$\Delta S^* = R(\ln A - \ln(RT/Nh) - 1)$$

These equations apply for both uni- and bimolecular reactions in solution[28b].

2.6. Treatment for error

In this work, all errors are quoted as ± (one standard deviation). Data (where appropriate) were weighted by the reciprocal of the square of its associated error. The formulae used in calculations and computer programs are to be found in Beer's monograph[88].

CHAPTER 3

THE KINETICS AND MECHANISM OF THE FORMATION AND DECAY OF PEROXYNITROUS ACID IN PERCHLORIC ACID SOLUTION, AND LEAST-SQUARES ANALYSIS OF SPECTROPHOTOMETRIC DATA FOR SERIES FIRST-ORDER REACTIONS

3.1. Introduction

Peroxynitrous acid has been established as the intermediate of reactions (3.1) and (3.2) largely by stabilisation at a high pH as the peroxynitrite anion[89,90].

$$HNO_2 + H_2O_2 \longrightarrow HOONO + H_2O \qquad (3.1)$$

$$HOONO \longrightarrow NO_3^- + H^+ \qquad (3.2)$$

The unstable peroxynitrous acid has been estimated kinetically[91] to have a pK_a of 6.6 and an impure solid peroxynitrite salt has been prepared[92]. There have been several previous kinetic investigations[89,92-5] of these two reactions above pH4 (Table 1), where the rates can be measured by conventional methods, but an extension of these studies to higher acidities was prevented on account of the rapidity of the reactions. It was found relatively easy to extend these studies to higher acidities by using the stopped-flow method, and it was possible to establish the nature of an additional acid catalysed pathway for the decomposition of peroxynitrous acid, which previous workers had postulated to be present[91].

The formation of peroxynitrous acid was also studied at higher acidities to gain information about the various species postulated to be formed in aqueous acidic solutions of nitrous acid[96-7].

The three species which are found to be most reactive in solutions of nitrous acid are N_2O_3, $H_2NO_2^+$ and NO^+, which are formed according to the following equilibria (in the presence of co-ordinating anions, X^-, a further species, NOX, is possible).

$$2HNO_2 \rightleftharpoons N_2O_3 + H_2O \qquad (3.3)$$

$$HNO_2 + H^+ \rightleftharpoons H_2NO_2^+ \quad \text{rapid } K_1 \qquad (3.4)$$

$$H_2NO_2^+ \underset{k_{-2}}{\overset{k_2}{\rightleftharpoons}} NO^+ + H_2O \qquad (3.5)$$

Mechanistically, it is relatively easy to detect N_2O_3 as the attacking species, since in this case, the rate law is then of the form:

$$\text{Rate} = k\,[HNO_2]^2\,[\text{substrate}]$$

However, it is not so easy to distinguish between $H_2NO_2^+$ and NO^+ as the reactive intermediates, since under many conditions both reactants give rise to a rate law of the form:

$$\text{Rate} = k\,[H^+]\,[HNO_2]\,[\text{substrate}] \qquad (3.6)$$

When $H_2NO_2^+$ is involved $k = k_4K_1$, where k_4 is the rate constant for $H_2NO_2^+$ attacking the substrate. If NO^+ is the reactive intermediate, the rate constants associated with equilibrium (3.5) become important and water competes with the substrate for NO^+. Definition of k_3 as the rate constant for the reaction between NO^+ and substrate, and application of the steady state approximation to NO^+ gives:

$$-d[\text{substrate}]/dt = \frac{k_3k_2K_1[H^+]\,[HNO_2]\,[\text{substrate}]}{k_{-2}\,[H_2O] + k_3\,[\text{substrate}]} \qquad (3.7)$$

Under conditions where $k_{-2}[H_2O] \gg k_3\,[\text{substrate}]$ this law reduces to equation (3.6) with $k = k_3k_2K_1/k_{-2}\,[H_2O]$. Since in aqueous solution $[H_2O] \gg [\text{substrate}]$, in most cases (unless $k_3 \gg k_{-2}$) equation (3.6) will be the rate law observed. However, in the case where $k_3\,[\text{substrate}] \gg k_{-2}\,[H_2O]$ then equation (3.7) reduces to:

$$-d[\text{substrate}]/dt = k_2K_1\,[H^+]\,[HNO_2] \qquad (3.8)$$

Under these conditions the rate determining step is the formation of NO^+ according to reaction (3.5) and the rate of reaction becomes independent of the substrate concentration. Cases where this behaviour has been observed have been reviewed[98]. In all of these cases interpretation of the results suffers from the possible complication[98] that buffer anions, (X^-), were present which might interfere by reacting with $H_2NO_2^+$ to give NOX rather than NO^+.

Table 1

Resumé of kinetic data of reactions (3.1) and (3.2)

T/K	Medium and I	Formation.[a] Reaction (3.1)	Decay.[a] Reaction (3.2)	Notes	Ref.
292.1	Varied (SO_4^{2-})	$k \simeq 1.5 \times 10^2$		Rate = $k[H^+][H_2O_2][HNO_2]$	89
274±1	0.5 (Cl^-)		$k_{1d} = 0.1$	pH 4 - 9	
				$K_a = 2.5 \times 10^{-7}$	91
298.1	0.25		$k_{1d}/K_a = 5.7 \times 10^8$	pH > 11	
				$K_a < 10^{-8.3}$ at 275K	92
298.1	0.3 mol^{-1}	$k_2 = 3.5 \times 10^8$		Eqn.(3.7) applies	
	(PO_4^{3-})	$k_3/k_{-2}[H_2O] = 2.4$		pH 4 - 6	93
298.1	PO_4^{3-} [b]	$k^1 \simeq 3 \times 10^7$		Rate = $k^1[H^+][HNO_2]$[c]	94
				pH 7.08; $[H_2O_2] = 1.07$ mol l^{-1}	
274	b		$k_{1d} = 0.1$	pH unknown	95
273.7	1.0($NaClO_4$)	$k_3/k_{-2}[H_2O] = 2.32$	$k_{1d} = 0.053$	Eqn.(3.7) applies	This
		$k_2K_1 = 617$	$k_{2d} = 0.60$	pH < 2	work[e]

a Units are mol l^{-1} and s^{-1} b Ionic strength not quoted c Order with respect to $[H_2O_2]$ not established

d $\Delta H^*(k_{1d}) - \Delta H(K_a) = 12.5$ kcal mol^{-1} $\Delta S^*(k_{1d}) - \Delta S(K_a) = 26$ cal $mol^{-1}K^{-1}$ e $\Delta H^*(k_{1d}) = 19.6$ kcal mol^{-1};

$\Delta S^*(k_{1d}) = 7.4$ cal mol^{-1} K^{-1}

In the present reaction Halfpenny and Robinson[89], from initial rate studies, found the rate law (3.6) to hold at low peroxide concentrations, but Anbar and Taube's[93] results at higher peroxide concentrations, in the region pH 4-6, followed the rate law (3.7). Moreover, at high peroxide concentrations of about 4 mol l^{-1}, the latter workers obtained a limiting rate in agreement with equation (3.8) and, therefore, ascribed the reaction to attack of H_2O_2 on NO^+. However, it has been suggested that the phosphate ion used as a buffer in Anbar and Taube's experiments may have interfered in this case[99].

Therefore, to try to resolve this ambiguity, the formation of peroxynitrous acid was studied in the absence of interfering anions, and at higher acidities where the formation of NO^+ is expected to be more important[98].

The spectrum of the peroxynitrite anion has been reported[92] but not that of peroxynitrous acid. In this work the latter's spectrum was obtained for the first time using a continuous-flow mixing cell.

3.2. Experimental

Materials. Sodium nitrite was A.R. grade. It was dried at ca. 383K before use, and solutions were prepared by weight. Solutions of A.R. hydrogen peroxide were standardised by ceric sulphate titration[100]. Sodium perchlorate was prepared by careful neutralisation of A.R. sodium carbonate with A.R. perchloric acid, followed by boiling to remove CO_2. These solutions were standardised by evaporation at ca. 393K and weighing of the $NaClO_4$ residue.

Kinetics. The stopped-flow apparatus was a modified Gibson-Milnes machine, which has been described elsewhere[13]. This equipment was found to be more convenient than the low temperature apparatus described in Chapter 2, but both machines were found to give identical results. Temperature control was ± 0.1K.

3.3. Results

Kinetics. All experiments were carried out under pseudo-first-order conditions, with $[H^+]$ and $[H_2O_2]$, concentrations in the range 0.01 to 1.0 mol l^{-1}, in large excess over $[HNO_2]$ (ca. 10^{-3} mol l^{-1}). To avoid the slow

decomposition of nitrous acid solution[101], the reactions were initiated by mixing the nitrite ion solution with a solution containing hydrogen peroxide and perchloric acid. Both of these solutions were adjusted to an ionic strength of 1.0 with sodium perchlorate. At the lower acidities allowance was made for the small amount of acid consumed by nitrite ion in estimating the free acid concentrations listed in Tables 2 and 3. The pK_a of nitrous acid (3.002) reported[101] at I = 1.0 ($NaClO_4$) and 298.1K was used for this purpose.

Under the conditions of the experiments, reaction (3.2) commences before reaction (3.1) has completely ended, and it became necessary to take into account the slower decay process in estimating the rate constants for the rapid formation. To enable this to be done reaction (3.2) was studied first. Kinetics of reaction (3.2). The reaction was studied at 303 nm where the absorbance first increases rapidly due to reaction (3.1), and then decreases at a slower rate (reaction (3.2)). This behaviour is consistent with the known spectra of the reactants and products, and the spectrum of the intermediate peroxynitrous acid, as reported later. The pseudo-first-order rate constants for the decay process were readily obtained in the usual way from the final part of the absorbance-time curve, where reaction (3.1) is complete. Good first-order rate plots were obtained in all cases for at least three half-lives. The rate of the reaction did not vary upon changing the concentration of H_2O_2 by a factor of ca. 5, or by adding a ten-fold excess of nitrate ion over nitrite. The results are collected in Table 2, the rate constants being an average of 2 - 4 estimations at each condition. Figure 10 shows how the observed rate constants vary linearly with the acidity. A least-squares analysis of the results, using computer program LSAD (Appendix), at 273.7K gives:

$$10^2 k_d = (5.27 \pm 0.10) + (59.6 \pm 0.8)\ [H^+]\ s^{-1} \quad (3.9)$$

Some runs were carried out under the same conditions but in a 0.5 mol l^{-1} phosphate buffer at pH 2.33. The value of k_d under these conditions ($5.44 \times 10^{-2} s^{-1}$) is in good agreement with equation (3.9). At 310.7K other

Table 2

Kinetic data for the reaction $HOONO \xrightarrow{H^+} NO_3^- + H^+$

$I = 1.0$ ($NaClO_4$), $[H_2O_2] = 4.25 \times 10^{-2}$ mol l^{-1},

$[HNO_2]$ used to generate HOONO = ca. 10^{-3} mol l^{-1}

Temperature = 273.7K

$10^2[H^+]$/mol l^{-1}	$10^2 k_d/s^{-1}$	$10^2[H^+]$/mol l^{-1}	$10^2 k_d/s^{-1}$
0.374[a]	5.44	24.8	20.2
1.89	6.93	29.7	22.6
2.88	6.97	34.8	25.8
3.88	7.10	38.7[b]	28.4[b]
4.88	8.29	44.7	31.5
6.87	9.75	49.7	33.8
8.86	10.2	59.7	41.2
10.9	11.8	69.6	47.8
12.9	12.4	79.6	52.3
14.8	14.8	89.5	61.3
19.8	17.1	99.5	64.9

Temperature = 310.7K

4.9	5.24
9.6	6.16
38.7	11.1

a pH 2.33 (phosphate buffer), omitted in estimating the coefficients of equation (3.9)

b Values of $10^2 k_d$ at $[H_2O_2] = 0.209$ mol l^{-1}, and added $[NO_3^-] = 10^{-2}$ mol l^{-1} were 28.6 and 28.4 s^{-1} respectively at this acidity

FIGURE 10

Kinetics of the reaction $HOONO \xrightarrow{H^+} NO_3^- + H^+$

at 273.7K and I = 1.0($NaClO_4$).

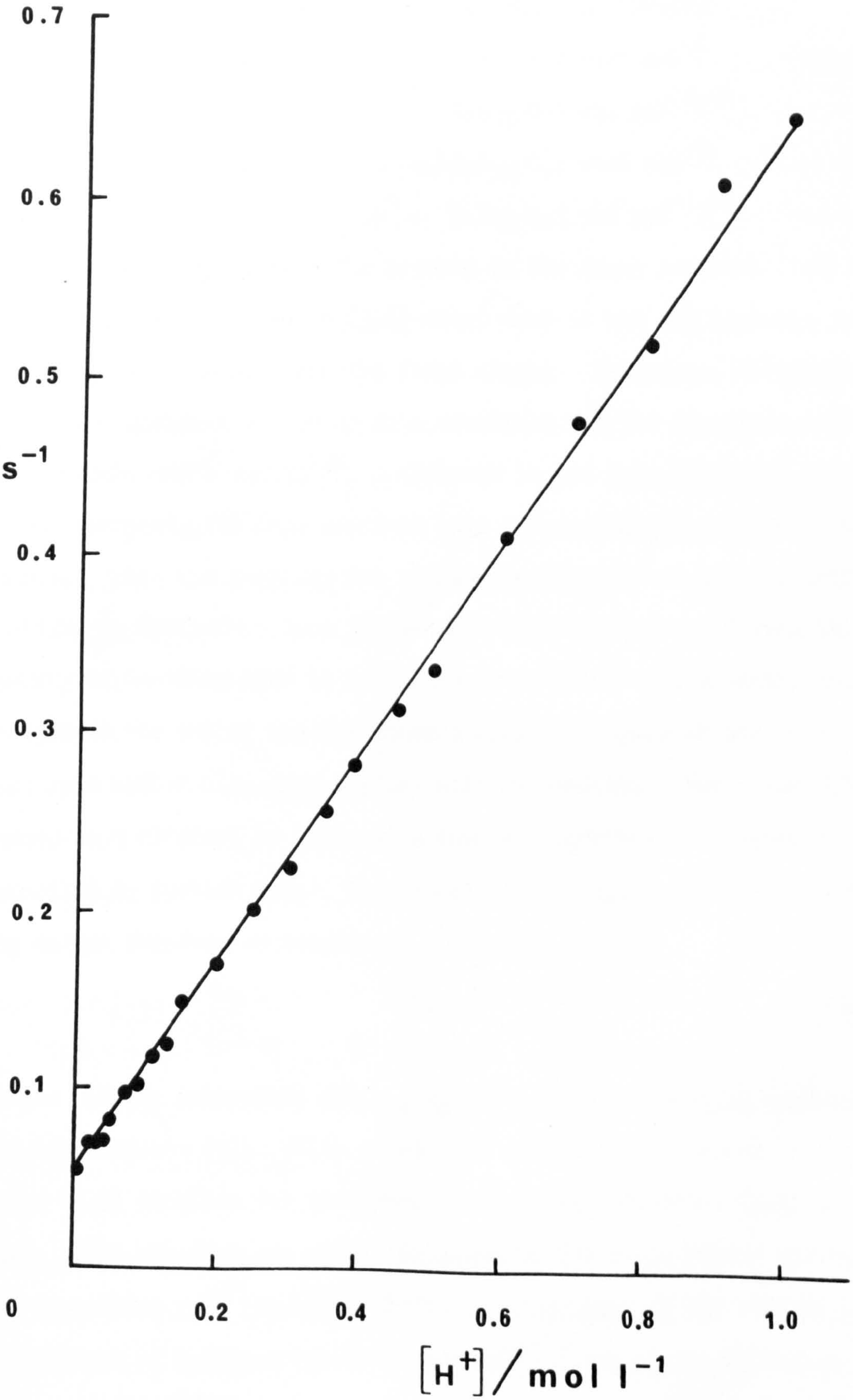
0.7
0.6
0.5
0.4
0.3
0.2
0.1
0
k_d / s^{-1}
0.2
0.4
0.6
0.8
1.0
$[H^+] / mol\ l^{-1}$

runs gave:

$$10^2 k_d = (443 \pm 8) + (1730 \pm 49)\ [H^+]s^{-1}$$

Analysis of the two sets of data at different temperatures gave approximate values for the activation parameters at 298.1K:

Acid independent pathway: $\Delta H^* = 19.6 \pm 0.2$ kcal mol^{-1}

$\Delta S^* = 7.4 \pm 0.7$ cal $mol^{-1}K^{-1}$

Acid dependent pathway: $\Delta H^* = 14.8 \pm 0.2$ kcal mol^{-1}

$\Delta S^* = 5.3 \pm 0.7$ cal $mol^{-1}K^{-1}$

Kinetics of reaction (3.1). The overlap of the decay reaction (3.2) with that of the formation reaction (3.1) meant that it was not possible to obtain an infinity reading for the first stage. Therefore, first attempts to derive the pseudo-first-order rate constants for the formation reaction utilised Swinbourne's method[102]. Although linear rate plots for individual runs were obtained, the data obtained were inconsistent and the results were scattered. This was probably due to Swinbourne's method being relatively insensitive to deviations from first-order behaviour, coupled with the difficulty in deciding when to terminate measurement of the oscilloscope trace towards the end of the formation stage. Analysis of the runs by the initial rate method also gave a great deal of scatter. Formation rate constants were obtained by means of a computer program, the theory of which is described in section 3.6. In general, this program fits absorbance data to any series first-order reaction,

$$A \xrightarrow{k_f} B \xrightarrow{k_d} C$$

where the unknown parameters are k_f, k_d and ϵ_B, the extinction coefficient of the intermediate (B). With a modified form of this program, and using equation (3.9) to allow for the decay process (k_d), reaction (3.1) was then studied. The reaction was mainly followed at 350 nm to reduce the background absorbance from the excess hydrogen peroxide. A few runs at lower concentrations of hydrogen peroxide were carried out at 303 nm whilst studying reaction (3.2). Since the extinction coefficient (ϵ) of the intermediate peroxynitrous acid was not known with any certainty, the program

was used in a two parameter mode to find the best fit values to k_f and ϵ. A knowledge of k_d makes the least-squares procedure simpler and more accurate and it is only necessary to follow the initial stage of the two consecutive reactions to enable good values of k_f to be obtained. Values of ϵ remained reasonably constant ($\pm$ 10%) for all the runs at the same wavelength and also agreed reasonably with the values obtained later from the spectrum of peroxynitrous acid. Absorbance data were fitted with a mean square error of less than 0.001 (<1%) in all cases. The values obtained for k_f are collected in Table 3. The order with respect to acid was established by keeping $[H_2O_2]$ constant (4.25×10^{-2} mol l^{-1}) and varying the acid concentration (Table 3, runs 6 - 12). The results are plotted in Figure 11 and confirm that the reaction is first-order in acid. Analysis of these data gives $k_f/[H^+] = 46.0 \pm 2.4$ l mol^{-1}s^{-1}. The reaction is not simply first-order in $[H_2O_2]$ as can be seen from the variation of $k_f/[H^+]$ with $[H_2O_2]$ in Table 3 and Figure 12. The values of $k_f/[H^+]$ tend towards a maximum at high $[H_2O_2]$. This behaviour is in agreement with equation (3.7) (substrate = $[H_2O_2]$) where

$$k_f = k_3k_2K_1[H^+]\,[H_2O_2] \;/\; (k_{-2}[H_2O] + k_3[H_2O_2])$$

Rearrangement of this equation gives:

$$[H^+]/k_f = (k_{-2}[H_2O]/k_3k_2K_1)\,[H_2O_2]^{-1} + (k_2K_1)^{-1} \qquad (3.10)$$

The average values of $[H^+]/k_f$ are plotted against $[H_2O_2]^{-1}$ in Figure 13 and a weighted least-squares analysis of these data gives:

from the intercept $10^3\,(k_2K_1)^{-1} = 1.62 \pm 0.21$ mol l^{-1} s

and from the slope: $10^4\,(k_{-2}[H_2O]/k_2k_3K_1) = 6.97 \pm 0.08$ mol^{2}l^{-2} s

Hence $k_2K_1 = 617 \pm 80$ mol^{-1}l s^{-1} and $k_3/k_{-2}[H_2O] = 2.32 \pm 0.28$ l mol^{-1}.

3.4. Spectrum of peroxynitrous acid

With the aid of equations (3.9) and (3.10), it was possible to design an experiment to enable the spectrum of peroxynitrous acid to be obtained in a 0.1 mol l^{-1} perchloric acid solution. The spectrum was recorded at 276$\pm$1K with a Cary 14 spectrophotometer, using a continuous-flow cell (pathlength 0.5 cm) in conjunction with a T piece mixer. The conditions

TABLE 3

Kinetic data for the reaction $HNO_2 + H_2O_2 \xrightarrow{H^+} HOONO + H_2O$

$I = 1.0(NaClO_4)$, $[HNO_2]$ = ca. 10^{-3} mol l^{-1}, Temperature = 273.7K

Run No.	$10^2[H^+]$[a] / mol l^{-1}	$10^2[H_2O_2]$[b] / mol l^{-1}	k_f[c] / s^{-1}	$k_f/[H^+]$[d] / l mol^{-1} s^{-1}
1	10.0	1.08	1.50 ± 0.03	15.0
2	67.7	2.13	17.6 ± 0.5	26.0
3	87.0	2.13	22.3 ± 0.5	25.6
4	96.7	3.10	24.6 ± 0.5	25.4
5	10.0	3.20	3.89 ± 0.10	38.9
6	96.0	4.25	42.3 ± 0.17	44.1
7	2.33	4.25	1.43 ± 0.04	61.4
8	4.74	4.25	2.88 ± 0.14	60.7
9	9.59	4.25	4.31 ± 0.40	44.9
10	24.1	4.25	11.0 ± 0.2	45.6
11	38.6	4.25	19.7 ± 0.4	51.0
12	48.3	4.25	21.6 ± 0.2	44.7
13	10.0	10.6	10.5 ± 0.3	105
14	2.32	10.6	3.27 ± 0.10	141
15	2.32	21.0	4.25 ± 0.43	183
16	2.32	42.3	6.40 ± 0.56	276
17	2.32	48.6	7.34 ± 0.12	316
18	2.32	64.0	8.35 ± 0.56	360
19	2.32	85.6	9.2 ± 1.4	397
20	2.32	107	10.1 ± 0.8	435

a Free acid concentration. Allowance was made for the small amount of acid consumed by NO_2^-

b Average value allowing for a very small amount consumed during the reaction

c Average of 2 - 4 estimations

d Subject to same percentage error as the k_f values

FIGURE 11

Kinetics of the reaction

$$HNO_2 + H_2O_2 \xrightarrow{H^+} HOONO + H_2O$$

at constant $[H_2O_2] = 4.25 \times 10^{-2}$ mol l^{-1}

Temperature = 273.7K and I = 1.0($NaClO_4$).

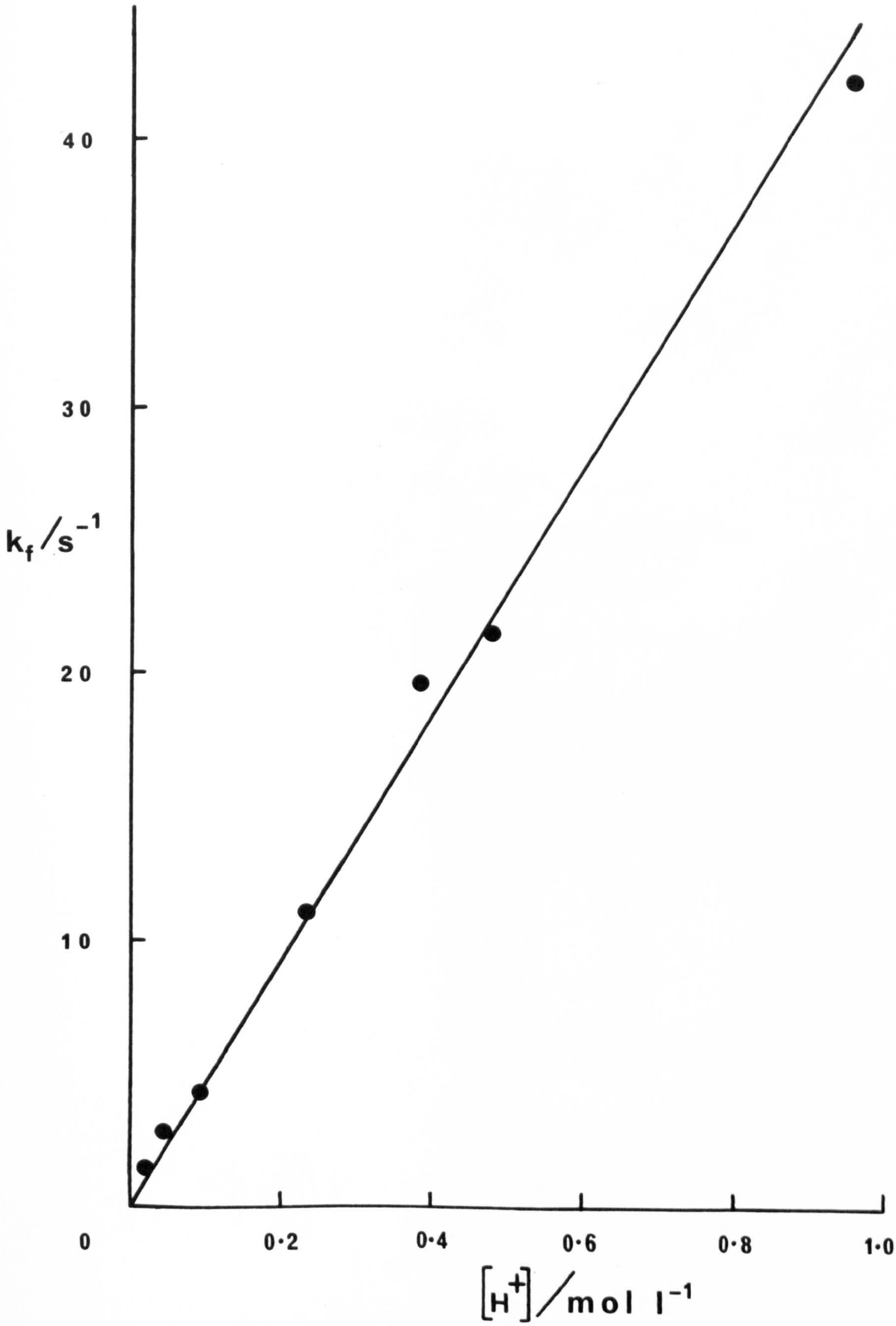
40
30
20
10
0
0·2
0·4
0·6
0·8
1·0
k_f / s^{-1}
$[H^+] / mol\ l^{-1}$

FIGURE 12

Variation of $k_f/[H^+]$ versus $[H_2O_2]$

for the reaction $HNO_2 + H_2O_2 \xrightarrow{H^+} HOONO + H_2O$

Temperature 273.7K and I = 1.0($NaClO_4$).

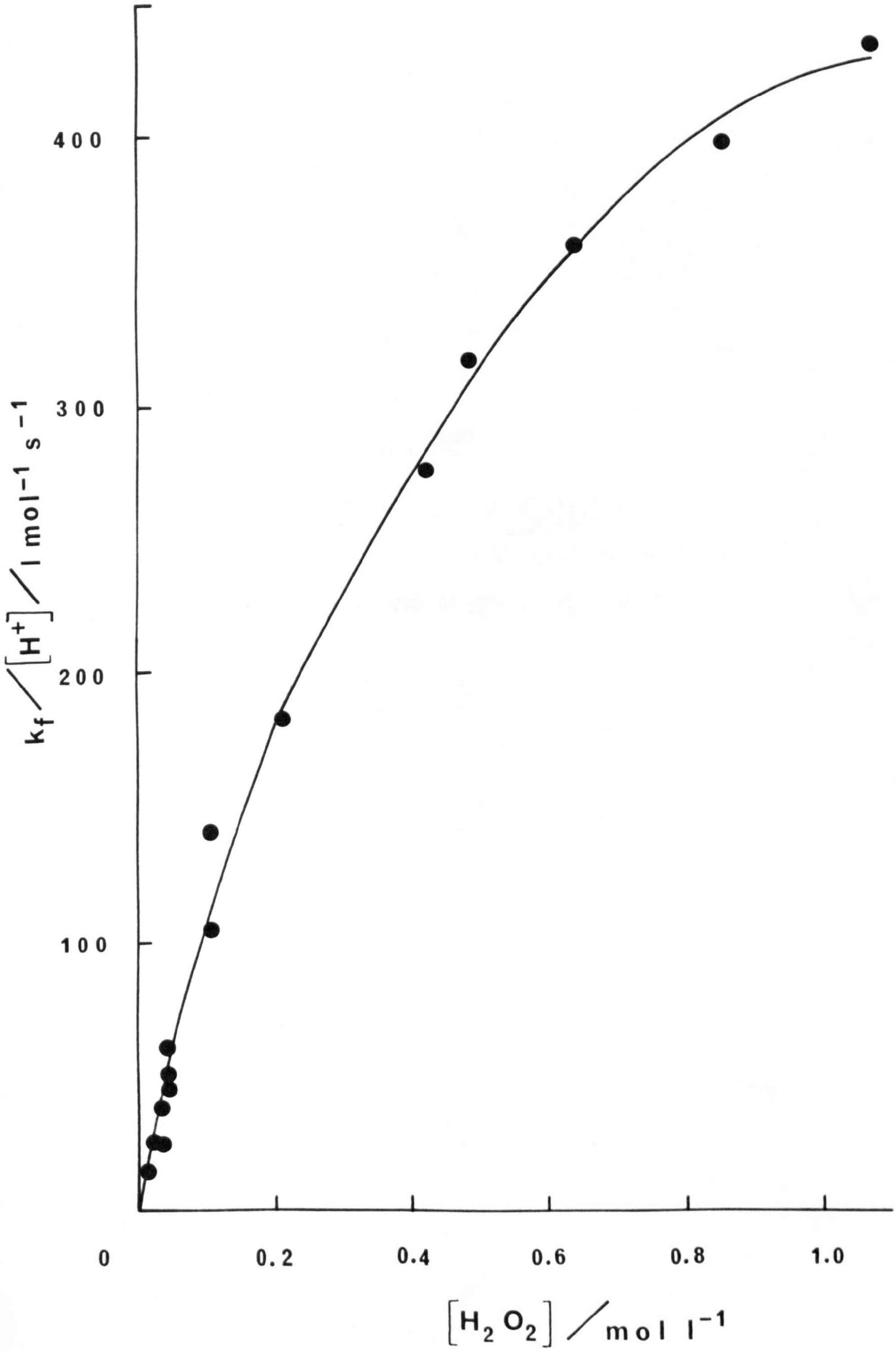
400
300
200
100
$k_f / [H^+] / l\ mol^{-1}\ s^{-1}$
0
0.2
0.4
0.6
0.8
1.0
$[H_2O_2] / mol\ l^{-1}$

FIGURE 13

Variation of $[H^+]/k_f$ versus $[H_2O_2]^{-1}$

for the reaction $HNO_2 + H_2O_2 \xrightarrow{H^+} HOONO + H_2O$

Temperature = 273.7K and I = 1.0($NaClO_4$).

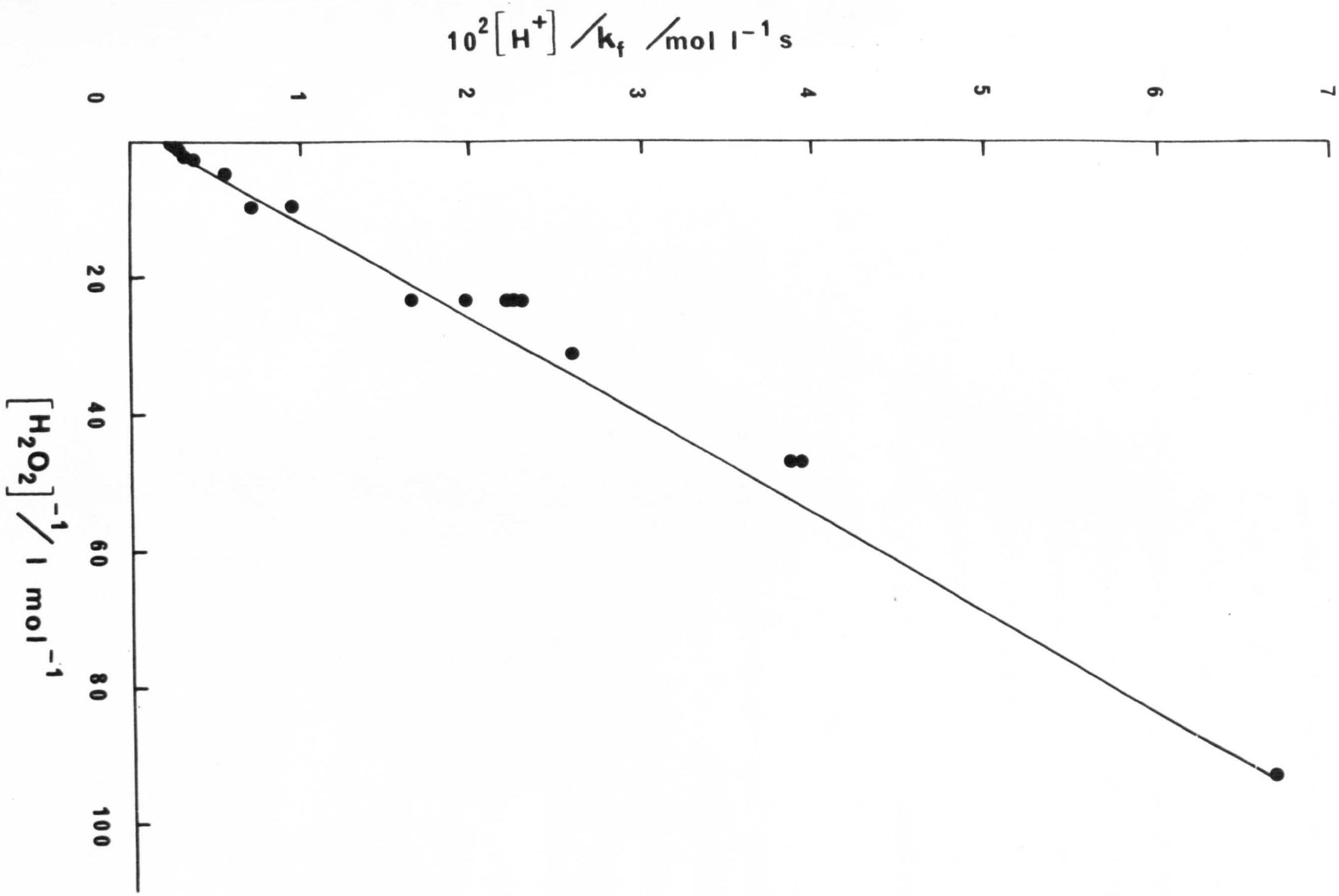
$10^2[H^+]\,/k_f\,/\text{mol l}^{-1}\text{s}$
0
1
2
3
4
5
6
7
8
20
40
60
80
100
$[H_2O_2]^{-1}/\text{l mol}^{-1}$

were chosen so that reaction (3.1) was complete within the time of mixing, ca. 5×10^{-3} s and reaction (3.2) had progressed to a negligible extent within the time of observation, ca. 10^{-2} s. The spectrum which was recorded under continuous-flow conditions was that of a mixture of peroxynitrous acid (2.5×10^{-2} mol l^{-1}) and excess hydrogen peroxide (0.25 mol l^{-1}). By stopping the flow, reaction (3.2) was allowed to proceed to completion and the final spectrum corresponded to that of the product, nitrate ion, plus the excess of hydrogen peroxide. This spectrum was corrected for a small absorbance from the nitrate ion and then subtracted from the spectrum obtained under continuous-flow conditions to give the spectrum of the peroxynitrous acid shown in Figure 14. The correction for the background absorbance from the hydrogen peroxide was less than 1% of the total optical density above 310 nm.

3.5 Discussion

The peroxynitrite anion has a single peak in its spectrum[90] above 250 nm with an extinction coefficient of 1670 ± 50 (302 nm)[92]. In this work, peroxynitrous acid was found to have at least three peaks in the region 320 - 350 nm with much smaller extinction coefficients. It is interesting to compare the vibrational fine structure which appears in the spectrum of peroxynitrous acid with its absence in the peroxynitrite anion. This behaviour is analogous to that found for nitrous acid compared to nitrite anion[103]. It would be interesting to see if fine structure appears in the spectrum of the peroxynitrite anion in non-aqueous solvents as is found for the nitrite anion[104].

The present results are consistent with the recent studies of reaction (3.2) above pH 4, and a comparison of these is given in Table 1. In addition, the acid catalysed route for isomerisation to nitrate ion that previous workers[91] had indicated is now established. The following mechanism is consistent with the present rate data.

FIGURE 14

Spectrum of peroxynitrous acid.

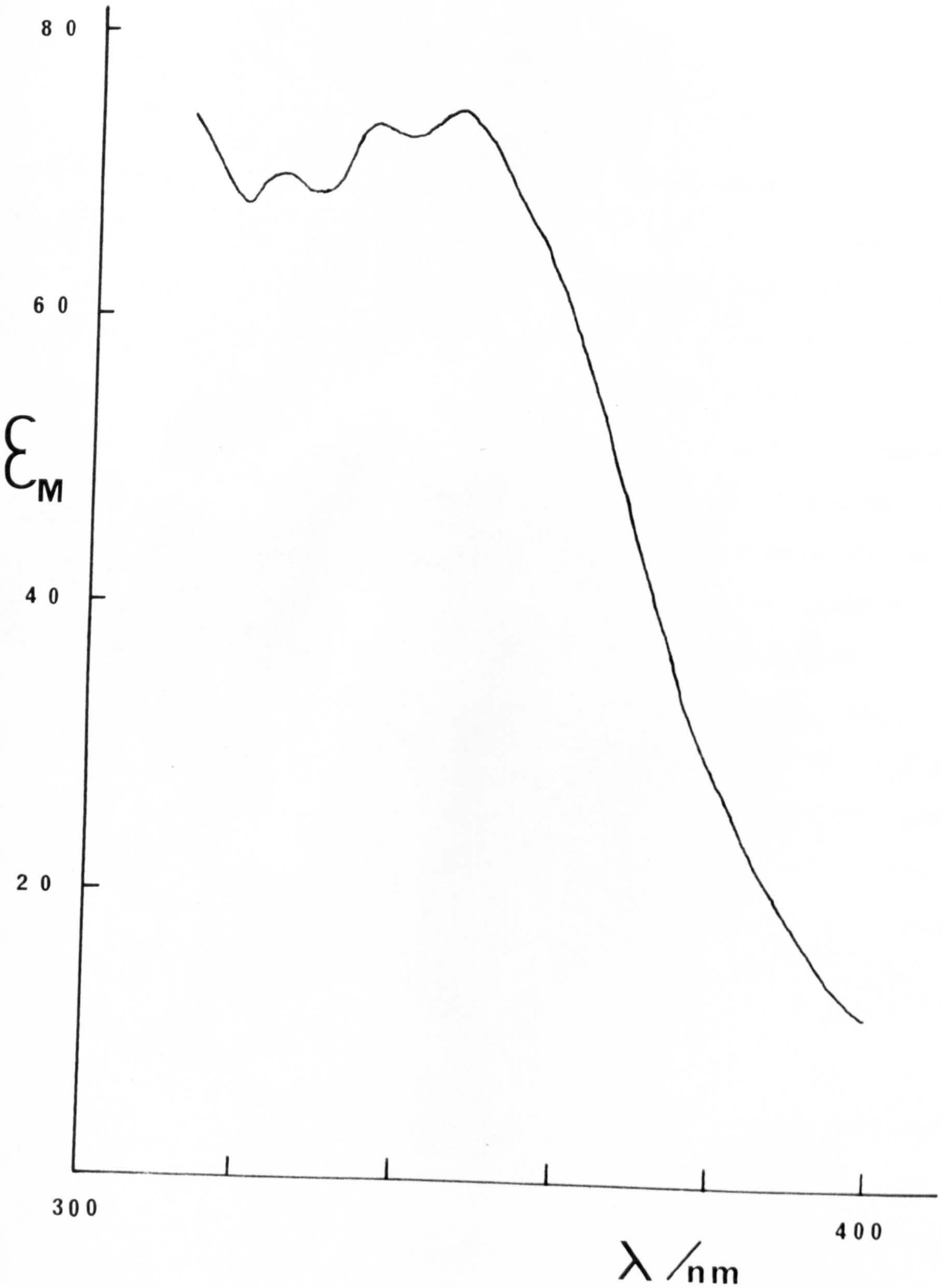
8 0
6 0
4 0
2 0
ε_M
300
400
λ /nm

$$HOONO \xrightarrow{k_{1d}} NO_3^- + H^+$$

$$H^+ \text{ rapid} \quad \rightleftharpoons$$

$$H_2OONO^+ \xrightarrow{k_{2d}} NO_3^- + 2H^+$$

Defining $K_4 = [H_2NO_3^+] / [HOONO]\,[H^+]$,

$$k_d = k_{1d} + k_{2d}K_4[H^+]$$

Acid catalysis is a well known feature of peroxide mechanisms[94,105], even though in general protonation of peroxides is not at all extensive. In this case it is to be expected by analogy with other systems[94] that $K_4 \ll 1$ and so from equation (3.9) $k_{2d} \gg k_{1d}$. The reason for this strong acid catalysis is seen to arise from the reduced activation enthalpy: $\Delta H^*(k_{1d}) = 19.6 \pm 0.2$ kcal mol^{-1}, whereas $\Delta H^*(k_{2d}) + \Delta H(K_4) = 14.8 \pm 0.2$ kcal mol^{-1}. The constant in brackets indicates the origin of the corresponding enthalpy term. A value for the enthalpy of protonation of peroxynitrous acid is unknown but a value has been estimated[94] for the enthalpy of formation of $H_3O_2^+$ from H_2O_2 and H_3O^+; $\Delta H = +4.2 \pm 1.2$ kcal mol^{-1}. A similar value is to be expected for $\Delta H(K_4)$ and hence $\Delta H^*(k_{2d}) \ll \Delta H^*(k_{1d})$. This behaviour is consistent with the trend in stability $OONO^- > HOONO > H_2NO_3^+$, in which successive protonation of the peroxynitrite ion results in a gradual weakening of the O–O bond. It is not, however, possible to predict the position at which protonation occurs. Values have been estimated previously[92] for :

$$\Delta H^*(k_{1d}) - \Delta H(K_a) = 12.5 \text{ kcal mol}^{-1}$$

$$\text{and } \Delta S^*(k_{1d}) - \Delta S(K_a) = +26 \text{ cal mol K}^{-1}$$

where $K_a = [OONO^-]\,[H^+] / [HOONO]$. Hence from the values obtained in this work for $\Delta H^*(k_{1d})$ and $\Delta S^*(k_{1d})$ it can be estimated that at 298.1K $\Delta H(K_a) \sim 7$ kcal mol^{-1} and $\Delta S(K_a) \sim -19$ cal mol^{-1} K^{-1}. Although these values are reasonable for the dissociation of a weak acid, they should be regarded as only approximate, since they lead to a pK_a value of 9.4 which is almost certainly too large[91-2]. Reaction (3.2) was originally proposed

to involve a free radical mechanism[89] but this conclusion has been opposed in view of the low activation energy for the process[92]. However, a recent study of this reaction has offered further evidence for homolytic decomposition of HOONO and, moreover, suggested that the low activation energy is not incompatible with the production of radicals[106].

The results obtained for the formation of peroxynitrous acid in acidic solutions are in general agreement with the mechanism originally proposed by Anbar and Taube[93]. Their tracer studies showed that reactions (3.1) and (3.2) involve the transfer of two oxygen atoms from H_2O_2 to the product, NO_3^-. (At high concentrations of NO_2^- a further reaction occurs in which HOONO reacts with NO_2^- to give NO_3^- with a net transfer of only one O atom from H_2O_2). There can be little doubt that the active species is NO^+ rather than $H_2NO_2^+$ since a limiting rate is obtained at high hydrogen peroxide concentration as predicted by equation (3.7). At 273.7K, NO^+ reacts much more rapidly with H_2O_2 than with H_2O:

$$k_3/k_{-2}\,[H_2O] = 2.32 \pm 0.28 \text{ l mol}^{-1}$$

and since in aqueous solution $[H_2O] = 55.5$, $k_3/k_{-2} = 129 \pm 16$.

At 298.1K Anbar and Taube[93] found $k_3/k_{-2}\,[H_2O] = 2.4$, in good agreement with the value of this work at 273.7K. The calculated value of k_2K_1 at 273.7K is 617 ± 80 l mol^{-1} s^{-1} which is somewhat higher than the value of 230 l mol^{-1} s^{-1} obtained at 273.1K from the reaction between hydrazoic and nitrous acids[99]. However, in the latter study the possibility that $H_2NO_2^+$ was the reactive species was suggested to be more likely.

3.6 Analysis of spectrophotometric data for a series first-order reaction by the method of least-squares

The reaction between hydrogen peroxide and nitrous acid provides an example of a series reaction of the type,

$$A \xrightarrow{k_1} B \xrightarrow{k_2} C$$

This particular reaction has the simplifying feature that it may be studied under pseudo-first-order conditions. Methods of obtaining values

of k_1 and k_2 for a series first-order reaction are well known[28c]. However, these methods are unsuitable in the present case since the extinction coefficient of the intermediate (B) is unknown, and hence it is not possible to measure the concentration of B directly. To enable the rate constants k_1, k_2 and the extinction coefficient of the intermediate to be obtained a least-squares method of analysing the spectrophotometric data was devised.

The differential rate equations for the three species of a series first-order reaction can be integrated to give[28c]:

$$A/A_o = \exp(-k_1 t);$$

$$B/A_o = k_1 [\exp(-k_2 t) - \exp(-k_1 t)] / (k_1 - k_2);$$

$$C/A_o = 1 + [(k_2 \exp(-k_1 t) - k_1 \exp(-k_2 t)) / (k_1 - k_2)],$$

where A_o = initial concentration of A, and it is assumed B=C=0 when t=0.

The optical density (D) of the solution at time t (pathlength 1 cm) is then

$$D = \epsilon_A A + \epsilon_B B + \epsilon_C C$$

where ϵ_A, ϵ_B, ϵ_C are the molar extinction coefficients of A, B and C respectively.

Taking $A_o = 1$,

$$D = (\epsilon_A - \epsilon_C) \exp(-k_1 t) + k_1 (\epsilon_B - \epsilon_C) [\exp(-k_2 t) - \exp(-k_1 t)] / (k_1 - k_2) + \epsilon_C \quad (3.11)$$

Least-squares analysis

Values of k_1, k_2 and ϵ_B can best be determined by least-squares fitting to a set of N values of D obtained at various times t throughout the course of the reaction. Equation (3.11) is non-linear, so iteration is necessary, starting from approximate values of the three parameters derived from the observed trace. The three normal equations are:

$$\sum_{i=1}^{N} w_i (\partial D/\partial k_1)^2 \delta k_1 + \sum_{i=1}^{N} w_i (\partial D/\partial k_1)(\partial D/\partial k_2) \delta k_2$$

$$+ \sum_{i=1}^{N} w_i (\partial D/\partial k_1)(\partial D/\partial \epsilon_B) \delta \epsilon_B = \sum_{i=1}^{N} w_i (\partial D/\partial k_1) \Delta_i$$

$$\sum_{i=1}^{N} w_i \, (\partial D/\partial k_2) \, (\partial D/\partial k_1)\, \delta k_1 + \sum_{i=1}^{N} w_i \, (\partial D/\partial k_2)^2 \, \delta k_2$$

$$+ \sum_{i=1}^{N} w_i \, (\partial D/\partial k_2) \, (\partial D/\partial \epsilon_B)\, \delta \epsilon_B = \sum_{i=1}^{N} w_i \, (\partial D/\partial k_2)\, \Delta_i$$

$$\sum_{i=1}^{N} w_i \, (\partial D/\partial \epsilon_B) \, (\partial D/\partial k_1)\, \delta k_1 + \sum_{i=1}^{N} w_i \, (\partial D/\partial \epsilon_B) \, (\partial D/\partial k_2)\, \delta k_2$$

$$+ \sum_{i=1}^{N} w_i \, (\partial D/\partial \epsilon_B)^2 \, \delta k_2 = \sum_{i=1}^{N} w_i \, (\partial D/\partial \epsilon_B)\, \Delta_i$$

w_i is a weighting factor (unit weights are used in the analyses reported here). Δ_i is the difference between the observed optical density at time t, and that calculated using the estimated values of k_1, k_2 and ϵ_B. The partial derivatives required for the normal equations can be obtained numerically, and this is satisfactory unless k_1 approaches k_2. To include this situation it is better to use the analytical formulae below. From equation (3.11):

$$(\partial D/\partial k_1)_{k_2,\epsilon_B} = \frac{(\epsilon_B - \epsilon_C)}{(k_1 - k_2)^2} \, (k_1 - k_2) \left[\exp(-k_2 t) - \exp(-k_1 t) + k_1 t \exp(-k_1 t) \right]$$

$$- k_1 \left[\exp(-k_2 t) - \exp(-k_1 t) \right] - t\,(\epsilon_A - \epsilon_C) \exp(-k_1 t) \; ; \qquad (3.12)$$

$$(\partial D/\partial k_2)_{k_1,\epsilon_B} = \frac{k_1(\epsilon_B - \epsilon_C)}{(k_1 - k_2)^2} \left[\exp(-k_2 t) - \exp(-k_1 t) \right.$$

$$\left. - (k_1 - k_2) t \exp(-k_2 t) \right] \; : \qquad (3.13)$$

$$(\partial D/\partial \epsilon_B)_{k_1,k_2} = k_1 \left[\exp(k_2 t) - \exp(-k_1 t) \right] / (k_1 - k_2) \; ; \qquad (3.14)$$

If $k_1 = k_2$, all these expressions are indeterminate, and serious loss of accuracy will occur if the rate constants are nearly equal. To avoid the difficulty a series expansion can be used. Substituting for k_2 from $R = (k_1 - k_2)/k_1$ in equation (3.11) gives:

$$D = (\epsilon_A - \epsilon_C)\exp(-k_1 t) + (\epsilon_B - \epsilon_C) \exp(-k_1 t) \left[\exp(k_1 R t) - 1 \right] / R + \epsilon_C$$

Series expansion of exp (k_1Rt), neglecting terms in R^4 and higher gives

$$D = (\epsilon_A - \epsilon_C) \exp(-k_1t) + (\epsilon_B - \epsilon_C) \exp(-k_1t) \times (k_1t + Rk_1^2t^2/2 + R^2k_1^3t^3/6 + R^3k_1^4t^4/24) + \epsilon_C$$

The partial derivatives are then:

$$(\partial D/\partial k_1)_{R,\epsilon_B} = \exp(-k_1t)(\epsilon_B - \epsilon_C)\left[t + Rk_1t^2 + R^2k_1^2t^3/2 + R^3k_1^3t^4/6\right.$$

$$\left. -t(k_1t + Rk_1^2t^2/2 + R^2k_1^3t^3/6 + R^3k_1^4t^4/24)\right] - t\exp(-k_1t)(\epsilon_A - \epsilon_C); \quad (3.15)$$

$$(\partial D/\partial R)_{k_1,\epsilon_B} = (\epsilon_B - \epsilon_C)\exp(-k_1t)(k_1^2t^2/2 + Rk_1^3t^3/3 + R^2k_1^4t^4/8); \quad (3.16)$$

$$(\partial D/\partial \epsilon_B)_{k_1,R} = \exp(-k_1t)(k_1t + Rk_1^2t^2/2 + R^2k_1^3t^3/6 + R^3k_1^4t^4/24). \quad (3.17)$$

These derivatives are related to equations (3.12) - (3.14) by the equations:

$$(\partial D/\partial k_1)_{k_2,\epsilon_B} = (\partial D/\partial k_1)_{R,\epsilon_B} + (\partial D/\partial R)_{k_1,\epsilon_B}(\partial R/\partial k_1)_{k_2,\epsilon_B}$$

$$(\partial D/\partial k_2)_{k_1,\epsilon_B} = (\partial D/\partial R)_{k_1,\epsilon_B}(\partial R/\partial k_2)_{k_1,\epsilon_B}$$

$$(\partial D/\partial \epsilon_B)_{k_1,k_2} = (\partial D/\partial \epsilon_B)_{k_1,R}$$

where

$$(\partial R/\partial k_1)_{k_2,\epsilon_B} = k_2/k_1^2 \text{ and } (\partial R/\partial k_2)_{k_1,\epsilon_B} = -1/k_1$$

In practice equations (3.15) - (3.17) have been found adequate when $R < 0.01$ and equations (3.12) - (3.14) are used when $R > 0.01$. The normal equations can then be solved for δk_1, δk_2 and δ_{ϵ_B} which are the estimated shifts to k_1, k_2 and ϵ_B respectively, e.g. k_1 (improved) = k_1 (previous) + δk_1.

Ambiguity

Analysis of some test data gave two sets of values of k_1, k_2 and ϵ_B which fitted the observations equally well. An examination of equation (3.11) shows that two solutions will always be possible. Equation (3.11)

can be arranged as follows:

$$D = \exp(-k_1 t)\,[\epsilon_A (k_1 - k_2) - k_1 \epsilon_B + k_2 \epsilon_C]/(k_1 - k_2)$$
$$+ [k_1 \exp(-k_2 t)\,(\epsilon_B - \epsilon_C)]/(k_1 - k_2) + \epsilon_C$$

The two solutions correspond to an interchange of k_1 and k_2. Suppose k_1, k_2, ϵ_B and k_1', k_2', ϵ_B' are the two sets of solutions, $k_1' = k_2$, $k_2' = k_1$ and for D to be unaltered, the following two equations must hold:

$$\epsilon_A (k_1 - k_2) - k_1 \epsilon_B + k_2 \epsilon_C = k_2 (\epsilon_B' - \epsilon_C)$$
$$\epsilon_A (k_2 - k_1) - k_2 \epsilon_B' + k_1 \epsilon_C = k_1 (\epsilon_B - \epsilon_C)$$

Both of these equations reduce to

$$\epsilon_B' = \epsilon_A + k_1 (\epsilon_B - \epsilon_A) / k_2 \qquad (3.18)$$

The two solutions correspond to rapid formation of a weakly absorbing intermediate, or slow formation of a strongly absorbing intermediate. If $k_1 = k_2$, both values of ϵ_B are the same.

The important corollary is that an optical density which rapidly increases and slowly declines does not necessarily imply a fast first and slow second reaction. This can be illustrated by considering an experiment involving the formation and decay of peroxynitrous acid in acidic solution. Figure 15 shows the observed absorbances and those calculated by the least-squares procedure. The reaction shown was studied at 273.7K and 320 nm. Pseudo-first-order conditions were used, with $[H^+]$ held constant by phosphate buffering at pH 1.57, and $[H_2O_2]$ in large excess over $[HNO_2]$. In this example, the calculated optical density is given by equation (3.11) either with $k_1 = 3.76 \pm 0.02\ s^{-1}$, $10^2 k_2 = 8.54 \pm 0.03\ s^{-1}$ and $\epsilon_B = 58.3 \pm 0.1$, or with $10^2 k_1 = 8.54 \pm 0.03\ s^{-1}$, $k_2 = 3.76 \pm 0.02\ s^{-1}$ and $\epsilon_B = 2039 \pm 1$. The quoted errors are the standard deviations. It is mathematically impossible to distinguish the correct from the incorrect solution from a single set of data, unless the value of ϵ_B' happens to be physically meaningless e.g. far too large or negative. The ambiguity may be resolved if the ratio k_1/k_2 is varied, in which case ϵ_B' will vary according to equation (3.18) whilst ϵ_B remains constant. For this reaction it is relatively easy to vary k_1/k_2 since both reactions are pseudo-first-order.

FIGURE 15

A comparison of observed absorbance-time data of a series first-order reaction, to those calculated using the least-squares procedure described in section 3.6.

The reaction is the formation and decay of peroxynitrous acid at 320 nm and

pH = 1.57 (phosphate buffer)

Temperature = 273.7K

Initial $[HNO_2]$ = 3 x 10^{-3} mol l^{-1}

$[H_2O_2]$ = 0.15 mol l^{-1}

Circles represent experimental observations.

The continuous line was calculated from the least-squares parameters.

Formation and decay of Peroxynitrous Acid at 320nm.

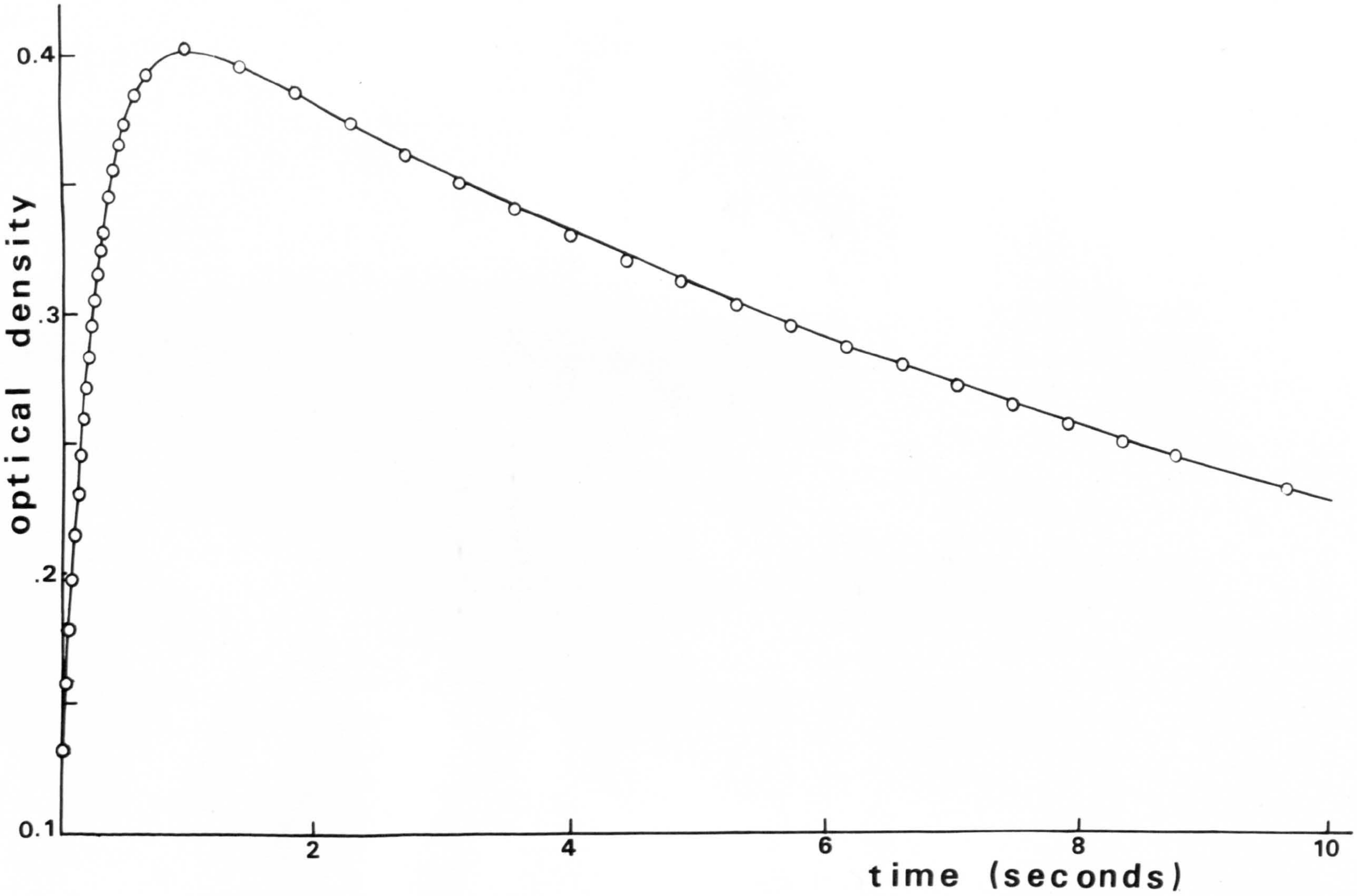

A further set of data, obtained at pH 2.26 under otherwise identical conditions, showed that the true value of ϵ_B is 58.3. In this case, therefore, the first stage of the reaction is faster.

Where reactions are not followed under pseudo-first-order conditions, the ratio k_1/k_2 may be varied by changing the temperature, provided that the two stages of the reaction do not have identical activation energies. However this approach also requires that ϵ_B does not vary substantially with temperature.

Convergence

The initial estimates of k_1, k_2 and ϵ_B must not be too far from the correct values or the least-squares refinement may oscillate rather than converge. In particular if k_1 and k_2 are nearly equal, the calculated shifts may be such that the rate constants are interchanged, and oscillation between the two solutions occurs. In this situation, dampening of the shifts may be necessary, and good data are required if convergence is to be achieved.

Errors

After convergence, the errors in k_1, k_2 and ϵ_B can be estimated as follows. If the 3 x 3 matrix with coefficients a_{ij} on the left-hand side of the normal equations is inverted to give the inverse matrix with coefficients b_{ij}, then the standard deviation σ_j of variable j is given by

$$\sigma_j = \left[(b_{jj} \sum_{i=1}^{N} w_i \Delta_i^2) / (N - 3) \right]^{\frac{1}{2}}$$

An increase in N by more frequent sampling of a continuously recorded curve will produce a decrease in the calculated standard deviations, but this may not be genuine since adjacent observations may cease to be independent. This problem can be overcome by a non-linear weight matrix as in electron diffraction studies[107], but this is probably unnecessary in kinetic work. The calculated standard deviations may, however, be underestimated with data taken from a continuous curve.

In many experiments the exact zero time for data is difficult to ascertain, e.g. with fast reactions in stopped-flow experiments one is

limited by the rather imprecise dead-time of the apparatus. In this situation a zero time correction may be necessary. This is readily obtained by comparing the observed and calculated optical densities of the first few observations after cycles of least-squares fitting have given approximate values of the unknown parameters. If necessary, the corrected times may then be used to generate improved values of k_1, k_2 and ϵ_B, and the whole process repeated until convergence is obtained.

The procedures described in this section are implemented in the Algol computer program SPORK, on an Elliott 4130 computer. A listing of this program is given in the Appendix.

CHAPTER 4

THE KINETICS OF FORMATION AND DISSOCIATION OF THE MONO-COMPLEXES OF THE MANGANESE(II) ION WITH 2,2'-BIPYRIDYL AND 1, 10-PHENANTHROLINE AND OF FORMATION OF THE MONO-(2,2,'2''-TERPYRIDYL)MANGANESE(II) ION IN ANHYDROUS METHANOL

Note: In the following, bipy, phen and terpy will be used as abbreviations for 2,2'-bipyridyl, 1,10-phenanthroline and 2,2,'2''-terpyridyl, respectively.

4.1. Introduction

In Chapter 1 a general outline of the kinetics of metal complex formation of the divalent metal ions of the first transition series was given. Despite the proliferation of the rapid-reaction techniques, several of the metal ions of this series remain relatively unstudied. Due to their high lability, data on the Mn(II), Cr(II), Cu(II) and Zn(II) ions, in particular, are sparse. The high rates of reaction of the Cu(II) and Cr(II) ions have been ascribed to Jahn-Teller distortion[50]. The Zn(II) and Mn(II) ions are expected to be very labile, for d^{10} and high spin d^5 ions lack any Ligand Field Stabilisation Energy.

Kinetic studies of Mn(II) formation reactions may also be expected to be complicated by the low stability of these complexes. The Irving-Williams stability order predicts an increase in complex stability in the sequence Mn(II) < Fe(II) < Co(II) < Ni(II) < Cu(II) > Zn(II). As fast reactions require the use of low concentrations to give a measurable rate, it may be impossible to arrange the experimental conditions to ensure significant complex formation, and hence a detectable optical change. With a labile metal ion whose complexes have low stabilities, it may also be expected that the dissociation rate will be appreciable. The dissociation rate will, therefore, contribute to the observed formation rate constant, adding to the difficulty of obtaining the true formation rate constant. Thus, for the following reaction, (M^{2+} is a metal ion, and L a ligand):

$$M^{2+} + L \underset{k_d}{\overset{k_f}{\rightleftharpoons}} M\text{-}L^{2+}$$

the pseudo-first-order rate constant (k_{obs}), with metal ion in excess, is given by[28d]:

$$k_{obs} = k_f [M^{2+}] + k_d \qquad (4.1)$$

This sort of problem is shown by the data of Wilkins et al. In aqueous solution, they were able to measure[108] the rate constant and corresponding activation parameters for the formation of the Mn(terpy)$^{2+}$ ion, whose stability constant is fairly large. However, with 1,10-phenanthroline as the ligand, which forms a complex of lower stability, only a single rate constant at lowered temperature was obtainable[109]. The 2,2'-bipyridyl complex of the Mn(11) ion was too unstable at the low reactant concentrations necessary to enable the formation rate to be measured[109]. The Mn(II) ion reacting with 2,2'-bipyridyl and 1,10-phenanthroline was, therefore, considered a suitable system for investigation with the low temperature stopped-flow apparatus. Large concentrations of metal ion can be used to force the reaction to completion, and low temperatures used to offset the increase in rate.

The heterocyclic amines 2,2'-bipyridyl, 2,2',2''-terpyridyl and 1,10-phenanthroline have been extensively used as ligands in kinetic studies[108-9]. Their properties are particularly suitable for kinetic investigations with labile metal ions. In aqueous solution, at least, their metal complexes have been thoroughly examined thermodynamically[110] so that the nature and concentration of the species present are well characterised. The ligands have absorption bands in the near-ultraviolet region, sufficiently well separated from those of their metal complexes. The extinction coefficients are large, which enables dilute solutions to be used, and their chelating nature leads to relatively high stability, so that with most metal ions even low concentrations of metal ion and ligand lead to complete complex formation. The three ligands are weakly basic, thus,

studies in the neutral or weakly acid region avoid interference and difficulties in interpretation arising from the presence of protonated species.

The configurations of the three ligands in solution are shown below.

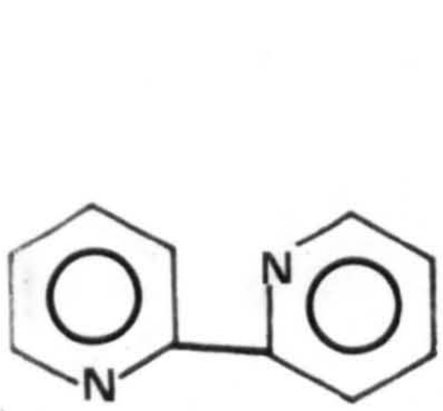

(I)

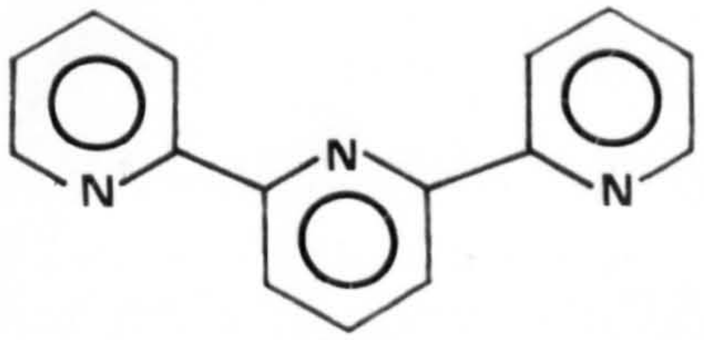

(II)

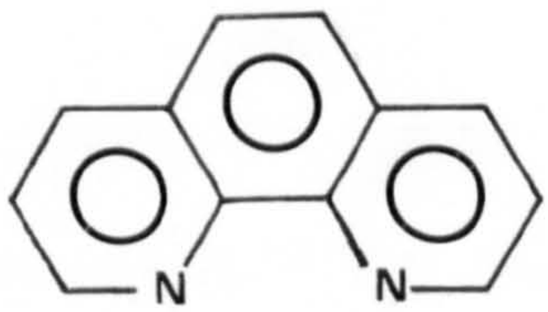

(III)

In aprotic solvents 2,2'-bipyridyl (I) and 2,2',2"-terpyridyl (II) exist in solution in <u>trans</u> and <u>trans-trans</u>-planar configurations, respectively[111]. The 1,10-phenanthroline molecule (III) is, of course, rigidly held in a <u>cis</u>-planar configuration.

For this work, methanol was chosen as solvent. The metal salts are freely soluble in it, and the freezing point and viscosity of methanol were suitable in the temperature range expected to be required. Moreover the methanol exchange rate at the Mn(II) ion has been reported[112], and this is an important requirement in understanding the kinetics of formation.

In addition to those of the 2,2'-bipyridyl and 1,10-phenanthroline complexes, the kinetics of formation of the $Mn(terpy)^{2+}$ ion in anhydrous methanol were also investigated for comparison with the aqueous work[108].

4.2. <u>Experimental</u>

<u>Materials</u>. A.R. grade methanol was dried by refluxing over magnesium turnings and distilled[113]. The water content was estimated by Karl Fischer titration and found to be < 0.01% by weight.

Manganese perchlorate was prepared from electrolytic grade manganese metal (Hopkin and Williams) and A.R. perchloric acid. The salt was re-crystallised from water several times to remove excess acid. The anhydrous salt was obtained by heating at 353-373K and 0.1mm Hg over P_2O_5 for two days[112]. Karl Fischer titration of stock methanolic solutions showed the dried salt contained 1% by weight of water. At the concentrations of metal ion used in the kinetic runs, the water content was at most 0.02% by weight.

Stock solutions of manganese perchlorate were estimated for manganese(II) ion by E.D.T.A. titration[114].

Sodium perchlorate (Analar, Hopkin and Williams) was dried at 393K for one week. Karl Fischer titration of ca. 2 mol l^{-1} solutions in methanol showed the water content to be the same as the solvent. The stock solution was standardised by evaporation of aliquots at 393K and weighing of the $NaClO_4$ residue.

Methanolic solutions of perchloric acid were prepared by adding ca. 5 ml of 72% perchloric acid to ca. 300 ml of methanol. An attempt was made to dry this solution by refluxing, and passing the condensed vapour through a bed of molecular sieves, before returning it to the solution[115]. Karl Fischer titration revealed a water content of 0.09% by weight.

Mercuric chloride and silver perchlorate were both A.R. grade materials. They were dried in the same way as manganese perchlorate. Methanolic solutions of mercuric perchlorate were prepared by the addition to methanol of accurately weighed amounts of mercuric chloride and silver perchlorate in stoicheiometric amounts. Silver chloride was removed by filtration, and the mercuric perchlorate solution was checked to ensure it was free of both silver and chloride ions.

2,2'-Bipyridyl (B.D.H.) and 1,10-phenanthroline monohydrate (Hopkin and Williams) were both A.R. grade and were used without further purification. 2,2',2"-Terpyridyl (Hopkin and Williams) was recrystallised from water/methanol solution and sublimed *in vacuo* at 353K. The white sublimate had m.p. 359.5K (lit. 395.5K)[108].

All stock solutions were made up, and all dilutions were performed, in a dry box under an atmosphere of nitrogen. Volumetric flasks were sealed by "Subaseals". Samples were withdrawn by hypodermic syringe under an atmosphere of dry nitrogen and injected into the reservoirs of the low temperature stopped-flow apparatus. The reservoirs were also kept under dry nitrogen. To avoid contamination of the terpy solutions caused by the

ligand leaching metal ions from volumetric flasks, the flasks were pre-rinsed with a strong solution of E.D.T.A. A new solution of terpy was made immediately prior to the experiments.

Additions of sodium perchlorate were made from burettes, the taps of which were encased in a glove box flushed with dry nitrogen. The tops of the burettes were protected by silica-gel guard tubes.

Spectra to determine observation wavelengths were run on a Cary 14 spectrophotometer.

4.3. Kinetics

The low temperature stopped-flow apparatus was employed to study the kinetics of the reactions. All formation runs were performed under pseudo-first-order conditions with the metal ion in large excess over the ligand. Metal ion concentrations were in the range 10^{-3} to 5×10^{-2} mol l^{-1} and ligand concentrations in the range $1 - 5 \times 10^{-5}$ mol l^{-1}. The formation reactions of the mono-complexes of bipy and phen were followed at 300 nm, and the reaction of the Mn(II) ion with terpy at 290 nm. Preliminary experiments on the reaction between the Mn(II) ion and bipy were performed without any ionic strength control. The order of the formation process with respect to the metal ion deviated from unity at the higher metal ion concentrations used. As this may have been due to the large metal ion concentrations employed, and hence varying ionic strength, all kinetic runs to establish the formation and dissociation rate constants were carried out at an ionic strength of 0.2 ($NaClO_4$).

The dissociation rate constants of the $Mn(bipy)^{2+}$ complex were obtained by decomposing it with both perchloric acid and mercuric ion. The perchloric acid induced dissociation of the $Mn(phen)^{2+}$ complex was also studied. The Mn(II) complex solutions were made by mixing a large excess of the metal ion with ligand. The runs were performed under pseudo-first-order conditions with acid or mercuric ion in large excess over the ligand. The acid dissociation of the $Mn(bipy)^{2+}$ ion was followed at 310 nm and that of the $Mn(phen)^{2+}$ ion at 315 nm. The mercuric ion induced dissociation of the

$Mn(bipy)^{2+}$ ion was monitored at 315 nm.

4.4. Results

a) Formation reactions

Good first-order plots, extending over at least three half-lives were obtained in all cases. While stability constants for these systems are known in aqueous solution[110], no data are available for methanol solution. However, with such large excess of metal ion over ligand (up to 10^3:1) it is assumed that the kinetic data refer to formation of the mono-complexes. The concentration dependence with respect to metal ion was studied. The observed pseudo-first-order rate constants are listed in Table 4 (Mn(II) + terpy), Table 5 (Mn(II) + phen) and Table 6 (Mn(II) + bipy), and shown plotted against metal ion concentration in Figure 16 (Mn(II) + terpy), Figure 17 (Mn(II) + phen) and Figure 18 (Mn(II) + bipy). Reference to these three figures shows that the metal ion concentration dependence is somewhat different for the reaction with each ligand. The reaction between Mn(II) and terpy is first-order in metal ion. A plot of observed rate constant against Mn(II) concentration for the reaction with bipy is also linear, but does not pass through the origin. The variation of k_{obs} with Mn(II) concentration for the reaction with phen is more complex. At low metal ion concentrations the plot is linear and gives an intercept, but at higher metal ion concentrations the plot curves upwards. However, the rates at higher Mn(II) concentrations are very large in this case, and the errors involved make it difficult to decide whether or not the curvature is significant. The rate constants and activation parameters for the formation of the $Mn(phen)^{2+}$ ion are derived by considering all k_{obs} values. Analyses of all the data by the method of least-squares (computer program LSAD, Appendix) gave slopes with a maximum standard deviation of 5%. The effect upon the activation enthalpy by considering only the runs at metal ion concentrations below ca. 0.03 mol l^{-1} Mn(II), where the plots are more linear, is only 0.8 kcal mol^{-1}.

TABLE 4

Observed rate constants for the reaction of the Mn(II) ion with 2,2,'2''-terpyridyl in anhydrous methanol

I=0.2 ($NaClO_4$) [terpy] ca. 1×10^{-5} mol l^{-1}

T/K	$10^2[Mn^{2+}]$/mol l^{-1}	k_{obs}/s^{-1}
273.7	0.101	0.67 ± 0.01
"	1.01	7.44 ± 0.12
"	2.02	13.9 ± 0.3
"	3.04	21.2 ± 0.5
262.4	1.01	2.78 ± 0.07
"	3.04	7.56 ± 0.13
"	5.05	13.8 ± 0.2
251.5	0.101	0.072 ± 0.001
"	1.01	0.819 ± 0.014
"	3.04	2.39 ± 0.09
"	5.05	3.99 ± 0.03

FIGURE 16

Kinetic data for the reaction of the manganese(II) ion with 2,2',2"-terpyridyl in anhydrous methanol

$I = 0.2$ ($NaClO_4$)

■ at 273.7K

● at 262.4K

▼ at 251.5K

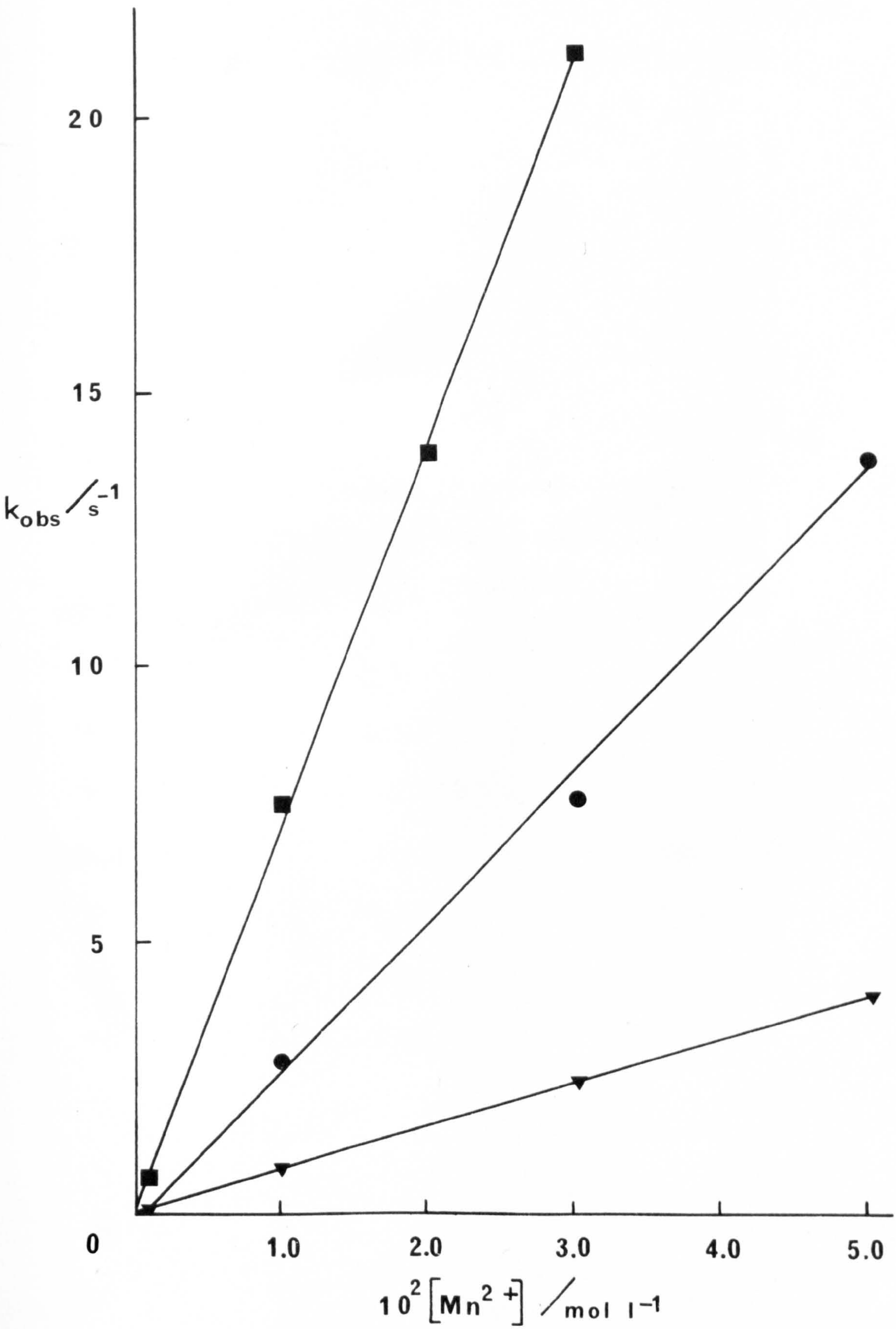
20
15
10
5
0
k_{obs} / s^{-1}
1.0
2.0
3.0
4.0
5.0
$10^2 [Mn^{2+}]$ / mol l^{-1}

TABLE 5

Observed rate constants for the reaction of the Mn(II) ion with 1,10-phenanthroline in anhydrous methanol

$I = 0.2$ ($NaClO_4$) [phen] ca. 5×10^{-5} mol l^{-1}

T/K	$10^2[Mn^{2+}]$/mol l^{-1}	k_{obs}/s^{-1}
251.8	0.10	3.47 ± 0.05
"	0.50	11.9 ± 0.4
"	0.99	21.7 ± 0.3
"	1.53	32.5 ± 0.1
"	2.44	58.9 ± 0.7
"	3.51	95.7 ± 1.5
239.8	0.125	1.24 ± 0.02
"	1.22	8.88 ± 0.27
"	3.01	23.5 ± 0.8
"	5.00	47.3 ± 1.0
226.9	0.10	0.299 ± 0.009
"	1.53	2.05 ± 0.03
"	3.51	6.23 ± 0.17
"	4.96	11.7 ± 0.2

FIGURE 17

Kinetic data for the reaction of the manganese(II) ion with 1,10-phenanthroline in anhydrous methanol.

$I = 0.2$ ($NaClO_4$)

■ at 251.8K

▲ at 239.8K

● at 226.9K

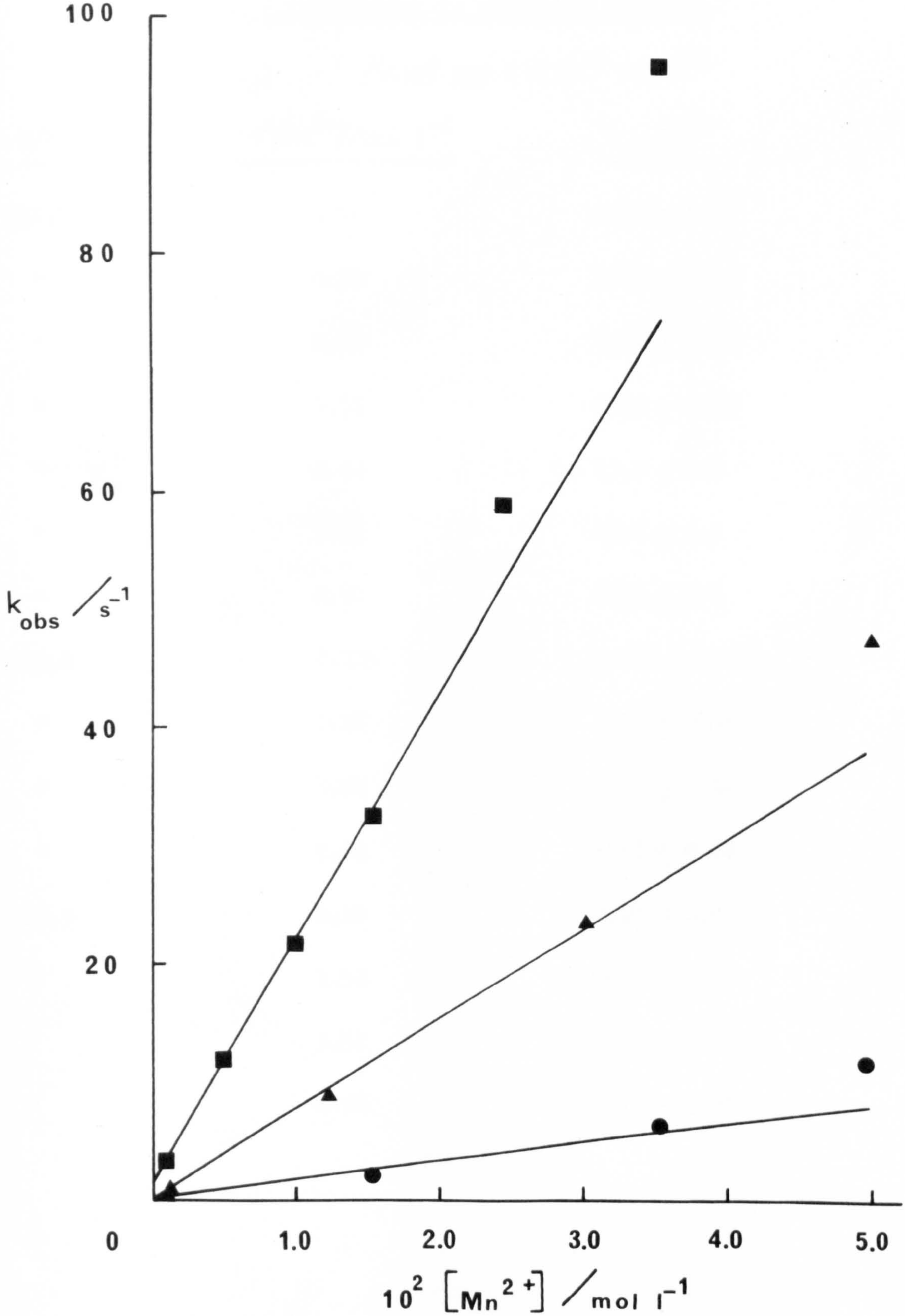
100
80
60
40
20
0
k_{obs} / s^{-1}
1.0
2.0
3.0
4.0
5.0
10^2 [Mn^{2+}] / mol l^{-1}

TABLE 6

Observed rate constants for the reaction of the Mn(II) ion with 2,2'-bipyridyl in anhydrous methanol

I = 0.2 ($NaClO_4$) [bipy] ca. 1 x 10^{-5} mol l^{-1}

T/K	$10^2[Mn^{2+}]$/mol l^{-1}	k_{obs}/s^{-1}
251.8	0.10	2.72 ± 0.03
"	0.50	4.89 ± 0.10
"	0.99	6.47 ± 0.27
"	1.53	9.29 ± 0.29
"	2.44	12.4 ± 0.3
"	3.51	15.6 ± 0.3
"	4.96	22.1 ± 0.1
239.8	0.125	0.624 ± 0.012
"	1.22	2.13 ± 0.01
"	3.01	4.16 ± 0.12
"	5.00	6.17 ± 0.08
226.9	0.10	0.21 ± 0.01
"	1.53	0.67 ± 0.02
"	3.51	1.14 ± 0.01
"	4.96	1.53 ± 0.01

FIGURE 18

Kinetic data for the reaction of the manganese(II) ion with 2,2'-bipyridyl in anhydrous methanol.

$I = 0.2$ ($NaClO_4$)

● at 251.8K

▼ at 239.8K

■ at 226.9K

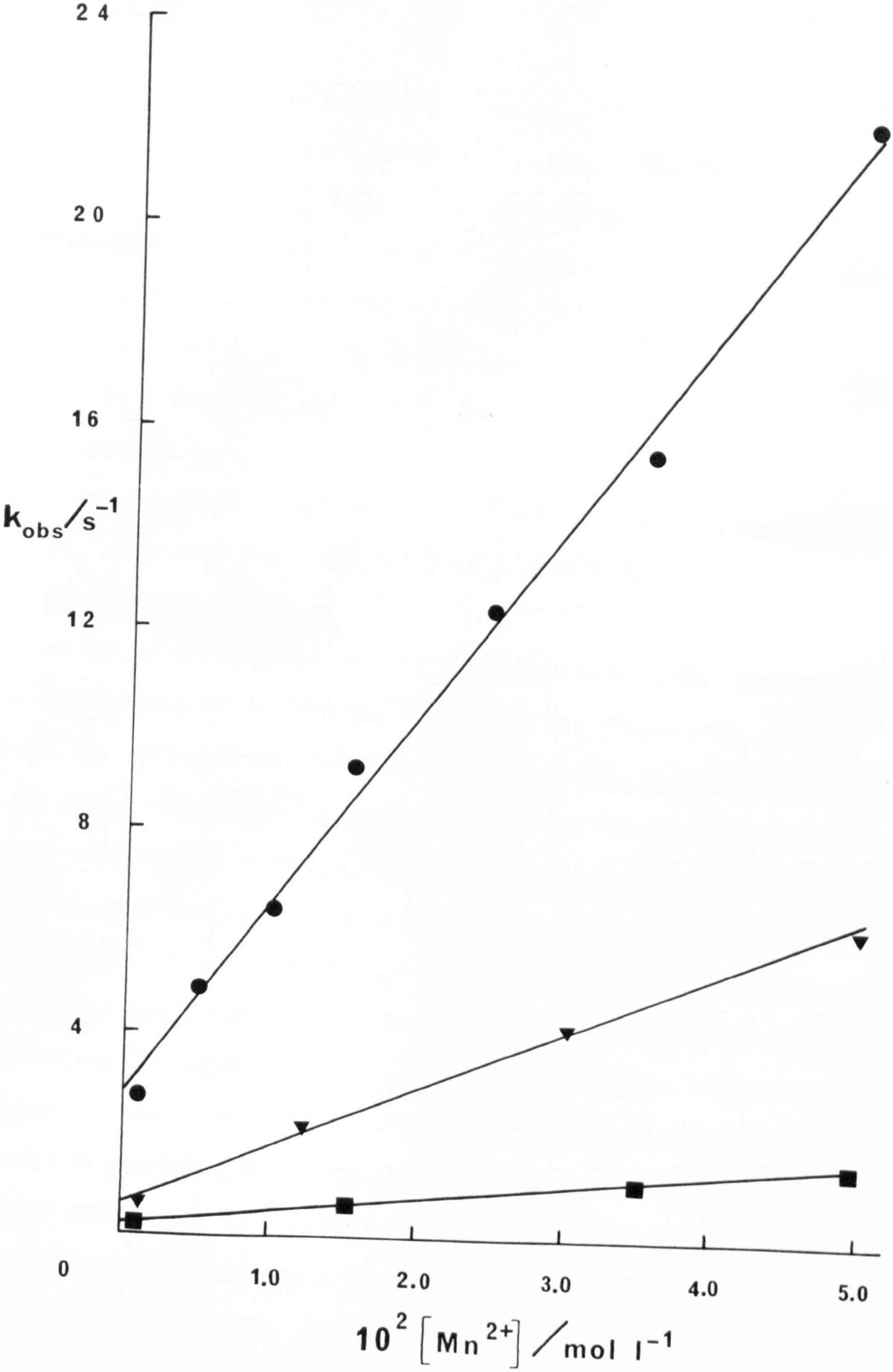
24
20
16
12
8
4
0
k_{obs}/s^{-1}
1.0
2.0
3.0
4.0
5.0
$10^2 [Mn^{2+}] / mol\ l^{-1}$

The activation enthalpies of the three formation reactions are collected in Table 8.

The effect of ionic strength (adjusted with sodium perchlorate), upon the reaction of the Mn(II) ion and phen at 251.8K is shown in Table 9(a). The rate decreases by a factor of about three over the range studied, (I = 0.03 to 0.4). The retardation is particularly marked in the region I = 0 - 0.2. This behaviour is in contrast to that observed for similar reactions in aqueous solution, which are reported[108] to be ionic strength independent, and also to the work of Pearson and Ellgen[74], who found the rate constant for the formation of the $Ni(bipy)^{2+}$ ion in methanol solution to increase by 40% with a change of ionic strength from 0.06-0.2. With such few data it is difficult to attribute this to any one cause. It could possibly be due to a combination of medium effects, ion pair formation between the Mn^{2+} and ClO_4^- ions, and inner-sphere perchlorate complexes.

b) Dissociation reactions

At the lowest concentration of Mn(II) ion used in the study of the acid dissociation of the $Mn(bipy)^{2+}$ complex, two stages were observed. An initial fast reaction was followed by a much larger transmission change of slower rate. The faster stage is assignable to the big species as they usually dissociate more rapidly than mono-complexes[3b]. The second stage was first-order and gave a linear rate plot for several half-lives. This interpretation is supported by the observation of only one reaction at the higher metal ion : ligand ratio, and this rate constant agreed reasonably with that of the second stage of the two stage reaction. The rate constants were independent of the acid concentration. Only one reaction was observed for acid dissociation of the $Mn(phen)^{2+}$ complex at both metal ion concentrations used. The acid induced dissociation rate constants are listed in Table 7 and activation parameters in Table 8.

The reaction between mercuric ion and bipy was shown to be too fast for flow methods in the temperature range used to effect the dissociation of the bipy complex. The mercuric ion induced rate constants were independent of the

TABLE 7

Observed rate constants for the dissociation of the mono-(2,2'-bipyridyl)Mn(II) ion and mono-(1,10-phenanthroline)Mn(II) ion in anhydrous methanol

Dissociation of the mono-(2,2'-bipyridyl)Mn(II) ion by perchloric acid

$[bipy] = 1.03 \times 10^{-5}$ mol l^{-1}, I = 0.2 ($NaClO_4$)

T/K	$10^3[Mn^{2+}]$/mol l^{-1}	$10^2[H^+]$/mol l^{-1}	k_{obs}/s^{-1}
287.7	9.7	5.8	15.5 ± 0.4
274.2	1.07	1.25	6.36 ± 0.01[a]
"	9.7	5.8	5.00 ± 0.08
"	1.07	5.8	5.96 ± 0.09[a]
262.9	9.7	5.8	1.54 ± 0.02

Dissociation of the mono-(1,10-phenanthroline)Mn(II) ion by perchloric acid

$[phen] = 5.2 \times 10^{-5}$ mol l^{-1}, I = 0.2 ($NaClO_4$)

T/K	$10^3[Mn^{2+}]$/mol l^{-1}	$10^2[H^+]$/mol l^{-1}	k_{obs}/s^{-1}
287.7	9.7	5.8	5.89 ± 0.04
274.2	1.07	12.5	1.77 ± 0.02
"	1.07	5.8	1.66 ± 0.03
"	9.7	5.8	1.82 ± 0.02
262.9	9.7	5.8	0.58 ± 0.02

Dissociation of the mono-(2,2'-bipyridyl)Mn(II) ion by mercuric perchlorate

$[Mn^{2+}] = 9.8 \times 10^{-3}$ mol l^{-1}, $[bipy] = 2 \times 10^{-5}$ mol l^{-1}, I = 0.2 ($NaClO_4$)

T/K	$10^3[Hg^{2+}]$/mol l^{-1}	k_{obs}/s^{-1}
289.9	10.0	11.8 ± 0.1
"	2.00	11.6 ± 0.1

a Rate constant derived from second step of a two stage reaction.

TABLE 8

Kinetic data for the formation and dissociation of the mono-complexes of Mn(II) with 2,2',2"-terpyridyl, 2,2'-bipyridyl and 1,10-phenanthroline, and kinetically derived stability constants in anhydrous methanol at 298.1K[a] and I = 0.2 ($NaClO_4$)

	terpy	bipy	phen
k_f [b]	5.3×10^3	1.7×10^4	8.1×10^4
ΔH_f^* [c]	12.8 ± 1.0	11.7 ± 0.01	10.4 ± 0.4
ΔS_f^* [d]	1.3 ± 4.0	0	0
k_a [e]		37	14
ΔH_a^* [c]		13.4 ± 0.5	13.5 ± 0.3
ΔS_a^* [d]		-6.4 ± 1.9	-8.1 ± 0.9
k_a [f]		11.7[g]	
$\log K_1$		2.9[6]	3.8

a extrapolated from data at lower temperatures

b units of 1 mol^{-1} s^{-1}

c units of kcal mol^{-1}

d units of cal mol^{-1} K^{-1}

e rate constants for dissociation induced by perchloric acid, units of s^{-1}

f rate constant for dissociation induced by mercuric ion, units of s^{-1}

g at 289.9K

TABLE 9 (a)

Variation of the observed rate constant with ionic strength for the reaction of the Mn(II) ion with 1,10-phenanthroline in anhydrous methanol at 251.8K

$[Mn^{2+}] = 1.01 \times 10^{-2}$ mol l^{-1}, $[phen] = 5.0 \times 10^{-5}$ mol l^{-1}

I	k_{obs}/s^{-1}	k_f [a]$/s^{-1}$
0.03	45.0 ± 0.8	43.4
0.20	25.3 ± 0.6	23.7
0.30	19.8 ± 0.6	18.2
0.40	15.9 ± 0.1	14.3

a k_f calculated by subtraction of the intercept, ($1.59 s^{-1}$), of the k_{obs} versus $[Mn^{2+}]$ plot, (Figure 17), from k_{obs}

TABLE 9 (b)

Comparison of intercepts obtained from formation studies of the mono-(2,2'-bipyridyl)Mn(II) and mono-(1,10-phenanthroline)Mn(II) ions at 251.8K and the acid induced dissociation rate constants extrapolated to 251.8K

Ligand	Intercept/s^{-1}	k_a/s^{-1}
bipy	2.77 ± 0.16	0.49
phen	1.59 ± 0.14 [b]	0.18

b intercept obtained from the linear portion of the k_{obs} versus $[Mn^{2+}]$ plot below ca. 1.5×10^{-2} mol l^{-1} Mn^{2+} (Figure 17)

mercuric ion concentration. These rate constants are tabulated in Table 7.

4.5. Discussion

Formation reactions

Before discussing possible mechanisms of the formation reactions, it is necessary to consider the effect upon the kinetics of the traces of water present. The highest concentration of water in any of the solutions is about 0.02% by weight, which corresponds to a molarity of ca. 9×10^{-3} mol l^{-1}. The molar ratio of water to metal ion is highest (ca. 5:1) at the lowest metal ion concentration used. This ratio decreases to 1:4 at the highest metal ion concentration. Water is known to be strongly preferred to alcohols in the inner co-ordination sphere of transition metal ions, to the extent that some water molecules remain co-ordinated until essentially all bulk water content has been eliminated[116-7]. Recent solvent exchange[118] and complex formation studies[79] of the Ni(II) and Co(II) ions in water/methanol mixtures, show that the mixed solvated species are more labile than the fully methanolated ions. There are, however, no equivalent data on the Mn(II) ion available. Inspection of the data of Pearson and Ellgen[74], MacKellar and Rorabacher[79] and Bennetto and Caldin[119] shows that only at water concentrations far higher than those used in this work does the water have a significant effect upon the formation rate constants. Lux and Neiboom[118a] were able to estimate the stability constants for the 5:1 and 4:2 methanol:water species of the Co(II) ion in methanol, and also the rate of methanol exchange of these mixed solvated ions. If similar stability constants, and labilities relative to the fully methanolated ion are applicable to the Mn(II) ion in methanol, then calculations show that even at the highest water to metal ion ratio, the concentration of the mixed solvate species will be extremely small, and its contribution to the kinetics negligible.

Extrapolation to 298.1K of the second-order formation rate constants of the three complexes studied, gives the values shown in Table 8. Comparison of these rate constants to the second-order rate constant for

solvent exchange[112] (2.3×10^5 l $mol^{-1}s^{-1}$) at the same temperature, shows that all three ligands react at a rate that is somewhat less than that of solvent exchange. This behaviour is similar to the pattern observed for reactions of this type in aqueous solution, and is suggestive of the dissociative process commonly accepted to apply in aqueous solution. The order of increasing rate constants, phen > bipy > terpy, is the same as that consistently obtained in aqueous solution with a number of metal ions.[33]

By analogy with similar formation reactions in aqueous solution, an attempt could be made to interpret the data in terms of the outer-sphere complex scheme outlined in Chapter 1. A value of K_o could be calculated from equation (1.2) with the exponential term set to unity[71]. Alternatively, and possibly more realistically in view of the uncertainty in calculating K_o values for large neutral multidentate ligands[47], an "experimental" K_o value could be derived from the identity $K_o = k_f/k_o$ from a similar reaction in aqueous solution. This value could be doubled to allow for the increased size of the methanolated ion over the aquo ion[79]. Equally, as there is no direct evidence for outer-sphere association with neutral ligands, the variation in rate constants of the three ligands studied could plausibly be explained by postulating a D mechanism involving no outer-sphere complexes, and which is showing some discrimination between the three ligands.

However, closer comparison with either of the above mechanisms is unwarranted when the activation enthalpies of solvent exchange[112] (6.8 kcal mol^{-1}) and complex formation (Table 8) are considered. In aqueous solution, the enthalpies of activation of formation are usually very similar to that for water exchange at the metal ion. As can be seen from Table 8, the activation enthalpies (ΔH_f^*) of the complex formations studied in this work are considerably greater than that (ΔH_{ex}^*) of methanol exchange at the Mn(II) ion. The difference cannot be accounted for by outer-sphere association. The enthalpy of formation of an outer-sphere complex with a neutral ligand will be very small[77]. Thus, although the formation rate constants are expected to be close to the solvent

exchange rate constant at 298.1K, at the temperatures at which the formation kinetics were measured, they are much less than the solvent exchange rate than the outer-sphere scheme or a D mechanism would predict.

The large activation enthalpies suggest that there is an additional energy barrier besides that associated with solvent loss. A possible explanation could be some form of steric effect. Rorabacher and MacKellar[79] have suggested that the formation of the mono-(2,2'-bipyridyl)Ni(II) ion in methanol/water mixtures[77] may involve a steric effect and/or a rate determining ring closure. For the bipy complex, if a rate determining ring closure were applicable here, then the enthalpy diagram shown in Figure 19(a) would apply. (ΔH_{ex}^{*} is the enthalpy of activation for the formation of the first bond, including any small amount due to outer-sphere association, and is taken as the enthalpy of activation of solvent exchange, and ΔH_{2}^{*} is the overall enthalpy of activation for the formation reaction).

In the introduction to this chapter, it was mentioned that bipy and terpy exist in solution in <u>trans</u> and <u>trans-trans</u> configurations, respectively. It is reasonable to assume that these ligands approach the metal ion in this configuration and that the first metal-ligand bond is formed before rotation of the remaining rings into the <u>cis</u> position. As the methanol molecules in the inner-sphere of the metal ion are larger than water molecules, they could conceivably offer some barrier to the rotation of the remaining pyridine rings required to complete chelate formation.

The formation of the terpy complex could possibly involve steric hindrance in both the second and third bond formations. The activation enthalpies of the bipy and terpy complexes are, however, very similar. A possible enthalpy profile for the terpy complex formation is shown in Figure 19(b). The unidentate and bidentate intermediates would approximate to the mono-pyridyl and mono-bipy complexes of Mn(II). The enthalpy of formation of the bipy complex is expected to be greater than that of the pyridyl complex ($|\Delta H_{2}| > |\Delta H_{1}|$, Fig. 19(b)). If steric effects are involved in the second and third metal-ligand bond formations, then the activation

FIGURE 19

Figure 19(a)

Enthalpy-reaction co-ordinate profile for successive bond formation of a metal ion to a bidentate ligand where ring closure is the rate determining step.
(Charges omitted, L-L = a bidentate ligand).

Figure 19(b)

Possible enthalpy-reaction co-ordinate profile for the reaction: Mn^{2+} + terpy $\longrightarrow$ $Mn(terpy)^{2+}$ in methanol solution.
(Charges omitted, L-L-L = 2,2',2''-terpyridyl).

Figure 19 (a)

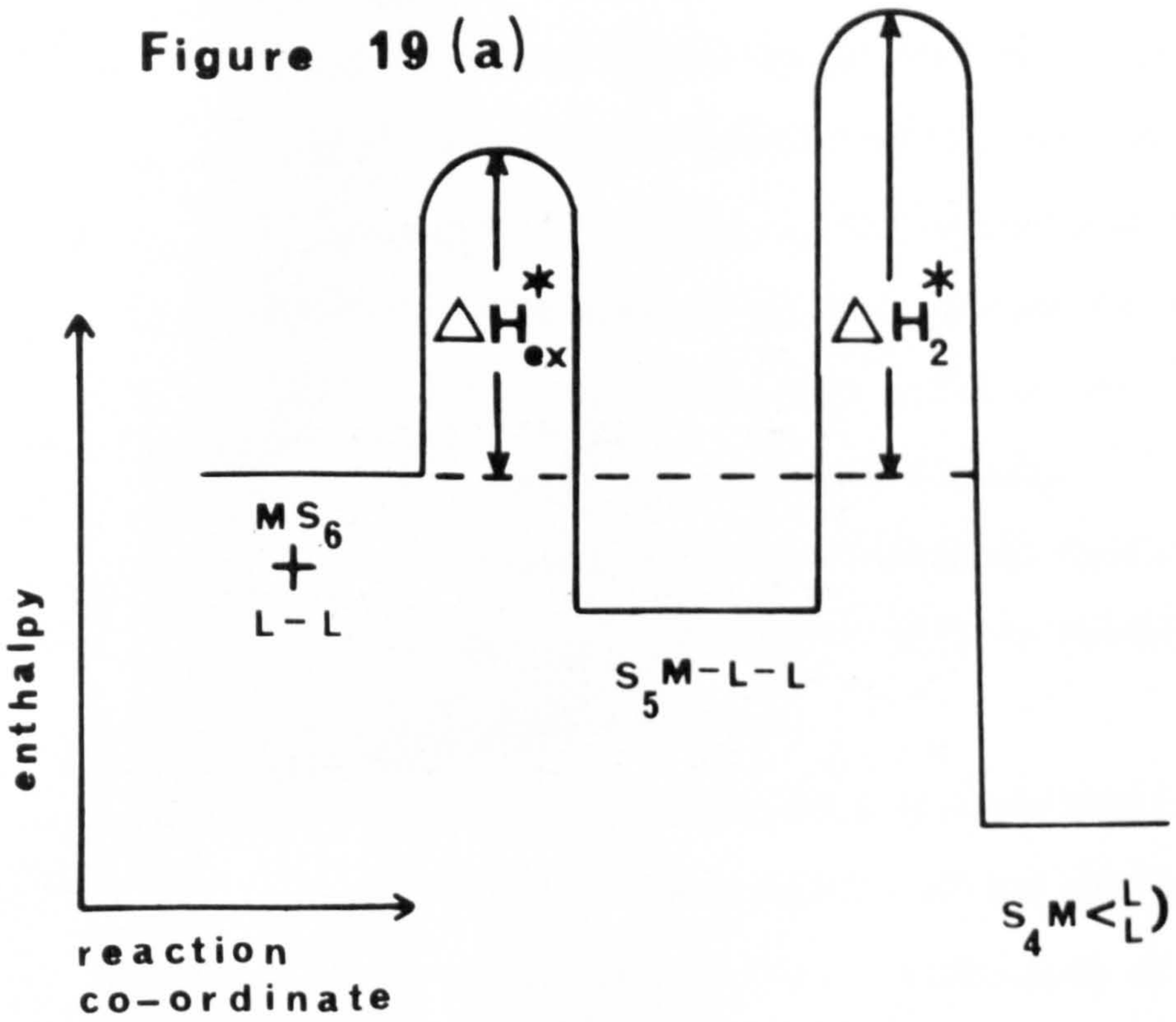

Figure 19 (b)

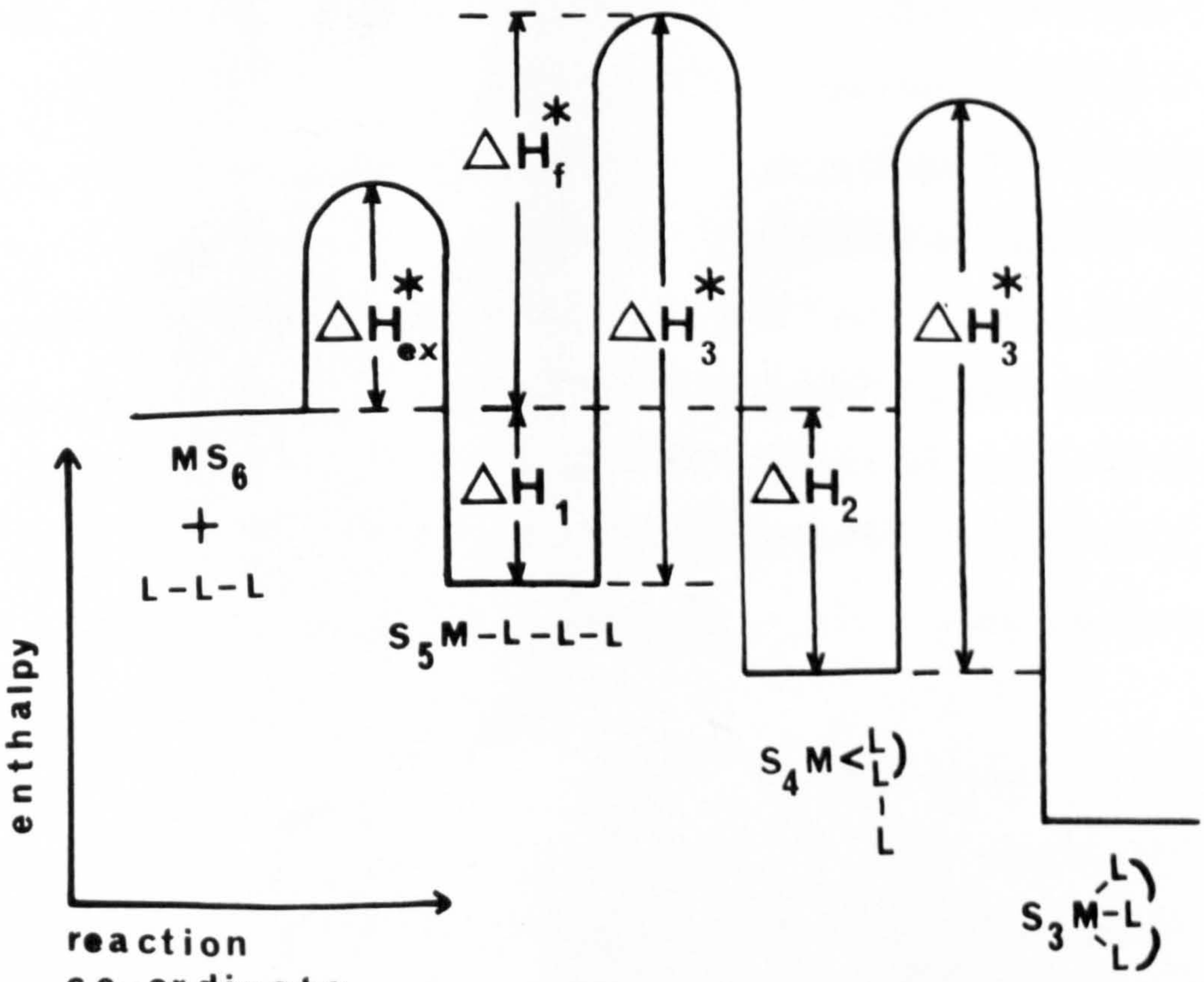

enthalpies (ΔH_3^*, Fig. 19 (b)) for these two steps would be very similar. If this is the case it can be seen from Figure 19 (b) that the formation of the second metal-ligand bond determines the overall activation enthalpy (ΔH_f^*) of the formation reaction. Moreover, as the enthalpy barrier is possibly due to rotation of a pyridyl residue and this process is common to both the formation of bipy and terpy complexes, this could account for the similarity of the activation enthalpies for these two ligands.

In a later section of this chapter, additional evidence that ring closure may be rate determining for the bipy complex will be presented from consideration of the dissociation rate constants.

However, the postulate of rate determining ring closure does not readily explain why the activation enthalpy for the formation of the phen complex is so large. The difference between the activation enthalpies of the phen and bipy complexes is only 1.3 kcal mol^{-1}, and is similar to the difference between the activation enthalpies of the bipy and terpy complexes. As phen is a rigid molecule, once first bond formation has occured, the second nitrogen atom is expected to be in a favourable position to complete chelate formation. There is, however, no positive evidence which precludes the formation of a species which involves the ligand bent back from the metal ion with a strained bond to the one co-ordinating nitrogen[120]. Equally though, the high activation enthalpy of the phen reaction suggests the possibility that the formation of the first bond could be sterically hindered. This could arise because the rigidity of the phen molecule places both of the nitrogen containing sides of the heterocyclic rings in the vicinity of the metal ion. Unlike bipy and terpy, phen cannot twist one heterocyclic ring perpendicular to the other which might aid penetration of one nitrogen atom to form the first bond.

For a series of complex formation reactions in non-aqueous solvents, Bennetto and Caldin report[80] large variations between the activation enthalpies of formation and the respective solvent exchange. According to their hypothesis[82] , for a given complex formation reaction, there should be

a linear relationship between the quantity $\triangle\triangle H^{*}$ (= $\triangle H_{f}^{*} - \triangle H_{ex}^{*}$) and the enthalpy of vaporisation of the solvent ($\triangle H_{evap}$). The intercept of such a plot at $\triangle\triangle H^{*} = 0$, should correspond to the heat of vaporisation of the ligand as a liquid. When the results of this work are placed upon such a plot the agreement with the data already presented[82] is not good. The correlation of the quantities $\triangle\triangle H^{*}$ and $\triangle H_{evap}$ is believed[82] to arise from the effect of the incoming ligand upon the solvent structure. In this work, however, the large amount of sodium perchlorate used to control the ionic strength may also modify the solvent structure. Small cations such as Na^{+} are known[77] to increase the degree of order of a solvent. Thus, the experimental conditions used here may invalidate a comparison with the work of Bennetto and Caldin[80,82].

Dissociation reactions

The intercepts that occurred on the k_{obs} versus $[Mn^{2+}]$ plots for the formation of the mono-bipy and mono-phen complexes (Figures 17 and 18) could conceivably have been equated to the neutral dissociation rate constants (k_{d} in equation (4.1)). However, the independent measurement of the dissociation rate constants, induced by both mercuric ion and perchloric acid (Table 7) shows this not to be so. Notably, the acid dissociation rate constants, when extrapolated to 251.8K, are considerably smaller than the intercepts (Table 9 (b)). Although some error must be involved in such a large extrapolation, the difference between the intercepts and the acid dissociation rate constants is still significant. For a flexible bidentate ligand, such as bipy, acid catalysis of dissociation is well known[3b]. The reaction scheme believed to apply is shown below, (omitting charges and co-ordinated solvent molecules).

$$
\begin{array}{ccccc}
 & \overset{k_{-2}}{\underset{k_{2}}{\rightleftharpoons}} & & \xrightarrow{k_{-1}} & \\
M\!<\!\begin{matrix}L\\L\end{matrix} & & M\text{-}L\text{-}L & & M + L\text{-}L \\
 & & \Big\downarrow H^{+} \;\; \Big\uparrow K_{1} & & \\
 & & M\text{-}L\text{-}LH^{+} & \xrightarrow{k_{-3}} & M + L\text{-}LH^{+}
\end{array}
\qquad (4.2)
$$

where $K_{1} = [M\text{-}L\text{-}LH^{+}]/[M\text{-}L\text{-}L][H^{+}]$ and $k_{-3} > k_{-1}$

Applying the steady-state approximation to the partly dissociated species the first-order dissociation rate constant is:

$$k_{obs} = \frac{k_{-2}(k_{-1} + K_1 k_{-3}[H^+])}{k_{-1} + k_2 + K_1 k_{-3}[H^+]} \qquad (4.3)$$

Under the conditions used here (Table 7) the measured rate constants are independent of acid concentration, which implies $K_1 k_{-3}[H^+] \gg (k_2 + k_{-1})$ and $k_{obs} = k_{-2}$, $(= k_a)$.

By analogy with Wilkins' et al. data[109] for the dissociation of some metal complexes by other metal ions, the mercuric ion induced rate constant can be equated to the rate constant under neutral conditions, i.e. $[H^+] = 0$, and $k_{obs} = (k_{-2}k_{-1})/(k_2 + k_{-1})$, $(= k_n)$. Hence the acid dissociation rate constant will always be greater than or equal to the rate constant under neutral conditions.

The dissociations of phen complexes are not acid catalysed[3b]. This is believed to be due to the rigidity of the phen molecule, which prevents protonation of the unidentate intermediate. The rate constants listed in Table 7 for the phen complexes are therefore expected to be the same as those under neutral conditions.

Hence, for both the phen and bipy complexes the intercepts observed in the complex formation studies cannot be due to the neutral dissociation rate. Similar unexplained large intercepts were obtained[80] during studies on the formation of the $Ni(bipy)^{2+}$ ion in acetonitrile and acetone, and the $Ni(terpy)^{2+}$ ion in acetonitrile. A possibility that the intercepts refer to the dissociation of a unidentate intermediate, with rate constant k_{-1} (equation (4.2)) can be rejected as not compatible with the observed kinetic order of the formation reactions. It is, however, interesting that the size of the intercepts, bipy > phen > terpy parallels the complex stability.

With bidentate ligands where acid catalysis occurs, the ratio of the acid (k_a) to neutral (k_n) dissociation rate constants is $k_a/k_n = (k_2 + k_{-1})/k_{-1}$. For the bipy complex the experimental value of this ratio is 1.73 at 289.9K, and $k_2/k_{-1} = 0.73$. From equation (1.7) it can be seen that this is the

condition for the ring closure step to contribute to the rate constant for complex formation. This ratio of k_2/k_{-1} can be compared to the estimated[47] values of k_2/k_{-1} in aqueous solution of 20, 75 and 1.3 for the $Ni(en)^{2+}$, $Ni(bipy)^{2+}$ and malonatoNi(II) ions, respectively. In the first two cases normal substitution is believed to apply, and in the formation of the latter complex two steps corresponding to unidentate formation and ring closure have been directly observed[70].

The effect of the ring closure rate upon the formation rate constant, k_f, of the $Mn(bipy)^{2+}$ ion can be put on a quantitative basis. If, at 289.9K $k_2/k_{-1} = 0.73$, then from equation (1.7), the value of k_f is reduced by a factor of 1/2.37 in comparison to the product $K_o k_1$. Hence, near room temperature the effect of the ring closure step is small. It follows that the first metal-ligand bond formation is normal.

Unfortunately, in the case of the phen complex, it is not possible to estimate k_2/k_{-1} in this manner, and no confident statement as to whether ring closure is involved can be made.

From the formation and dissociation rate constants under neutral conditions, the kinetic equilibrium constants, K_1 ($=k_f/k_d$) can be calculated for the $Mn(bipy)^{2+}$ and $Mn(phen)^{2+}$ ions in methanol. However, in view of extrapolations involved they can only be regarded as approximate. The values are tabulated in Table 8 and compared to the aqueous values below.

Stability constants for the mono-complexes of the Mn(II) ion with 2,2'-bipyridyl and 1,10-phenanthroline in water and methanol at 298.1K

Ligand	log K_1 (MeOH)[a]	log $K_1(H_2O)$[b]
phen	3.8	4.1
bipy	2.9[c]	2.6

a at I = 0.2 ($NaClO_4$)

b from ref. 110

c at 289.9K

The values of K_1 in methanol are remarkably similar to those in aqueous solution. In aqueous solution, because of the constancy of k_f values for

ligands of the same charge, the stability constant is largely determined by the dissociation rate constant. In contrast, in methanol solution the phen and bipy complex formation rates differ by a greater factor than the neutral dissociation rates.

A comparison of the neutral dissociation rate constants of some metal complexes in water, methanol and liquid ammonia is given in Table 10. The Mn(II) complexes dissociate at a slower rate in methanol than in water. This trend is parallel to the Co(II) and Ni(II) complexes. This is understandable in terms of the inner-sphere effects recently discussed by Rorabacher and MacKellar[79]. The rate of solvent exchange at the Mn(II) ion increases $NH_3 > H_2O > MeOH$ (Table 10). As this order is the same as that for solvent exchange at the Ni(II) and Co(II) ions, it implies that this is also the order of the bond strengths of these solvents to the Mn(II) ion. The substitution of weaker co-ordinating ligands in the inner solvation sphere decelerates the metal-ligand bond rupture rate for all other ligands in the inner-sphere[79].

4.6. Conclusions

A low temperature stopped-flow apparatus has been developed and used to study the rates and mechanisms of some complex formation reactions of the manganese(II) ion in methanol. The rate constants and activation enthalpies of the formations of the 2,2'-bipyridyl and 1,10-phenanthroline complexes could not have been measured by flow equipment at ambient temperatures but were easily obtained by use of the low temperature apparatus.

The pattern of these formation reactions in methanol has been found to be different from that for similar reactions in water. Extrapolation of the measured formation rate constants to room temperature, predicts that complex formation should proceed at a rate similar to methanol exchange at the manganese(II) ion. However, the activation enthalpies for the formation reactions are much larger than that of the solvent exchange process, whereas for similar reactions in aqueous solution the two

TABLE 10

Logarithmic values of the rate constants for the dissociation of some divalent metal ion complexes in various solvents at 298.1K[a], (units of k, s^{-1})

	← Pure solvents →		
M-L bond	CH_3OH	H_2O	NH_3
Ni - CH_3OH	3.0	5.9	
Ni - H_2O		4.5	
Ni - NH_3	-1.7 (est.)	0.6	5.0
Co - CH_3OH	4.3	6.8	
Co - H_2O		5.9	
Co - NH_3	0.3 (est.)	3.2	7.0
Mn - CH_3OH	5.98 [b]		
Mn - H_2O		7.5 [c]	
Mn - NH_3			7.6 [d]
Mn - bipy	1.07[e,f]	>2.3 [g]	
Mn - phen	1.15 [e]	2.08 [g]	

a from ref 79 unless otherwise stated

b ref. 112

c ref. 50

d ref. 121

e this work

f at 289.9K

g ref. 109

activation enthalpies are usually comparable.

Rate determining chelate ring closure has been suggested as one possibility to account for this. Consideration of the relative magnitude of the acid and mercuric ion induced dissociation rate constants of the $Mn(bipy)^{2+}$ ion does appear to confirm this. Similar steric effects are to be expected for the $Mn(terpy)^{2+}$ ion, and in this case, additional support for this hypothesis could be obtained by studying the acid and metal ion induced dissociations. The dissociations of terpy complexes are known to be acid catalysed[122], in a similar manner to their bipy analogues. If, in methanol solution, the formations of both the second and third metal-ligand bonds of the terpy complex are sterically hindered, then the acid and metal ion induced rate constants should be very similar.

The similarities of the activation enthalpies and formation rate constants of the phen and bipy complexes suggests that the rate of the phen complex formation is also controlled by ring closure. In view of the rigidity of the phen molecule, this is surprising. Unfortunately, it was not possible in this case to confirm whether or not ring closure is involved by comparison of the acid and metal ion induced dissociation rate constants. It is, perhaps, equally possible that the first metal-ligand bond formation is sterically hindered, and that the similarities of the formation rate constants and activation enthalpies for the phen and bipy complexes are fortuitous.

From the dissociation data of the $Mn(bipy)^{2+}$ ion it has been possible to show that near to room temperature the effect of the rate determining ring closure is small. This implies that the formation of the first metal-ligand bond is normal. This is possibly due to bipy being able to twist one ring perpendicular to the other. It would thus be expected that complex formation with a unidentate ligand, such as pyridine, would have an activation enthalpy similar to that of solvent exchange.

The three ligands used here all form five-membered chelate rings. In aqueous solution, it appears that even with the very labile Cr^{2+} and Cu^{2+} ions, the formations of mono-complexes of five-membered ring chelates are normal[69]. Steric control presumably arises in methanol solution because of the bulkiness of the methyl group of the co-ordinated solvent. As organic solvents are generally bulkier than water, rate determining ring closure could well occur with chelating ligands and the manganese(II) ion in the majority of cases. Obviously, these reactions must be studied in other solvents. It would be especially interesting to repeat this work in acetonitrile, where it has been found[80] that the Ni(II) ion reacts with bipy at a faster rate than the solvent exchange. In terms of the hypothesis of Bennetto and Caldin[82], concerning the effect of solvent structure on formation reactions, the results of this work offer little, either for or against. The presence of sodium perchlorate in this work is a complication. Perhaps further studies in other solvents, at lower metal ion concentrations and lower ionic strength will be more rewarding.

The work in this thesis has used neutral ligands. If, as Pearson and Kilgen's study[74] suggests, negatively charged ligands react at comparable or greater rates in non-aqueous solvents than in water, a low temperature stopped-flow apparatus should be very suitable for studying such reactions. Ion-pairing will be considerably greater in the lower dielectric media. Certainly if the relation $k_f = K_o k_{ex}$ applies, negatively charged ligands will probably react with labile metal ions in non-aqueous solvents faster than a conventional stopped-flow apparatus could measure. If the dissociative mechanism is applicable, the activation enthalpies (even assuming no steric effects) should be similar to those of solvent exchange. The latter enthalpies are often considerable[33] and hence the reactions should be slowed accordingly by low temperatures. For example, preliminary experiments on the formation of the mono-(8-hydroxyquinolato)Mn(II) ion in methanol, shows that at 226.4K the second-order formation rate constant is 8.3×10^2 l mol^{-1} s^{-1}, about four times greater than the formation rate

constant of the $Mn(phen)^{2+}$ ion at this temperature.

Non-aqueous solvents were first applied to kinetic studies of co-ordination reactions in order to permit the use of low temperatures for slowing down reactions which were considered instantaneous in water. Currently, the use of non-aqueous and mixed solvents has come under renewed interest as a means of investigating the role of the solvent itself in influencing reaction rates. As such studies are extended to the metal ions more labile than nickel(II), a low temperature stopped-flow apparatus will prove a useful instrument.

APPENDIX

COMPUTER PROGRAMS

The programs listed in this appendix are written in Elliot 4100 Algol and were used on an Elliot 4130 computer.

The author is grateful to Dr. P. Moore for the programs ACTPAR, SFORX and LSAD.

```
PROGRAM          SFDATA ;

REACTION RATES AND PLOTS FROM STOPPED-FLOW DATA;

"BEGIN"
"ARRAY"  XX, YY[0:30,0:30];
"ARRAY"AA,BB[0:30];
"ARRAY"EE[0:30];
"INTEGER"NS,J;
"INTEGER""ARRAY"N[0:30];
"INTEGER""ARRAY"CT[0:30];
"INTEGER"V;"REAL"W;
"READ" NS;
V:=50;W:=0.1;
"FOR" J:=0"STEP" 1"UNTIL" ( NS - 1) "DO"
"BEGIN""READ"CT[J],N[J];
"PRINT"``F'', `STOPPED-FLOW DATA`,``L3'';
"PRINT"`RUN NUMBER`,``S2'',SAMELINE,CT[J],``L3'';
"BEGIN""REAL"IO,MNF,K,C,D,F,G,M,DY;
"REAL"A,B,E;
"INTEGER"I;
"ARRAY"T,DT,Y[0:N[J]-1];
"READ"IO,INF,K;
"PRINT"``S'',SAMELINE,`T (MSECS)    D(T)      LOG[D(T)-D(INF)] + 2`,
``L2'';
"FOR"I:=0"STEP"1"UNTIL"N[J]-1"DO"
"BEGIN""READ"T[I],DT[I];
DT[I]:=INF-DT[I];
"END";
INF:=(LN(IO/INF))/2.303;
"FOR"I:=0"STEP"1"UNTIL"N[J]-1"DO"
"BEGIN"
T[I]:=K*T[I];
XX[I,J]:=T[I];
DT[I]:=(LN(IO/DT[I]))/2.303;
Y[I]:=LN(ABS(DT[I]-INF));
YY[I,J]:=((Y[I]/2.303)+2);
"PRINT"FREEPOINT(6),T[I],SAMELINE,``S4'',DT[I],``S6'',
((Y[I]/2.303) + 2 ) , ``L'' ;"END" ;
"PRINT"``L'',SAMELINE,``S'', `INFINITY`S3'',FREEPOINT(6),INF,``L5'';
"COMMENT"LEAST SQUARES ANALYSIS FOLLOWS;
"PRINT"`LEAST SQUARES ANALYSIS OF DATA ABOVE`,``L2'';
A:=B:=D:=E:=G:=0;
"FOR"I:=0"STEP"1"UNTIL"N[J]-1"DO"
"BEGIN"A:=A+T[I];
B:=B+Y[I];
D:=D+T[I]*T[I];
E:=E+T[I]*Y[I];
"END"; F:=N[J]*D-A*A;
M:=(N[J]*E-A*B)/F;
C:=(B*D-A*E)/F;
EE[J]:=XX[N[J]-1,J];
"FOR"I:=1"STEP"1"UNTIL"N[J]-1"DO"
"IF"YY[I,J]<0"AND"YY[I-1,J]"GE"0"THEN"EE[J]:=XX[I,J];
"FOR"I:=0"STEP"1"UNTIL"N[J]-1"DO"
G:=G+(M*T[I]+C-Y[I])↑2;
DY:=SQRT(G/(N[J]-2));
"PRINT"``S8'',SAMELINE,`K = `,FREEPOINT(6),(-1000*M),
` SECONDS(-1)`,``S6'',`ESD K = `,
(1000*DY*SQRT(N[J]/F)),``S`SECONDS(-1)`,``L2'';
"PRINT"`HALF-LIFE = `,SAMELINE,FREEPOINT(6),
(-0.693/M),``S`MILLISECONDS`;
```

```
BB[J]:=M/2.303;
AA[J]:=C/2.303 +2;
"END";
"END";
"BEGIN""INTEGER"M,I,MM,D,Z;
"REAL" XSCALE,YSCALE;
"REAL"QQ,LY;
"COMMENT" N = TOTAL NO. OF POINTS
V=X SCALE PLOTTER STEP
W = Y SCALE PLOTTER STEP
D=MAX VALUE OF X
E=LAST CO-ORDINATE PLOTTED;
PUNCH(5);
SETORIGIN(600,0);
XSCALE:=-1.0106;
YSCALE:=-1.0106;
LY:=1.0106;
"FOR" J:= 0 "STEP" 1 "UNTIL" (NS-1) "DO"
"BEGIN"
N[J]:=N[J]-1;
"FOR"I:=0"STEP"1"UNTIL'N[J]"DO"
"BEGIN"
"IF"YY[I,J]<LY"THEN"LY:=YY[I,J];
"IF"YY[I,J]>YSCALE"THEN"YSCALE:=YY[I,J];
"IF"XX[I,J]>XSCALE"THEN"XSCALE:=XX[I,J]    "END";
"END";
QQ:=(ENTIER(LY/W))*W;
"IF"LY<0.3"AND"LY>0.0"THEN"QQ:=0.0;
YSCALE:=YSCALE+NS*W-QQ;
"IF"XSCALE>500"THEN"V:=100;
"IF"XSCALE>1000"THEN"V:=500;
"IF"XSCALE>5000"THEN"V:=1000;
"IF"XSCALE>10000"THEN"V:=5000;
"IF"XSCALE>50000"THEN"V:=10000;
"IF"XSCALE>100000"THEN"V:=50000;
M:=ENTIER(YSCALE/W+1.0);
Z:=ENTIER(XSCALE/V+1.0);
YSCALE:=2000/W/M;
XSCALE:=1600/V/Z;
MOVEPEN(0,0);
"FOR"I:=1"STEP"1"UNTIL"Z"DO"
"BEGIN"DRAWLINE(I*XSCALE*V,0);
DRAWLINE(I*XSCALE*V,20);
DRAWLINE(I*XSCALE*V,0);
"END";
"FOR"I:=1"STEP"1"UNTIL"M"DO"
"BEGIN"DRAWLINE(1600,I*YSCALE*W);
DRAWLINE(1580,I*YSCALE*W);
DRAWLINE(1600,I*YSCALE*W);
"END";
"FOR"I:=Z-1"STEP"-1"UNTIL"0"DO"
"BEGIN"DRAWLINE(I*XSCALE*V,2000);
DRAWLINE(I*XSCALE*V,1980);
DRAWLINE(I*XSCALE*V,2000);
"END";
"FOR"I:=M-1"STEP"-1"UNTIL"0"DO"
"BEGIN"DRAWLINE(0,I*YSCALE*W);
DRAWLINE(20,I*YSCALE*W);
DRAWLINE(0,I*YSCALE *W);
"END";
"COMMENT"AXES NOW COMPLETE;
```

```
"FOR"I:=0"STEP"1"UNTIL"M"DO"
"BEGIN"
MOVEPEN(-300,I*YSCALE*W-15,0);
"PRINT"WAY(0,5),ALIGNED(3,3),(I*W+QQ);
"END";
"FOR" I:=0"STEP"1"UNTIL"Z"DO""BEGIN"
MOVEPEN(I*XSCALE*V-210,-60);
"PRINT"WAY(0,5),I*V;
"END";
MOVEPEN(200,2050);
"PRINT" WAY(0,5),'SFDATA RUN NO ';
"FOR" J:=0"STEP" 1"UNTIL" ( NS - 1) "DO"
"BEGIN"
"FOR"I:=0"STEP"1"UNTIL"N[J]"DO"
"BEGIN"MOVEPEN(XSCALE*XX[I,J], YSCALE*(YY[I,J]+J*W-QQ));
CENCHARACTER(J+1);
"END";
MOVEPEN(0,(AA[J]+J*W-QQ)*YSCALE);
DRAWLINE(EE[J]*XSCALE,(AA[J]+BB[J]*EE[J]+J*W-QQ)*YSCALE);
MOVEPEN(1300,1900-J*50);
"PRINT"WAY(0,3),ALIGNED(4,0),CT[J];
MOVEPEN(1500,1910-J*50);
CENCHARACTER(J+1);
MOVEPEN(500+150*J,2050);
"PRINT"WAY(0,5),ALIGNED(4,0),CT[J];
"END";
MOVEPEN(-330,600);
"PRINT"WAY(1,5),'LOG[D(T)-D(INF)]+2';
MOVEPEN(750,-200);
"PRINT" WAY(0,5),'TIME (MSECS)';
MOVEPEN(0,3500);
"END";
"COMMENT" INPUTS AS FOLLOWS: "&RUN" CARD, M(NO. OF LINES TO BE PLOTTED
PER SET OF AXES, MAX OF 8), CT[A](DATA LABEL OF FIRST PLOT),
N[A](NO. OF POINTS IN PLOT "A"), IO[A](100% TRANSMISSION),
INF[A](INFINITY READING), K[A](TIME FACTOR, 1 MM = K MS),
T[1A](TIME IN MM), I[1A](INTENSITY AT TIME T[1A]).....T[NA], I[NA],
CT[B], N[B], ETC.....CT[M], N[M], ETC.....
CONTROL CARD;
"END"OFPROGRAM;
```

```
PROGRAM      ACTPAR ;

ACTIVATION PARAMETERS;

"BEGIN""INTEGER"N;"READ"N;
"PRINT"'CALCULATION OF ACTIVATION PARAMETERS FOR SYSTEM :'L9'';
"BEGIN""REAL"A,B,C,D,F,G,H,M,P,DM,DC,DDY;
"INTEGER"I;"ARRAY"X,Y,DY,W[1:N];
A:=B:=D:=F:=G:=H:=0;
"PRINT"' TEMPERATURE          RATE                WEIGHT'L'';
"PRINT"'(CENTIGRADE)       CONSTANT'L2'';
"FOR"I:=1"STEP"1"UNTIL"N"DO"
"BEGIN""READ"X[I],Y[I],DY[I];
"IF"DY[I]-1=0"THEN""GOTO"L1;
DY[I]:=DY[I]/Y[I];

L1:W[I]:=1/(DY[I]*DY[I]);
"PRINT"''S3'',SAMELINE,ALIGNED(3,1),X[I],''S7'',
SCALED(4),Y[I],''S6'',W[I],'L';
```

```
X[I]:=1000/(273.1+X[I]);Y[I]:=LN(Y[I]);
H:=H+W[I];A:=A+W[I]*X[I];
B:=B+W[I]*X[I]*Y[I];D:=D+W[I]*Y[I];
F:=F+W[I]*X[I]*X[I];"END";
P:=H*F-A*A;M:=(H*B-A*D)/P;C:=(F*D-A*B)/P;
"FOR"I:=1"STEP"1"UNTIL"N"DO"G:=G+((M*X[I]+C-Y[I])↑2)*W[I];
DDY:=SQRT(G/(N-2));DM:=DDY*SQRT(H/P);DC:=DDY*SQRT(F/P);
"PRINT"``L4`ARRHENIUS PARAMETERS :`L2``;
"PRINT"``S2`ENERGY OF ACTIVATION = `,SAMELINE,
ALIGNED(2,2),-1.9872*M,``S4`E.S.D. = `,1.9872*DM,` KCALS. PER MOLE`;
"PRINT"``L``,SAMELINE,``S8`LOG10(A-FACTOR) = `,
ALIGNED(2,2),C/2.303,``S4`E.S.D. = `,DC/2.303,``L3``;
"PRINT"`ENTHALPY OF ACTIVATION = `,SAMELINE,
ALIGNED(2,2),-1.9872*(M+0.2981),
``S4`E.S.D. = `,1.9872*DM,` KCALS. PER MOLE AT 25 DEGREES CENTIGRADE`;
"PRINT"``L``,SAMELINE,` ENTROPY OF ACTIVATION = `,
ALIGNED(2,2),1.9872*(C-30.4575),``S4`E.S.D. = `,
1.9872*DC,` E.U.`,``S12`AT 25 DEGREES CENTIGRADE`F``;"END";
"COMMENT"INPUTS AS FOLLOWS: N(NO. OF POINTS), T[1](CENTIGRADE),
K[1](RATE CONSTANT AT T[1], UNITS OF MOLES AND SECS.), E.S.D. K[1].....
T[N], K[N], E.S.D. K[N];
"COMMENT" IF EQUAL WEIGHTING OF POINTS REQUIRED SET ALL ESD K VALUES
TO UNITY;
"END" OF PROGRAM;
```

```
PROGRAM      LSAD

WEIGHTED LINEAR LEAST SQUARES ANALYSIS;

"BEGIN""INTEGER"CT,N;"READ"CT,N;
"PRINT"`WEIGHTED LINEAR LEAST SQUARES ANALYSIS`L3``;
"PRINT"`OUTPUT`,SAMELINE,DIGITS(4),CT,``L``;
"BEGIN""REAL"A,B,C,D,F,G,H,M,P,DM,DC,DDY;
"INTEGER"I;"ARRAY"X,Y,DY,W[1:N];
A:=B:=D:=F:=G:=H:=0;
"FOR"I:=1"STEP"1"UNTIL"N"DO""BEGIN""READ"X[I],Y[I],DY[I];
W[I]:=1/(DY[I]*DY[I]);
H:=H+W[I];A:=A+W[I]*X[I];B:=B+W[I]*X[I]*Y[I];D:=D+W[I]*Y[I];
F:=F+W[I]*X[I]*X[I];"END";
P:=H*F-A*A;M:=(H*B-A*D)/P;C:=(F*D-A*B)/P;
"FOR"I:=1"STEP"1"UNTIL"N"DO"G:=G+((M*X[I]+C-Y[I])↑2)*W[I];
DDY:=SQRT(G/(N-2));
DM:=DDY*SQRT(H/P);DC:=DDY*SQRT(F/P);
"PRINT"``S4``,SAMELINE,`C = `,C,``S6``,`ESD C = `,DC,``L``;
"PRINT"``S4``,SAMELINE,`M = `,M,``S6``,`ESD M = `,DM,`L`;
"PRINT"`ESD Y = `,SAMELINE,DDY,``L4``; "END";
"COMMENT"INPUTS AS FOLLOWS: CT(DATA LABEL), N(NO. OF POINTS),
X[1],Y[1],ESD Y[1].....................
X[N],Y[N],ESD Y[N];
"COMMENT" IF WEIGHTING IS NOT REQUIRED SET ALL ESD Y VALUES
TO UNITY;
"END"OFPROGRAM;
```

```
PROGRAM          SFORK ;
ANALYSIS OF SPECTROPHOTOMETRIC DATA FOR A SERIES FIRST-ORDER REACTION;

"BEGIN""REAL"TA,EPA,EPB,EPC,PL,DB,K1,K2,STDF;
"REAL"DF,STSDELTAS,D,PO;
"REAL"TIM;
     "REAL"K,INC;
"INTEGER"CT,CYCLE,N,TX,TY,TZ;
"INTEGER"MODE;
"READ"MODE;
"READ"CT,N,TA,EPA,EPB,EPC,PL,DB,K1,K2;
     "READ"K,INC;
TX:=TY:=TZ:=0;DF:=STDF:=1;
"PRINT"´´F`SERIES FIRST-ORDER REACTIONS´L2``;
"PRINT"´OUTPUT `,SAMELINE,DIGITS(4),CT,
´´S4`UNKNOWN PARAMETER(S) ARE:  `;
"IF"MODE=0"THEN""PRINT"´K1, K2 AND EPB´L2``;
"IF"MODE=1"THEN""PRINT"´K2 AND EPB´L2``;
"IF"MODE=2"THEN""PRINT"´K1 AND EPB´L2``;
"IF"MODE=3"THEN""PRINT"´K1 AND K2´L2``;
"IF"MODE=12"THEN""PRINT"´EPB´L2``;
"IF"MODE=23"THEN""PRINT"´K1´L2``;
"IF"MODE=13"THEN""PRINT"´K2´L2``;
"BEGIN"
"ARRAY"T,DD[1:N];
"ARRAY"X,Y,Z[1:3,1:3];
"REAL""PROCEDURE"DCALC(KK1,KK2,EEPB,TT,DD1,DD2,DD3);
"VALUE"KK1,KK2,EEPB,TT;"REAL"KK1,KK2,EEPB,TT;
"REAL"DD1,DD2,DD3;
"BEGIN""REAL"A,B,C,S,E,F,G,P,Q,R;
G:=EEPB-EPC;P:=EPA-EEPB;Q:=EPC-EPA;
D:=(KK1-KK2)/KK1;
"COMMENT"IF ABS(K1-K2)<0.01*K1, USE A REPHRASING IN TERMS OF K1 AND
K1*(1-D) = K2 FOLLOWED BY A SERIES EXPANSION TO POWER 4 OF EXP(K1*D*TT);
"IF"ABS(D)"LE"0.01"THEN""GOTO"SMALL;
S:=EXP(-KK1*TT);
E:=EXP(-KK2*TT);
F:=KK1-KK2;
R:=S*(KK1*P+KK2*Q)+(KK1*E*G);
A:=TA*S;B:=(KK1*TA*(E-S))/F;C:=TA-A-B;
DD1:=(TA*PL*(-TT*S*(KK1*P+KK2*Q)+P*S+E*G)/F)-TA*PL*R/(F*F);
DD2:=(TA*PL*(S*Q-TT*KK1*E*G)/F)+TA*PL*R/(F*F);
DD3:=PL*TA*KK1*(E-S)/F;
"IF"MODE=1"THEN"DD1:=0;
"IF"MODE=2"THEN"DD2:=0;
"IF"MODE=3"THEN"DD3:=0;
"IF"MODE=12"THEN"DD1:=DD2:=0;
"IF"MODE=13"THEN"DD1:=DD3:=0;
"IF"MODE=23"THEN"DD2:=DD3:=0;
DCALC:=PL*(EPA*A+EEPB*B+EPC*C);
"GOTO"EX;
SMALL:A:=KK1*TT;E:=EXP(-A);
TY:=TY+1;
Q:=-Q;
B:=(A+.5*A*A*D+.16667*A*A*A*D*D+A*A*A*A*D*D*D/24);
C:=PL*TA;
DD1:=C*(-TT*E*(Q+G*B)+E*G*(TT*(1+D*A+.5*D*D*A*A+.16667*D*D*D*A*A*A)));
DD2:=C*E*G*(A*A)*(.5+.33333*A*D+.125*A*A*D*D);
DD3:=C*E*B;
"IF"MODE=1"THEN"DD1:=0;
"IF"MODE=2"THEN"DD2:=0;
```

```
"IF"MODE=3"THEN"DD3:=0;
"IF"MODE=12"THEN"DD1:=DD2:=0;
"IF"MODE=13"THEN"DD1:=DD3:=0;
"IF"MODE=23"THEN"DD2:=DD3:=0;
DCALC:=C*(EPC+E*(Q+G*B));
DD1:=DD1+DD2*KK2/(KK1*KK1);
DD2:=-DD2/KK1;
EX:"END";
CYCLE:=0;
STSDELTAS:=105;
"PRINT"´ N =  ,SAMELINE,DIGITS(3),N,´´S2`TA = `,SCALED(4),TA,
´  EPA = `,EPA,´  EPC = `,EPC,´  PATH LENGTH = `,FREEPOINT(4),PL,
´  BACKGROUND ABSORBANCE = `,DB,´´L4``;
"PRINT"´DAMPING FACTOR = `,SAMELINE,FREEPOINT(3),DF,´´L2``;
"PRINT"´CYCLE´S6``,SAMELINE,´K1´S8`K2´S7`EPB´S7`SQ. ERROR´S6`STSDELTAS
´L2``;
"BEGIN""REAL"DK1,DK2,DEB,DELK1,DELK2,DELEB,SDK1S,SDK2S,SDEBS,
SDK1EB,SDK2EB,SDK1K2,DELTA,SDELTAS,SDELK1,SDELK2,SDELEB,DC,DET;
"REAL"STK1,STK2,STEPB;
"REAL"DIFF;
"INTEGER"I,J;
"FOR"I:=1"STEP"1"UNTIL"N"DO"
"BEGIN""READ"T[I],DO[I];
     T[I]:=T[I]*K;
     T[I]:=T[I]+INC;
DO[I]:=DO[I]-DB;
"END";
START:SDELTAS:=SDK1S:=SDK2S:=SDEBS:=SDK1EB:=SDK2EB:=SDK1K2:=
SDELK1:=SDELK2:=SDELEB:=0;
DIFF:=0;
"FOR"I:=1"STEP"1"UNTIL"N"DO"
"BEGIN"DC:=DCALC(K1,K2,EPB,T[I],DK1,DK2,DEB);
DELTA:=DO[I]-DC;
SDK1S:=SDK1S+DK1*DK1;
SDK2S:=SDK2S+DK2*DK2;
SDEBS:=SDEBS+DEB*DEB;
SDK1EB:=SDK1EB+DK1*DEB;
SDK2EB:=SDK2EB+DK2*DEB;
SDK1K2:=SDK1K2+DK1*DK2;
SDELK1:=SDELK1+DELTA*DK1;
SDELK2:=SDELK2+DELTA*DK2;
SDELEB:=SDELEB+DELTA*DEB;
SDELTAS:=SDELTAS+DELTA*DELTA;
"END";
"IF"TX=1"THEN""GOTO"LABEL2;
"PRINT"DIGITS(3),CYCLE,SAMELINE,´´S3``,FREEPOINT(6),K1,
´´S2``,K2,´´S2``,EPB,´´S3``,SCALED(6),SDELTAS,´´S3``,STSDELTAS;
LABEL2:
"IF"CYCLE=100"THEN""GOTO"LABEL;
"IF"SDELTAS=STSDELTAS"THEN""GOTO"EXIT;
"IF"(ABS(STSDELTAS-SDELTAS))*DF"LE"10-13"THEN""GOTO"EXIT;
"IF"DF<10-6"THEN""GOTO"EXIT;
"IF"STSDELTAS<SDELTAS"THEN""BEGIN"
"IF"ABS(D)>0.01"THEN""GOTO"LABELD;
"IF"TY-(2*N)"LE"0"THEN""GOTO"LABEL3;
LABELD:
DF:=DF*0.1;
"IF"TX=1"THEN""GOTO"LABEL4;
"PRINT"´´L2`DAMPING FACTOR = `,SAMELINE,FREEPOINT(7),DF,´´L``;
LABEL4:
K1:=STK1;K2:=STK2;EPB:=STEPB;STSDELTAS:=SDELTAS;CYCLE:=CYCLE+1;
LABEL3:"END"
```

```
"IF"CYCLE=100"THEN""GOTO"EXIT;
"IF"STSDELTAS=SDELTAS"THEN""GOTO"START;
"IF"SDELTAS<STSDELTAS"THEN""BEGIN"
STSDELTAS:=SDELTAS;
STK1:=K1;STK2:=K2;STEPB:=EPB;
"END";
"COMMENT"MATRIX INVERSION FOLLOWS;
LABEL:
X[1,1]:=SDK1S;X[1,2]:=SDK1K2;X[1,3]:=SDK1EB;
X[2,1]:=SDK1K2;X[2,2]:=SDK2S;X[2,3]:=SDK2EB;
X[3,1]:=SDK1EB;X[3,2]:=SDK2EB;
X[3,3]:=SDEBS;
"IF"MODE"NE"0"THEN""BEGIN""IF"MODE>3"THEN""GOTO"LABEL5;
X[MODE,MODE]:=1;
LABEL5:
"IF"MODE=12"THEN"X[1,1]:=X[2,2]:=1;
"IF"MODE=13"THEN"X[1,1]:=X[3,3]:=1;
"IF"MODE=23"THEN"X[2,2]:=X[3,3]:=1;
"END";
Y[1,1]:=X[2,2]*X[3,3]-X[3,2]*X[2,3];
Y[1,2]:=-(X[2,1]*X[3,3]-X[3,1]*X[2,3]);
Y[1,3]:=X[2,1]*X[3,2]-X[3,1]*X[2,2];
Y[2,1]:=-(X[1,2]*X[3,3]-X[3,2]*X[1,3]);
Y[2,2]:=X[1,1]*X[3,3]-X[3,1]*X[1,3];
Y[2,3]:=-(X[1,1]*X[3,2]-X[3,1]*X[1,2]);
Y[3,1]:=X[1,2]*X[2,3]-X[2,2]*X[1,3];
Y[3,2]:=-(X[1,1]*X[2,3]-X[2,1]*X[1,3]);
Y[3,3]:=X[1,1]*X[2,2]-X[2,12*X[1,2];
DET:=X[1,1]*Y[1,1]+X[1,2]*Y[1,2]+X[1,3]*Y[1,3];
Z[1,1]:=Y[1,1]/DET;Z[1,2]:=Y[2,1]/DET;Z[1,3]:=Y[3,1]/DET;
Z[2,1]:=Y[1,2]/DET; Z[2,2]:=Y[2,2]/DET;Z[2,3]:=Y[3,2]/DET;
Z[3,1]:=Y[1,3]/DET;Z[3,2]:=Y[2,3]/DET;Z[3,3]:=Y[3,3]/DET;
"IF"CYCLE=100"THEN""GOTO"OUTPUT;
DELK1:=Z[1,1]*SDELK1+Z[1,2]*SDELK2+Z[1,3]*SDELEB;
DELK1:=DELK1*DF;
DELK2:=Z[2,1]*SDELK1+Z[2,2]*SDELK2+Z[2,3]*SDELEB;
DELK2:=DELK2*DF;
DELEB:=Z[3,1]*SDELK1+Z[3,2]*SDELK2+Z[3,3]*SDELEB;
DELEB:=DELEB*DF;
D:=(K1-K2)/K1;
"IF"ABS(D)"LE"0.01"THEN""GOTO"SM2;
"GOTO"SM3;
SM2:"IF"TX=1"THEN""GOTO"SM3;
"PRINT"´ (K1 - K2)/K1 < ONE PERCENT`;
SM3:
K1:=K1+DELK1;K2:=K2+DELK2;EPB:=EPB+DELEB;
CYCLE:=CYCLE+1;
"IF"MODE>3"THEN""GOTO"LABEL8;
"IF"K1"LE"0"THEN"
"BEGIN"K1:=(K1-DELK1)*0.8;
K2:=(K2-DELK2)*1.2;
EPB:=(EPB-DELEB)*1.2;
"PRINT"´´L``S66`K1 NEGATIVE´L``;
"END";
"IF"K2"LE"0"THEN"
"BEGIN"K1:=(K1-DELK1)*1.2;
K2:=(K2-DELK2)*0.8;
EPB:=(EPB-DELEB)*1.2;
"PRINT"´´L``S66`K2 NEGATIVE´L``;
"END";
"IF"EPB"LE"0"THEN"
"BEGIN"K1:=(K1-DELK1)*1.2;
```

```
K2:=(K2-DELK2)*1.2;
EPB:=(EPB-DELEB)*0.8;
"PRINT"´´L``S6`EPB NEGATIVE´L``;
"END";
"IF"MODE=1"THEN"K1:=STK1;
"IF"MODE=2"THEN"K2:=STK2;
"IF"MODE=3"THEN"EPB:=STEPB;
LABEL8:
"IF"CYCLE=100"THEN""GOTO"EXIT"ELSE""GOTO"START;
EXIT:"IF"CYCLE=100"THEN""BEGIN"
K1:=STK1;K2:=STK2;EPB:=STEPB;
"GOTO"START;
OUTPUT:"END";
"PRINT"´´L4``,SAMELINE,´MINIMUM VALUES ARE:´L2``;
"PRINT"´  K1 = `,SAMELINE,SCALED(4),K1,´´L2``;
"PRINT"´  K2 = `,SAMELINE,SCALED(4),K2,´´L2``;
"PRINT"´ EPB = `,SAMELINE,SCALED(4),EPB,´´L4``;
"PRINT"´SUMS OF SQUARES OF RESIDUALS = `,SAMELINE,SCALED(4),SDELTAS,
´´L2``;
"PRINT"´´L2``,SAMELINE,´´S4``,´T´S6`OBSERVED´S3`CALCULATED´L``;
"PRINT"´(SECONDS) ABSORBANCE  ABSORBANCE DIFFERENCE´L2``;
"FOR"J:=1"STEP"1"UNTIL"N"DO"
"BEGIN"D:=`CALC(K1,K2,EPB,T[J],DK1,DK2,DEB);
"PRINT"FREEPOINT(5),T[J],SAMELINE,´´S4``,FREEPOINT(4),
DO[J]+DB,´´S6``,D+DB,´´S6``,DO[J]-D,´´L``;
"END";
"PRINT"´´L``,SAMELINE,´ K1 = `,SCALED(4),K1,´´S3``,´ESD (K1) = `,
SQRT((Z[1,1]*SDELTAS)/(N-3)),´´S2`SECONDS(-1)´L``;
"PRINT"´´L``,SAMELINE,´ K2 = `,SCALED(4),K2,´´S3``,´ESD (K2) = `,
SQRT((Z[2,2]*SDELTAS)/(N-3)),´´S2`SECONDS(-1)´L2``;
"PRINT"´EPB = `,SAMELINE,SCALED(4),EPB,´´S3``,´ESD(EPB) = `,
SQRT((Z[3,3]*SDELTAS)/(N-3)),´´S2`MOLES(-1) CM.(-1)´L``;
"PRINT"´´L`CORRELATION COEFFICIENTS ARE:´L``;
"PRINT"´(K1,K2)`,SAMELINE,FREEPOINT(4),´´S3``,
Z[1,2]/(SQRT(Z[1,1]*Z[2,2])),´´L``;
"PRINT"´(K1,EPB)`,SAMELINE,FREEPOINT(4),´´S2``,
Z[1,3]/(SQRT(Z[1,1]*Z[3,3])),´´L``;
"PRINT"´(K2,EPB)`,SAMELINE,FREEPOINT(4),´´S2``,
Z[2,3]/(SQRT(Z[2,2]*Z[3,3])),´´L2``;
"IF"MODE"GE"3"THEN""GOTO"LABEL7;LABEL9:
TX:=TX+1;"IF"TX=1"THEN""BEGIN"
"PRINT"´´L5`SEARCH FOR SECOND MINIMUM´L2``;
K1:=STK2;K2:=STK1;EPB:=EPA+(STK1*(EPB-EPA)/STK2);
DF:=STDF;
CYCLE:=0;STSDELTAS:=105;
"END";
"IF"TX=1"THEN""GOTO"START;
LABEL7:"IF"MODE=12"THEN""GOTO"LABEL9;
TZ:=TZ+1;"IF"TZ"LE"2"THEN"
"BEGIN""FOR"J:=1"STEP"1"UNTIL"N"DO"
"BEGIN"D:=DCALC(K1,K2,EPB,T[J],DK1,DK2,DEB);
DIFF:=DIFF+(DO[J]-D)*(DO[J]-D);
"END";
DIFF:=DIFF/N;DIFF:=SQRT(DIFF);
"PRINT"´´L`ROOT MEAN SQUARE DIFFERENCE = `,SAMELINE,DIFF,´´L2``;
D:=DCALC(K1,K2,EPB,T[1],DK1,DK2,DEB);
PO:=T[1];
"IF"ABS(DO[1]-D)"GE"DIFF"THEN"
"BEGIN"
TIM:=EPB-EPA;
TIM:=TIM/(EPB-DO[1]/(TA*PL));
TIM:=LN(TIM)/K1;
"FOR"I:=1"STEP"1"UNTIL"N"DO"
```

```
T[I]:=T[I]-PO+TIM;
"IF"TZ>1"THEN""GOTO"SM5;
"PRINT"'F',CORRECTION FOR POSSIBLE ZERO TIME ERROR APPLIED'L2';
"PRINT"'ERROR = ',SAMELINE,FREEPOINT(6),TIM-INC,' SECONDS'L2';
"GOTO"SM6;
SM5:"PRINT"'SECOND CORRECTION FOR POSSIBLE TIME ERROR APPLIED'L2';
"PRINT"'TOTAL TIME ERROR = ',SAMELINE,FREEPOINT(6),TIM,' SECONDS'L2';
SM6:"END";
TX:=TY:=CYCLE:=0;DF:=STDF;STSDELTAS:=105;
"END""ELSE""GOTO"SM4;
"IF"ABS(DO[1]-D)<DIFF"THEN""GOTO"SM4;
"IF"TZ"LE"2"THEN""GOTO"START;
SM4:"END";
"END";
"IF"MODE"NE"0"THEN""PRINT"'L4'CORRELATION COEFFICIENTS ARE NOT
MEANINGFUL IN THIS CASE'L';
"COMMENT"INPUTS AS FOLLOWS:  MODE (=0,1,2,3,12,13,23 ACCORDING AS
UNKNOWN PARAMETERS ARE K1 & K2 & EPB,K2 & EPB, K1 & EPB, K1 & K2,
EPB, K2, K1), CT (DATA LABEL), N (NO. OF POINTS),
TA (TOTAL INITIAL CONCN. OF A),  EPA, EPB, EPC (MOLAR EXTINCTION
COEFFICIENTS OF A, B, AND C RESPECTIVELY, EPB AN ESTIMATE),
PL(PATH LENGH OF OBSERVATION CELL),
DB (BACKGROUND ABSORBANCE, CONSTANT THROUGHOUT THE REACTION),
K1 ,K2 (ESTIMATES OF THE RATE CONSTANTS),
     K (ONE UNIT OF TIME = K SECONDS),
     INC (REAL TIME = INPUT TIME + INC, IN SECONDS),
T[I],DO[I] ... , T[N], DO[N] (T=TIME, DO=OBSERVED ABSORBANCE,
INCLUDING DB);
"END" OF PROGRAM;
```

REFERENCES

1. H. Taube, Chem. Rev., 1952, 50, 69.

2. D.R.Stranks in "Modern Co-ordination Chemistry", J.Lewis and R.G.Wilkins (eds.), Interscience, 1960.

3. F.Basolo and R.G.Pearson, "Mechanisms of Inorganic Reactions", 2nd. ed. Wiley, 1967.
   (a) Chpt. 2. (b) Chpt. 3.

4. C.H.Langford and H.B.Gray, "Ligand Substitution Processes", Benjamin, 1965.

5. E.F.Caldin, "Fast Reactions in Solution", Blackwell, Oxford, 1964.
   (a) Chpt. 2. (b) Chpt. 5. (c) Chpt. 11.

6. J.Bjerrum and K.G.Poulsen, Nature, 1952, 169, 463.

7. C.S.Garner and J.Bjerrum, Acta. Chem. Scand. 1961, 15, 2055.

8. K.Kustin (ed.), "Methods in Enzymology", 16, Academic Press, 1969.
   (a) pp 232-6. (b) pp 227-8. (c) p 24. (d) p 195.

9. Many contributors, Diss. Faraday Soc., 1954, 17, 114-234.
   (a) pp 194-205 (M.Eigen).

10. S.L.Friess, E.S.Lewis and A.Weissburger (eds.), "Techniques in Organic Chemistry", 2nd. ed., Interscience, 1963, Vol. 8, Pt. II.
    (a) pp 707-792 (R.J.W.Roughton and B.Chance).
    (b) pp 901-16 (M.Eigen and L.DeMaeyer).

11. B.Chance, R.H.Eisenhardt, Q.H.Gibson and K.K.Longberg-Holm (eds.), "Rapid Mixing and Sampling Techniques in Biochemistry", Academic Press, 1964.
    (a) pp 71-85 (P.Strittmatter)
    (b) pp 89-103 (J.N.Sturtevant)

12. E.M.Eyring and B.C.Bennion, Ann. Rev. Phys. Chem., 1968, 19, 129-60.

13. T.C.Watts, Ph.D. Thesis, University of Warwick, 1970.

14. J.F.Below, R.E.Connick and C.P.Coppel, J. Amer. Chem. Soc., 1958, 80, 2961.

15. H.Hartridge and F.J.W.Roughton, Proc. Roy. Soc.(A), 1923, 104, 376.

16. K.Dalziel, Biochem. J., 1953, 55, 79.

17. M.N.J.Dirken and H.J.Mook, J. Physiol., 1930, 70, 373.

18. B.Chance, J. Franklin Inst., 1940, 229, 455, 613, 737.

19. F.J.W.Roughton, Proc. Roy. Soc.(B), 1934, 115, 473.

20. B.Chance and V.Legallais, Rev. Sci. Instr., 1951, 22, 627.

21. Q.H.Gibson, J. Physiol., 1952, 117, 49P.

22. R.H.Prince, Z. Electrochem., 1960, 64, 13.

23. G.Dultz and N.Sutin, Inorg. Chem., 1963, 2, 917.

24. Q.H.Gibson and L.Milnes, Biochem. J., 1964, 91, 161.

25. R.J.De Sa and Q.H.Gibson, Rev. Sci. Instr., 1966, 37, 900.

26. B.G.Willis, J.A.Bittikofer, H.L.Pardue and D.W.Margerum, Anal. Chem., 1970, 42, 1340.

27. J.L.Dye and L.H.Feldman, Rev. Sci. Instr., 1966, 37, 154.

28. A.A.Frost and R.G.Pearson, "Kinetics and Mechanism", 2nd. ed., Wiley, 1961.

(a) pp 280-1. (b) pp 98-101. (c) pp 166-171. (d) p 186.

29. G.Czerlinski and M.Eigen, Z. Electrochem., 1959, 63, 652.

30. H.Hoffman, E.Yeager and J.Stuehr, Rev. Sci. Instr., 1968, 39, 649.

31. International Conference on the Mechanisms of Reactions in Solution, University of Kent, 1970, Unofficial Seminars on Advances in Fast-Reaction Techniques.

(a) J.E.Crooks. (b) G.W.Hoffmann.

32. G.Ertland and H.Gerischer, Z. Electrochem., 1961, 65, 629.

33. D.J.Hewkin and R.H.Prince, Co-ord. Chem. Rev., 1970, 5, 45.

34. T.R.Stengle and C.H.Langford, Co-ord Chem. Rev., 1967, 2, 349.

35. L.Burlamacchi, G.Martini and E.Tiezzi, J.Phys. Chem., 1970, 74, 1809.

36. D.C.McCain and R.J.Myers, J.Phys.Chem., 1968, 72, 4115.

37. N.Tanaka, H.Ogawa and M.Kamada, Bull. Chem. Soc. Japan, 1963, 36, 530.

38. J.E.Erman and G.G.Hammes, Rev. Sci. Instr., 1966, 37, 746.

39. Q.H.Gibson and C.Greenwood, Biochem. J., 1963, 86, 541.

40. R.L.Berger, B.Balko, W.Borcherdt and W.Friauf, Rev. Sci. Instr., 1968, 39, 486.

41. C.R.Allen, A.J.W.Brook and E.F.Caldin, Trans. Farad. Soc., 1960, 56, 788.

42. C.A.Tolman, J. Amer. Chem. Soc., 1970, 92, 4217.

43. R.R.Dewald and J.M.Brooks, Rev. Sci. Instr., 1970, 41, 1612.

44. M.Eigen and R.G.Wilkins, Adv. Chem. Sers., 1965, 49, 55.

45. K.Kustin and J.Swinhart, Prog. Inorg. Chem., 1970, 13, 107.

46. A.McAuley and J.Hill, Quart. Rev., 1969, 23, 18.

47. R.G.Wilkins, Acc. Chem. Res., 1970, 3, 408.

48. M.Eigen, Pure Appl. Chem., 1963, 6, 97.

49. M.Eigen and K.Tamm, Z. Electrochem., 1962, 66, 107.

50. T.J.Swift and R.E.Connick, J. Chem. Phys., 1962, 37, 307.

51. N.Fogel, J.M.J.Tai and J.Yarbourgh, J. Amer. Chem. Soc., 1962, 84, 1145.

52. H.Taube and F.A.Posey, J. Amer. Chem. Soc., 1953, 75, 1463.

53. C.H.Langford and W.R.Muir, J. Amer. Chem. Soc., 1967, 89, 3141.

54. N.Sutin, Ann. Rev. Phys. Chem., 1966, 17, 119.

55. G.Atkinson and S.Petrucci, J. Phys. Chem., 1966, 70, 3122.

56. G.Atkinson and S.Kor, J. Phys. Chem., 1967, 71, 673.

57. H.Brintzinger and G.G.Hammes, Inorg. Chem., 1966, 5, 1286.

58. P.M.Fuoss, J. Amer. Chem. Soc., 1958, 80, 5059.

59. M.Eigen, Z. Phys. Chem. (Frankfurt), 1954, 1, 176.

60. M.T.Beck, Co-ord. Chem. Rev., 1968, 3, 91.

61. C.H.Langford and T.R.Stengle, Ann. Rev. Phys. Chem., 1968, 19, 193.

62. A.Haim, R.J.Grassi and W.K.Wilmarth, Adv. Chem. Ser., 1965, 49, 31.

63. J.Halpern, J. Chem. Ed., 1968, 45, 372.

64. G.G.Hammes and J.I.Steinfeld, J. Amer. Chem. Soc., 1962, 84, 4639.

65. K.Kustin, R.F.Pasternack and E.M.Weinstock, J. Amer. Chem. Soc., 1966, 88, 4610.

66. A.Kowalak, K.Kustin, R.F.Pasternack and S.Petrucci, J. Amer. Chem. Soc., 1967, 89, 3126.

67. W.B.Makinen, A.F.Pearlmutter and J.E.Stuehr, J. Amer. Chem. Soc., 1969, 91, 4083.

68. R.F.Pasternack and K.Kustin, J. Amer. Chem. Soc., 1968, 90, 2295.

69. R.G.Pearson and C.P.Anderson, Inorg. Chem., 1970, 9, 39.

70. U.Nickel, H.Hoffmann and W.Jaenike, Ber. Bunsenges. Physik. Chem., 1968, 72, 526.

71. D.B.Rorabacher, Inorg. Chem., 1966, 5, 1891.

72. D.B.Rorabacher and D.B.Moss, Inorg. Chem., 1970, 9, 1314.

73. L.J.Kirschenbaum and K.Kustin, J. Chem. Soc.(A), 1970, 684.

74. R.G.Pearson and P.Ellgen, Inorg. Chem., 1967, 6, 1379.

75. P.Dickert, H.Hoffmann and W.Jaenike, Ber. Bunsenges. Physik. Chem., 1970, 74, 500.

76. G.Macri and S.Petrucci, Inorg. Chem., 1970, 9, 1009.

77. H.P.Bennetto, R.Bulmer and E.F.Caldin, in "Hydrogen Bonded Solvent Systems", A.K.Covington and P.Taylor (eds.), Taylor and Francis, London, 1968, p 335.

78. H.P.Bennetto and E.F.Caldin, Chem. Comm., 1969, 599.

79. W.J.MacKeller and D.B.Rorabacher, J. Amer. Chem. Soc., 1971, 93, 4379

80. H.P.Bennetto and E.F.Caldin, J. Chem. Soc.(A), 1971, 2191.

81. H.S.Frank and W.Y.Wen, Discuss. Faraday Soc., 1957, 24, 133.

82. H.P.Bennetto and E.F.Caldin, J.Chem.Soc.(A), 1971, 2198.

83. C.H.Langford and H.C.Tsien, Inorg. Chem., 1970, 9, 2345.

84. L.S.Frankel, Inorg. Chem., 1971, 10, 814.

85. R.B.Scott and F.G.Brickwedde, J. Res. Nat. Bur. Stand., 1931, 6, 401

86. R.E.Dodd and P.L.Robinson, "Experimental Inorganic Chemistry", Elsevier, 1954, pp 56-7.

87. P.Moore, S.F.A.Kettle and R.G.Wilkins, Inorg. Chem., 1966, 5, 220.

88. Y.Beers, "Introduction to the Theory of Error", 2nd. ed., Addison-Wesley, 1957.

89. E.Halfpenny and P.L.Robinson, J. Chem. Soc., 1952, 928.

90. G.Yagil and M.Anbar, J. Inorg. Nuc. Chem., 1964, 26, 453.

91. W.G.Keith and R.E.Powell, J. Chem. Soc.(A), 1969, 90.

92. M.N.Hughes and H.G.Nicklin, J. Chem. Soc.(A), 1968, 450.

93. M.Anbar and H.Taube, J. Amer. Chem. Soc., 1954, 76, 6243.

94. J.O.Edwards, "Peroxide Reaction Mechanisms", Wiley, N.Y., 1962.

95. J.D.Ray, J. Inorg. Nuc. Chem., 1962, 24, 1159.

96. J.H.Ridd, Quart. Rev., 1961, 15, 418.

97. T.A.Turney, "Oxidation Mechanisms", Butterworths, London, 1965, p 80.

98. T.A.Turney and G.A.Wright, Chem. Rev., 1959, 59, 497.

99. C.A.Bunton and G.Steadman, J. Chem. Soc., 1959, 3466.

100. P.Moore, Ph.D. Thesis, University of Sheffield, 1964.

101. P.Lumme and J.Tummavuori, Acta. Chem. Scand., 1965, 19, 617.

102. E.S.Swinbourne, J. Chem Soc., 1961, 2371.

103. T.A.Turney and G.A.Wright, J. Chem. Soc., 1958, 2415.

104. W.W.Fee, C.S.Garner and J.N.Mac B.Harrowfield, Inorg. Chem., 1967, 6, 87.

105. P.Moore, S.F.A.Kettle and R.G.Wilkins, Inorg. Chem., 1966, 5, 466.

106. L.R.Mahoney, J. Amer. Chem. Soc., 1970, 92, 5262.

107. Y.Murato and Y.Norino, Acta. Cryst., 1966, 20, 605.

108. R.H.Hoyler, C.D.Hubbard, S.F.A.Kettle and R.G.Wilkins, Inorg. Chem., 1966, 5, 622.

109. R.H.Hoyler, C.D.Hubbard, S.F.A.Kettle and R.G.Wilkins, Inorg. Chem., 1965, 4, 929.

110. L.G.Sillen and A.E.Martell (compilers), "Stability Constants of Metal-Ion Complexes", Special Publications No. 17, The Chemical Society, 1964.

111. W.R.McWhinnie and J.D.Miller, Adv. Inorg. Chem. Radiochem., 1969, 12, 135.

112. H.Levanon and Z.Luz, J. Chem. Phys., 1968, 49, 2031.

113. A.I.Vogel, "A text-book of Practical Organic Chemistry", 3rd. ed., Longmans, 1957, p 169.

114. A.I.Vogel, "A Text-book of Quantitative Inorganic Analysis", 3rd. ed., Longmans, 1962, p 434.

115. P.Arthur, W.M.Haynes and L.P.Varga, Anal. Chem., 1966, 38, 1630.

116. R.F.Pasternack and R.A.Plane, Inorg. Chem., 1965, 4, 1171.

117. N.J.Friedman and R.A.Plane, Inorg. Chem., 1963, 2, 11.

118. Z.Luz and S.Meiboom, J. Chem. Phys., 1964, 40,
(a) 1058. (b) 1066. (c) 2686.

119. H.P.Bennetto and E.F.Caldin, J. Chem. Soc.(A), 1971, 2207.

120. M.L.Sanduja and W.MacF.Smith, Canad. J. Chem., 1969, 47, 3773.

121. M.Grant, H.W.Dodgen and J.P.Hunt, J. Amer. Chem. Soc., 1969, 91, 6318.

122. R.Farina, R.Hogg and R.G.Wilkins, Inorg. Chem., 1968, 7, 170.